MODE OF ACTION OF EXOGLUCANASES FROM THE CELLULOLYTIC FUNGUS *Trichoderma reesei*: ACTIVITY ON REDUCING END-LABELED CELLOOLIGOSACCHARIDES AND TOPOGRAPHY OF ACTIVE SITES OF β-GLUCOSIDASE, CELLOBIOHYDROLASE I(D), AND CELLOBIOHYDROLASE II

BY

WILLIAM JOSEPH CHIRICO

A DISSERTATION PRESENTED TO THE GRADUATE SCHOOL
OF THE UNIVERSITY OF FLORIDA IN
PARTIAL FULFILLMENT OF THE REQUIREMENTS
FOR THE DEGREE OF DOCTOR OF PHILOSOPHY

UNIVERSITY OF FLORIDA

1984

This dissertation is dedicated to my parents,

Dominick and Catherine Chirico,

and to my Aunt and Uncle,

Inez and Frank Montalbano.

ACKNOWLEDGMENTS

I wish to express my sincere gratitude to Dr. Ross D. Brown, Jr., for his guidance and support during the course of this work. I would also like to thank the other members of my supervisory committee, Drs. Charles M. Allen, Jr., Kim J. Angelides, Vicent Chau, Michael Roberts, and Jesse F. Gregory, for their suggestions and support. I wish to thank Drs. Phil Laipis, Mike Kilberg, and Daniel Purich for their support.

I am also grateful to Charles duMee, John Denny, Larry Weissbach, Mark Eller, and Sal Pietromonaco for friendship and many valuable discussions.

I am extremely grateful for the excellent technical assistance of Cynthia Fazenbaker and Vicki Andersen who shared the duties of scraping TLC plates. I would also like to thank Jim Parkes for incorporating J.D. Allen's depolymerase computer model in my computer file. I wish to thank Cindy Zimmerman for typing the dissertation and Nancy Shaskey for drawing the figures.

Finally, I would like to thank Crystal Willis, without whose support, encouragement, and love this dissertation could not have been written.

TABLE OF CONTENTS

Page

ACKNOWLEDGMENTS.....iii

LIST OF TABLES.....vii

LIST OF FIGURES.....x

LIST OF ABBREVIATIONS AND SYMBOLS.....xv

ABSTRACT.....xvi

CHAPTER

1 INTRODUCTION.....1

Structure of Cellulose.....3
Cellulases.....4
Subsite Mapping of Enzymes.....12
Assessment.....15

2 EXPERIMENTAL PROCEDURES.....17

Materials.....17
Enzymes.....17
Substrates.....17
Chemicals.....18
Chromatographic Supplies.....18
Methods.....19
Carbohydrate Determination.....19
Protein Determination.....20
High Performance Liquid Chromatography (HPLC).....20
Preparation of Cellooligosaccharides.....21
Oxidation of Cellooligosaccharides.....21
Lactonization of Cellooligosaccharide Aldonic Acids.....22
Reduction of Aldonic Lactones with Sodium Borohydride.....23
Reduction of Lactones of Cellooligosaccharide Aldonic Acids with Sodium Boro[^{3}H]hydride.....24
Specificity of Radiolabeling.....25
Measurement of Radioactivity.....26
Preparation of [^{14}C-U]cellooligosaccharides.26

Thin-layer Chromatography (TLC).....27
Enzymic Assays.....31
Kinetic Analysis of Hydrolysis Data.....34
Determination of Kinetic Constants.....34
Evaluation of Subsite Affinities.....35

3 PREPARATION OF [1-^{3}H]CELLOOLIGOSACCHARIDES AND [^{14}C-U]CELLOOLIGOSACCHARIDES.....36

Introduction.....36
Results and Discussion.....38
Preparation of Cellooligosaccharides.....38
Oxidation of Cellooligosaccharides.....43
Lactonization of Cellooligosaccharide Aldonic Acids.....46
Reduction of Lactones of Cellooligosaccharide Aldonic Acids with Sodium Boro[^{2}H]hydride.....49
Purity and Stability of [1-^{3}H]Cellooligosaccharides.....53
Specificity of Radiolabeling.....54
Preparation of [^{14}C-U]Cellooligosaccharides.....54
Conclusions.....57

4 SEPARATION OF [1-^{3}H]CELLOOLIGOSACCHARIDES BY THIN-LAYER CHROMATOGRAPHY.....58

Introduction.....58
Results and Discussion.....60
Separation of [1-^{3}H]Cellooligosaccharides...60
Extraction of [1-^{3}H]Cellooligosaccharides...69
Conclusions.....71

5 MODE OF ACTION OF β-GLUCOSIDASE.....73

Introduction.....73
Results and Discussion.....75
Hydrolysis of [1-^{3}H]Cellooligosaccharides...75
Hydrolysis of [1-^{3}H]Cellooligosaccharides and [^{14}C-U]Cellooligosaccharides.....113
Inhibition of Methylumbelliferylglucoside (MUG) Hydrolysis by Cellooligosaccharides.....119
Subsite Mapping of β-Glucosidase.....135
Conclusions.....144

6 MODE OF ACTION OF CELLOBIOHYDROLASE I(D).....146

Introduction.....146
Results and Discussion.....148
Hydrolysis of [1-^{3}H]Cellooligosaccharides.....148

Hydrolysis of
[1-^{3}H]Cellooligosaccharides and
[^{14}C-U]Cellooligosaccharides.....184
Subsite Mapping of
Cellobiohydrolase I(D).....196
Conclusions.....205

7 MODE OF ACTION OF CELLOBIOHYDROLASE II.....206

Introduction.....206
Results and Discussion.....208
Hydrolysis of
[1-^{3}H]Cellooligosaccharides.....208
Hydrolysis of
[1-^{3}H]Cellooligosaccharides and
[^{14}C-U]Cellooligosaccharides.....240
Subsite Mapping of Cellobiohydrolase II....249
Conclusions.....258

8 GENERAL DISCUSSION.....260

Hydrolysis of [1-^{3}H]Cellooligosaccharides.....260
Synergism of Cellulolytic Enzymes.....263
Individual Roles of Cellulolytic Enzymes.....270
Methods of Subsite Mapping.....274
Future Experiments.....281

9 SUMMARY.....283

APPENDICES

A SUBSITE MAPPING OF ENZYMES.....286

B SAMPLE CALCULATIONS FOR BOND CLEAVAGE FREQUENCIES AND INITIAL RATES OF HYDROLYSIS OF [1-^{3}H]CELLOOLIGOSACCHARIDES.....304

C KINETIC EQUATIONS.....309

D SUBSITE AFFINITIES FOR ß-GLUCOSIDASE.....310

E KINETIC CONSTANTS FOR HYDROLYSIS OF ß-LINKED DISACCHARIDES OF GLUCOSE BY ß-GLUCOSIDASE.....311

F KINETIC CONSTANTS FOR HYDROLYSIS OF [1-^{3}H]CELLOOLIGOSACCHARIDES BY ß-GLUCOSIDASE, CBH I(D), AND CBH II.....312

BIBLIOGRAPHY.....313

BIOGRAPHICAL SKETCH.....323

LIST OF TABLES

Table		Page
3-1	Oxidation of Cellooligosaccharides	44
3-2	Lactonization of Calcium Salts of Cellooligosaccharide Aldonic Acids	48
3-3	Characteristic Infrared Bands of Calcium Salts of Cellooligosaccharide Aldonic Acids and Cellooligosaccharides Lactones	50
3-4	Reduction of Cellooligosaccharide Lactones with Sodium Boro[^{2}H]hydride	51
3-5	Preparation of [^{14}C-U]Cellooligosaccharides	56
4-1	Resolution of Cellooligosaccharides With Different Adsorbents, Impregnants and Solvents	61
4-2	Values of the Migration Parameter, R_F	68
4-3	Extraction of a Mixture of [1-^{2}H]Cellooligosaccharides From Thin-layer Chromatographic Plates	70
4-4	Extraction of Individual [1-^{2}H]Cellooligosaccharides From Thin-layer Chromatographic Plates	72
5-1	Kinetic Constants for [1-^{2}H]Cellooligosaccharide Hydrolysis by β-Glucosidase of *T. reesei*	83
5-2	Hydrolysis of [1-^{3}H]Cellopentaose and [^{14}C-U]Cellopentaose by β-Glucosidase	114
5-3	Initial Rates for β-Glucosidase Activity on [1-^{2}H]Cellopentaose and [^{14}C-U]Cellopentaose	116
5-4	Hydrolysis of [1-^{3}H]Cellohexaose and [^{14}C-U]Cellohexaose by β-Glucosidase	117
5-5	Initial Rates for β-Glucosidase Activity on [1-^{2}H] Cellohexaose and [^{14}C-U]Cellohexaose	118

5-6 Inhibition of ß-Glucosidase by Cellooligosaccharides.....134

6-1 Kinetic Constants for [1-^{3}H]Cellooligosaccharide Hydrolysis by Cellobiohydrolase I(D).....183

6-2 Hydrolysis of [1-^{3}H]Cellopentaose and [^{14}C-U]Cellopentaose by Cellobiohydrolase I(D).....185

6-3 Initial Rates of Cellobiohydrolase I(D) Activity on [1-^{3}H]Cellopentaose and [^{14}C-U]Cellopentaose.....189

6-4 Hydrolysis of [1-^{3}H]Cellohexaose and [^{14}C-U]Cellohexaose by Cellobiohydrolase I(D)...191

6-5 Initial Rates of Hydrolysis of Cellobiohydrolase I(D) Activity on [1-^{3}H]Cellohexaose and [^{14}C-U]Cellohexaose.....195

6-6 Subsite Affinities of CBH I(D) Calculated Using Values of V_{max}/K_m and Bond Cleavage Frequencies from [1-^{3}H]Cellooligosaccharides....197

7-1 Kinetic Constants for [1-^{3}H]Cellooligosaccharide Hydrolysis by Cellobiohydrolase II.....239

7-2 Hydrolysis of [1-^{3}H]Cellopentaose and [^{14}C-U]Cellopentaose by Cellobiohydrolase II....242

7-3 Initial Rates of Cellobiohydrolase II Activity on [1-^{3}H]Cellopentaose and [^{14}C-U]Cellopentaose.....243

7-4 Hydrolysis of [1-^{3}H]Cellohexaose and [^{14}C-U]Cellohexaose by Cellobiohydrolase II.....245

7-5 Initial Rates of Cellobiohydrolase II Activity on [1-^{3}H]Cellohexaose and [^{14}C-U]Cellohexaose.....250

7-6 Subsite Affinities of CBH II Calculated Using Values of V_{max}/K_m and Bond Cleavage Frequencies from [1-^{3}H]Cellooligosaccharides....252

B-1 Distribution of [1-^{3}H]Cellooligosaccharides from Hydrolysis of [1-^{3}H]Cellotetraose by CBH II(D).....305

B-2 Product Ratios for [1-^{3}H]Cellotetraose Hydrolysis by CBH I(D).....306

B-3 Concentration of [1-^{3}H]Cellooligosaccharides from Hydrolysis of [1-^{3}H]Cellotetraose by CBH I(D).....308

LIST OF FIGURES

Figure		Page
3-1	Synthesis of [1-^{3}H]cellooligosaccharides	40
3-2	Elution pattern from Bio-Gel P-2 column chromatography of cellooligosaccharides generated from acid hydrolysis of cellulose	42
4-1	Thin-layer chromatographic pattern of cellooligosaccharides	65
4-2	Thin-layer chromatographic pattern of [1-^{3}H]cellooligosaccharides	67
5-1	Time course hydrolysis of [1-^{3}H]cellobiose by β-glucosidase	78
5-2	Bond cleavage frequency plot for hydrolysis of [1-^{3}H]cellobiose by β-glucosidase	80
5-3	Lineweaver-Burk and Eadie-Hofstee plots for hydrolysis of [1-^{3}H]cellobiose by β-glucosidase	82
5-4	Time course hydrolysis of [1-^{3}H]cellotriose by β-glucosidase	85
5-5	Bond cleavage frequency plot for hydrolysis of [1-^{3}H]cellotriose by β-glucosidase	88
5-6	Lineweaver-Burk and Eadie-Hofstee plots for hydrolysis of [1-^{3}H]cellotriose by β-glucosidase	90
5-7	Time course hydrolysis of [1-^{3}H]cellotetraose by β-glucosidase	92
5-8	Bond cleavage frequency plot for hydrolysis of [1-^{3}H]cellotetraose by β-glucosidase	95
5-9	Lineweaver-Burk and Eadie-Hofstee plots for hydrolysis of [1-^{3}H]cellotetraose by β-glucosidase	97

5-10 Time course hydrolysis of [1-^{3}H]cellopentaose by β-glucosidase.....99

5-11 Bond cleavage frequency plot for hydrolysis of [1-^{3}H]cellopentaose by β-glucosidase.....101

5-12 Lineweaver-Burk and Eadie-Hofstee plots for hydrolysis of [1-^{3}H]cellopentaose by β-glucosidase.....104

5-13 Time course hydrolysis of [1-^{3}H]cellohexaose by β-glucosidase.....106

5-14 Bond cleavage frequency plot for hydrolysis of [1-^{3}H]cellohexaose by β-glucosidase.....108

5-15 Lineweaver-Burk and Eadie-Hofstee plots for hydrolysis of [1-^{3}H]cellohexaose by β-glucosidase.....111

5-16 Inhibition of β-glucosidase by cellobiose using 4-methylumbelliferyl-β-D-glucopyranoside as the substrate.....121

5-17 Inhibition of β-glucosidase by cellotriose using 4-methylumbelliferyl-β-D-glucopyranoside as the substrate.....123

5-18 Inhibition of β-glucosidase by cellotetraose using 4-methylumbelliferyl-β-D-glucopyranoside as the substrate.....125

5-19 Inhibition of β-glucosidase by cellopentaose using 4-methylumbelliferyl-β-D-glucopyranoside as the substrate.....127

5-20 Inhibition of β-glucosidase by cellohexaose using 4-methylumbelliferyl-β-D-glucopyranoside as the substrate.....129

5-21 Dixon replots of inhibition of β-glucosidase by cellobiose, cellotriose and cellotetraose....131

5-22 Dixon replots of inhibition of β-glucosidase by cellopentaose and cellohexaose.....133

5-23 Subsite map for β-glucosidase constructed using values of V_{max}/K_m for cellooligosaccharides.....138

5-24 Subsite map for β-glucosidase constructed using values of inhibition constants for cellooligosaccharides.....141

6-1 Time course hydrolysis of [1-^{3}H]cellotriose by CBH I(D).....151

6-2 Bond cleavage frequency plot for hydrolysis of [1-^{3}H]cellotriose by CBH I(D).....153

6-3 Effect of [1-^{3}H]cellotriose concentration on product ratios.....155

6-4 Eadie-Hofstee plot for hydrolysis of [1-^{3}H]cellotriose hydrolysis by CBH I(D).....157

6-5 Time course hydrolysis of [1-^{3}H]cellotetraose by CBH I(D).....161

6-6 Bond cleavage frequency plot for hydrolysis of [1-^{3}H]cellotetraose by CBH I(D).....163

6-7 Lineweaver-Burk and Eadie-Hofstee plots for hydrolysis of [1-^{3}H]cellotetraose by CBHI(D)....165

6-8 Time course hydrolysis of [1-^{3}H]cellopentaose by CBH I(D).....167

6-9 Bond cleavage frequency plot for hydrolysis of [1-^{3}H]cellopentaose by CBH I(D).....170

6-10 Lineweaver-Burk and Eadie-Hofstee plots for hydrolysis of [1-^{3}H]cellopentaose by CBH I(D)...172

6-11 Time course hydrolysis of [1-^{3}H]cellohexaose by CBH I(D).....174

6-12 Bond cleavage frequency plot for hydrolysis of [1-^{3}H]cellohexaose by CBH I(D).....176

6-13 Lineweaver-Burk and Eadie-Hofstee plots for hydrolysis of [1-^{3}H]cellohexaose by CBH I(D)....179

6-14 Bond cleavage frequencies of [1-^{3}H]cellooligosaccharide hydrolysis by CBH I(D).....181

6-15 Possible types of repetitive attack of CBH I(D) with [1-^{3}H]cellopentaose and [^{14}C-U]cellopentaose.....188

6-16 Possible types of repetitive attack of CBH I(D) with [1-^{3}H]cellohexaose and [^{14}C-U]cellohexaose.....193

6-17 Subsite map for CBH I(D) constructed using values of V_{max}/K_m and bond cleavage frequencies for [1-^{3}H]cellooligosaccharides.....200

6-18 Subsite map for CBH I(D) constructed using values of K_m, V_{max} and bond cleavage frequencies for [1-^{3}H]cellooligosaccharides.....203

7-1 Time course hydrolysis of [1-^{3}H]cellotriose by CBH II.....210

7-2 Bond cleavage frequency plot for hydrolysis of [1-^{3}H]cellotriose by CBH II.....212

7-3 Lineweaver-Burk and Eadie-Hofstee plots for hydrolysis of [1-^{3}H]cellotriose by CBH II.....214

7-4 Time course hydrolysis of [1-^{3}H]cellotetraose by CBH II.....217

7-5 Bond cleavage frequency plot for hydrolysis of [1-^{3}H]cellotetraose by CBH II.....219

7-6 Lineweaver-Burk and Eadie-Hofstee plots for hydrolysis of [1-^{3}H]cellotetroase by CBH II.....221

7-7 Time course hydrolysis of [1-^{3}H]cellopentaose by CBH II.....223

7-8 Bond cleavage frequency plot for hydrolysis of [1-^{3}H]cellopentaose by CBH II.....226

7-9 Lineweaver-Burk and Eadie-Hofstee plots for hydrolysis of [1-^{3}H]cellopentaose by CBH II.....228

7-10 Time course hydrolysis of [1-^{3}H]cellohexaose by CBH II.....230

7-11 Bond cleavage frequency plot for hydrolysis of [1-^{3}H]cellohexaose by CBH II.....232

7-12 Lineweaver-Burk and Eadie-Hofstee plots for hydrolysis of [1-^{3}H]cellohexaose by CBH II.....235

7-13 Bond cleavage frequencies of [1-^{3}H]cellooligosaccharide hydrolysis by CBH II.....237

7-14 Possible types of repetitive attack of CBH II with [1-^{3}H]cellohexaose and [^{14}C-U]cellohexaose.....247

7-15 Subsite map for CBH II constructed using values of V_{max}/K_m and bond cleavage frequencies for [1-^{3}H]cellooligosaccharides.....254

7-16 Subsite map for CBH II constructed using values of K_m, V_{max} and bond cleavage frequencies for [1-^{3}H]cellooligosaccharides.....257

8-1 Structure of cellulose I and cellulose II.....266

8-2 Orientation of glycosidic bonds in cellulose....269

A-1 Binding modes of cellotriose on a hypothetical four-subsite enzyme.....288

A-2 Combination of V_{max}/K_m values and bond cleavage frequencies for [1-^{3}H]cellotetraose and [1-^{3}H]cellotriose used to calculate subsite affinities.....301

LIST OF ABBREVIATIONS AND SYMBOLS

A	Substrate
CBH	Cellobiohydrolase
CM-Cellulose	Carboxymethylcellulose
G_i	Cellooligosaccharide of chain length i
HPLC	High performance liquid chromatography
k_{cat}	Turnover number
k_{+2}	Hydrolytic rate coefficient
K_i	Inhibition constant
K_{int}	Microscopic dissociaton constant for a binding mode in which the entire binding region is occupied
K_m	Michaelis constant
K_s	Dissociation constant for substrate
MUG	4-Methylumbelliferyl-β-D-glucopyranoside
MeUmb β(Glcp)n	4-Methylumbelliferyl-β-D-glycosides from cellobiose (n=2) to cellohexaose (n=6)
TLC	Thin-layer chromatography
V	Measured velocity
V_{max}	Maximum velocity

Abstract of Dissertation Presented to the Graduate School of the University of Florida in Partial Fulfillment of the Requirements for the Degree of Doctor of Philosophy

MODE OF ACTION OF EXOGLUCANASES FROM THE CELLULOLYTIC FUNGUS Trichoderma reesei: ACTIVITY ON REDUCING END-LABELED CELLOOLIGOSACCHARIDES AND TOPOGRAPHY OF ACTIVE SITES OF β-GLUCOSIDASE, CELLOBIOHYDROLASE I(D), AND CELLOBIOHYDROLASE II

BY

WILLIAM JOSEPH CHIRICO

December, 1984

Chairman: Ross D. Brown, Jr., Ph.D.
Major Department: Biochemistry and Molecular Biology

The activity of purified β-glucosidase, cellobiohydrolase I(D) and cellobiohydrolase II from Trichoderma reesei was studied using [1-^{3}H]cellooligosaccharides. Reducing end-labeled cellooligosaccharides of high specific radioactivity were synthesized by reducing lactones of cellooligosaccharide aldonic acids with sodium boro[^{3}H]hydride. A thin-layer chromatographic method for separating [1-^{3}H]cellooligosaccharides with high resolution and quantitatively extracting them from silica gel was developed.

The β-glucosidase was shown to bind [1-^{3}H]cellooligosaccharides in one productive mode and sequentially remove glucosyl residues from the nonreducing end. The β-glucosidase exhibited little tendency to repetitively attack [1-^{3}H]cellooligosaccharides. Values of V_{max} for hydrolysis

of [1-^{3}H]cellooligosaccharides remained constant as chain length increased, whereas corresponding values of K_m decreased. Values of inhibition constants determined for cellooligosaccharide inhibition of 4-methylumbelliferyl-ß-D-glucopyranoside hydrolysis were similar to corresponding values of K_m. The active site of ß-glucosidase was shown to comprise primarily three subsites, of which subsite 1 contributes the greatest proportion of binding energy.

Cellobiohydrolase I(D) was shown to bind [1-^{3}H]cellooligosaccharides in more than one productive mode. Bond cleavage frequency analysis indicated that cellobiohydrolase I(D) preferentially hydrolyzes glycosidic bonds at the reducing end. Product distribution resulting from activity on [^{14}C-U]cellooligosaccharides and [1-^{3}H]cellooligosaccharides suggests that cellobiohydrolase I(D) repetitively attacks cellooligosaccharides from the reducing end. Values of V_{max}/K_m for [1-^{3}H]cellooligosaccharide hydrolysis increase with increasing chain length. Subsite mapping procedures revealed that the active site of cellobiohydrolase I(D) comprises seven subsites with catalytic groups located between subsites 5 and 6.

Cellobiohydrolase II was also shown to bind [1-^{3}H]cellooligosaccharides in more than one productive mode; however, glycosidic bonds at the nonreducing end are preferentially hydrolyzed. Product distribution resulting from hydrolysis of [^{14}C-U]cellooligosaccharides and [1-^{3}H]cellooligosaccharides suggests that cellobiohydrolase

II repetitively attacks cellooligosaccharides from the nonreducing end. Values of V_{max}/K_m for [1-^{3}H]cellooligosaccharide hydrolysis increase with increasing chain length. Subsite mapping procedures show that the substrate binding region of cellobiohydrolase II comprises seven subsites with catalytic groups located between subsites 3 and 4.

The results are discussed in terms of the individual roles of exoglucanases during the saccharification of cellulose. A mechanism by which cellobiohydrolase I(D) and cellobiohydrolase II may synergistically degrade crystalline cellulose is proposed.

CHAPTER 1
INTRODUCTION

The utilization of cellulose, the world's most abundant renewable carbon source, for fuel, food and chemical feedstocks has received increasing attention as depletion of nonrenewable resources continues. The amount of photosynthetically fixed carbon dioxide which is converted to cellulose has been estimated by Ghose (1) at 10^{11} metric tons per year. Glucose, a product of cellulose hydrolysis, can serve as a substrate for fermentations to produce single-cell protein, ethanol and methane (2). Cellulose can be converted to soluble products by acid or enzymic hydrolysis. Although technology for acid hydrolysis exists, degradation of products, interaction of acid with noncellulosic substances in natural sources of cellulose, corrosion of equipment and high capital costs argue for development of alternative methods of conversion (3). Enzymic hydrolysis of cellulose has the advantage of efficiency and specificity; however, it is the most expensive process. Lignin and hemicellulloses, which are constituents of natural sources of cellulose, protect the substrate from enzymic hydrolysis and limit conversion to 50 percent (2). Removal of lignin and hemicelluloses from native cellulose or addition of hemicellulases is necessary to obtain higher yields of glucose (2).

An excellent source of cellulolytic enzymes is the fungus Trichoderma reesei QM 9414, which possesses the complete array of enzymes required for the conversion of cellulose to glucose (4). The component enzymes of the cellulase system act synergistically, in order to convert native, crystalline cellulose to soluble products (5). Since the product of one enzyme may serve as a substrate for another, purification and characterization of each component is a prerequisite for a clear description of the enzymic hydrolysis of cellulose. Although the extracellular, depolymerizing enzymes (6,7) and ß-glucosidase (8) of T. reesei have been purified and partially characterized, little quantitative information is available regarding the affinity of cellulolytic enzymes for cellulose (or cellooligosaccharides). In addition, the mechanism by which cellulolytic enzymes act synergistically and the topography of their active sites remain unknown. Since cellooligosaccharides are symmetric, the precise glycosidic bonds cleaved by cellulolytic enzymes have not been determined. Furthermore, the direction from which exo-glucanases remove glucosyl or cellobiosyl residues from cellulosic substrates has not been determined.

In this report, the synthesis of reducing end-labeled cellooligosaccharides and a quantitative method for separating them using thin-layer chromatography are described. The activity of cellobiohydrolase I(D) [CBH I(D)], cellobiohydrolase II (CBH II) and ß-glucosidase of T. reesei on

these asymmetrically labeled substrates provides information regarding substrate affinities, action patterns, topography of active sites and the direction from which substrates are degraded.

Structure of Cellulose

Cellulose is a linear polymer of β-1,4-D-glucosyl residues. Four crystalline forms of cellulose (I-IV) have been recognized on the basis of infrared spectra and X-ray diffraction studies (9). The chains in each structure have approximately the same backbone conformation, with a unit of cellobiose repeating every 10.3 A (10). The distinguishing feature of the structures is the arrangement of adjacent chains. Cellulose I (native cellulose) is found in plant cell walls. When native cellulose is dissolved and recrystallized, it is converted irreversibly to cellulose II, a form of cellulose more stable than cellulose I. Cellulose III and IV can be produced from cellulose I or II by treatment with liquid ammonia and hot glycerol, respectively (9).

The most crystalline, native cellulose is found in the cell walls of the alga Valonia ventricosa. The X-ray diffraction patterns of cellulose fibers isolated from cell walls of Valonia ventricosa indicate that intramolecular hydrogen bonds are located on both sides of the glycosidic linkage: one hydrogen bond between O2'-H---O6 and another between O3-H---O5' (9). The O6-H hydroxyl is bonded to O3 of an adjacent chain. Thus, native cellulose is seen as a series of hydrogen-bonded sheets of parallel chains which

are held together by van der Waal forces between hydrophobic faces of sugar rings. In contrast, X-ray patterns of cellulose II indicate that chains are arranged in an antiparallel fashion. Cellulose II also has intramolecular hydrogen bonds between O2'-H---O6 and another between O3-H---O5'. The orientation of $-CH_2OH$ groups allows formation of intermolecular hydrogen bonds between O6-H---O3, O6-H---O2 and O2-H---O2'. The additional intermolecular hydrogen bonding accounts for the increased stability of cellulose II.

Recently, Atalla and VanderHart (11) compared the solid-state carbon-13 nuclear magnetic resonance spectra of various native celluloses. The spectra were consistent with the presence of two distinct forms of cellulose, I_α and I_β, in each sample. They estimated that the relative amounts of I_α as a fraction of the total are Acetobacter xylinium = Valonia ventricosa > cotton = ramie > regenerated cellulose I. Thus, I_α is dominant in bacterial and algal cellulose, whereas I_β is dominant in celluloses from higher plants. Carbon-13 NMR spectra of cellulose II closely resembled that of I_β.

Cellulases

The cellulase system comprises 1,4-β-D-glucan-4-glucanohydrolases (EC 3.2.1.4), 1,4-β-D-glucan cellobiohydrolases (EC 3.2.1.91) and β-glucosidases (EC 3.2.1.21), which together act sequentially and cooperatively to convert native, crystalline cellulose to oligosaccharides and glucose. Endoglucanases randomly attack internal glycosidic

bonds of cellulose producing chain ends and soluble oligosaccharides. Cellobiohydrolases cleave cellobiosyl residues from ends of cellulose chains. Cellobiose, an inhibitor of the depolymerizing enzymes, and oligosaccharides are converted to glucose by the ß-glucosidase. Component enzymes have been purified and characterized from true cellulolytic organisms, such as Trichoderma viride (5,12-16), Trichoderma reesei (6,8,17), Trichoderma koningii (18,19) and Irpex lacteus (20).

Endo-1,4,-ß-D-glucanases catalyze the hydrolysis of internal glycosidic bonds of cellulose providing chain ends from which cellobiosyl residues are removed by exo-cellobiohydrolases (5). The most frequently used technique for evaluating endoglucanase activity is measurement of the reduction of viscosity of a carboxymethylcellulose (CM-cellulose) solution (21). Endoglucanases are differentiated from exo-cellobiohydrolases according to the anomeric configuration and identity of products from hydrolysis of polymeric substrates and cellooligosaccharides (22). Endoglucanases proceed with retention of configuration and form a variety of products, whereas exo-glucanases proceed with inversion of configuration and cleave almost exclusively cellobiosyl residues from the ends of substrates (22).

Gritzali (6) reported the purification of a single endoglucanase, which has a molecular weight of 45,200 and a neutral carbohydrate content of 14.2 percent (by weight), from extracellular filtrates of T. reesei. The

endoglucanase accounts for 15 percent (by weight) of the extracellular protein (5). Purification of endoglucanases from T. reesei has also been reported by Hakansson et al. (17), Ladisch et al. (23) and duMee (24). Bhikhabhai and Pettersson (25) recently reported the partial sequence of an endoglucanase from T. reesei. Cyanogen bromide peptides of the endoglucanase showed significant homology with the amino acid sequence of CBH I. Comparison of carbon-13 NMR spectra of three endoglucanases isolated by duMee indicates that oligosaccharides attached to endoglucanases are similar if not identical to those of CBH I(D) and CBH II of T. reesei (24).

The rate of hydrolysis of cellooligosaccharides by the endoglucanase from T. reesei increases from cellotetraose to cellopentaose; however, this trend does not extend to cellohexaose (6). Cellotetraose is hydrolyzed to glucose, cellobiose and cellotriose. Cellotriose is resistant to further degradation and its large concentration relative to glucose is indicative of transglycosylation by the endoglucanase. A variety of products are formed from cellopentaose and cellohexaose. The endoglucanase readily catalyzes hydrolysis of CM-cellulose and phosphoric acid-swollen cellulose. Microcrystalline cellulose is resistant to attack, whereas filter paper discs are degraded to short fibers.

The release of cellobiose from ends of cellulose chains is due primarily to the hydrolytic action of 1,4-ß-D-glucan cellobiohydrolases. Other names for this enzyme include

exo-glucanase and exo-cellulase (20). The activity of cellobiohydrolases is determined by measuring the reducing sugar released from a suspension of swollen or crystalline cellulose. Since each enzyme in the cellulase system produces reducing sugar, highly purified preparations are required for enzymic characterization. Cellobiohydrolases exhibit little activity toward CM-cellulose as measured by change in viscosity (5).

Two immunologically distinct cellobiohydrolases [CBH I(D) and CBH II] have been purified from extracellular filtrates of T. reesei grown on cellulose or incubated with sophorose (6). Mandels et al. (26) discovered that sophorose is a potent inducer of cellulase in T. viride QM 6a. Cellobiohydrolase I(D) has a molecular weight of 53,200 (6), contains 5.9 percent (by weight) of neutral carbohydrate (24) and is isoelectric at pH 3.95 (7), whereas the corresponding values for CBH II are 54,700 (6), 18.1 percent (24) and pH 4.9 (6), respectively. Cellobiohydrolase I(D) and CBH II constitute approximately 60 and 25 percent (by weight), respectively, of the extracellular protein produced by this fungus (5). Recently, duMee (24) reported that CBH I(D) contains 6 or 7 oligosaccharide chains linked through mannose to the protein, whereas CBH II contains approximately 25 oligosaccharide chains also linked through mannose to the protein. Complete amino acid sequence analysis of CBH I revealed that most of the neutral carbohydrate is located in a short region near the carboxy terminus (27).

The sites of attachment of three glucosamine residues were also determined. Fagerstam and Pettersson (7) reported that no homology exists within the first 20 amino acid residues of CBH I(D) and CBH II, although both enyzmes have a pyroglutamyl residue at the N-terminus of the polypeptide chain. The molecular cloning and characterization of the gene encoding CBH I of T. reesei have been reported by Shoemaker et al. (28). The nucleotide sequence shows that the gene contains two introns and that a signal peptide is located at the N-terminus.

Enzymic properties of cellobiohydrolases purified from extracellular filtrates of T. reesei QM 9414 on insoluble and soluble substrates have been reported (6). Cellobiohydrolase II cleaves cellooligosaccharides approximately 10-fold and polymeric substrates 2-fold more rapidly than CBH I(D) (6). Cellobiohydrolase I(D) and CBH II are optimally active at pH 5.2-5.6 and 4.9, respectively (6).

Phosphoric acid-swollen cellulose is hydrolyzed more rapidly than microcrystalline cellulose by CBH I(D) or CBH II (6). Cellobiohydrolase II produces exclusively cellobiose from phosphoric acid-swollen cellulose, whereas CBH I(D) yields some glucose in addition to cellobiose. Carboxymethylcellulose is mostly resistant to attack by either enzyme. The two cellobiohyrolases show strong synergistic activity in the hydrolysis of crystalline cellulose, thereby demonstrating their essential role in the degradation of cellulose (7).

The action patterns of CBH I(D) and CBH II have been investigated using high performance liquid chromatographic (HPLC) analysis of products formed during enzymic hydrolysis of cellooligosaccharides (6). Cellobiohydrolase I(D) catalyzes the hydrolysis of cellotriose forming glucose and cellobiose, whereas CBH II has little activity toward cellotriose. As the chain length of oligosaccharide substrate increases, CBH I(D) produces cellobiose and increasing proportions of glucose and cellotriose. In contrast, CBH II yields exclusively cellobiose from cellotetraose and a mixture of cellobiose and cellotriose from cellopentaose and cellohexaose. Each cellobiohydrolase yields cellobiose from hydrolysis of cellohexaose without concomitant formation of cellotetraose, indicating a sequential cleavage of cellobiosyl residues. Cellohexaose is hydrolyzed 2-fold more rapidly than cellotetraose or cellopentaose by CBH I(D) or CBH II.

Hsu et al. (29), using a cellobiohydrolase isolated from T. reesei QM 9414, reported that Km's for cellotriose and cellotetraose are 0.2 and 0.08 mM, respectively. Cellotetraose was hydrolyzed 27-fold faster than cellotriose. Since low sensitivity of HPLC analysis of cellooligosaccharides precludes initial rate studies, Hsu et al. (29) estimated kinetic constants from analysis of the entire time course of the reaction.

Recently, van Tilbeurgh et al. (30) reported the action patterns of CBH I(D) on a series of 4-methylumbelliferyl

glycosides derived from cellooligosaccharides. Cellobiohydrolase I(D) preferentially cleaves the glycosyl bond at the reducing end of the modified cellooligosaccharides. Whether the modification influences the action pattern of CBH I(D) is not known.

Cellobiohydrolases are also characterized by their affinities for inhibitors and substrates. Inhibition of depolymerizing enzymes by cellobiose is an important regulatory feature of the cellulase system. Inhibition constants of 2.1 and 0.2 mM for glucose and cellobiose, respectively, have been reported using a cellobiohydrolase from T. reesei (29). Using 4-methylumbelliferylcellobioside as the substrate, Brown and Greenberg (31) determined that glucose, cellobiose, cellotriose, cellotetraose, cellopentaose and cellohexaose inhibit and bind to one site on CBH I(D) with inhibition constants of 0.476 M, 90.4 μM, 28.4 μM, 14.1 μM, 14.6 μM and 7.6 μM, respectively. Similar information was not obtained for CBH II, because this enzyme exhibits little activity toward 4-methylumbelliferylcellobioside.

The ß-glucosidases catalyze the hydrolysis of aryl-ß-D-glucopyranosides and ß-linked glucose oligomers as well as transfer of glucosyl residues (32). Although the hydrolysis of dimers, trimers and tetramers of glucose is catalyzed by glucosidases and exo-glucanases, glucosidases are often reported to act more rapidly on short oligomers, whereas exo-glucanases prefer longer oligomers (22). Glucosidases proceed with retention of configuration, whereas

exo-glucanases proceed with inversion (22). The role of ß-glucosidase within the complement of cellulase enzymes is to cleave cellobiose, an inhibitor of the depolymerizing enzymes, to glucose (5,33).

Glucosidases have been purified from extracellular filtrates of several cellulolytic fungi, such as T. viride (16,34,35), T. koningii (19) and T. reesei (8). The ß-glucosidase purified from T. reesei (8) has a molecular weight of 74,600, contains 0.7 percent (by weight) carbohydrate and is isoelectric at pH 8.5. The ß-glucosidase constitutes about 0.4 percent (by weight) of the extracellular protein produced by this fungus. Transglucosylation reactions and hydrolysis of cellobiose, p-nitrophenyl-ß-D-glucopyranoside and 4-methylumbelliferyl-ß-D-gluconpyranoside are catalyzed by the ß-glucosidase. The enzyme has an unusually high affinity for its product, D-glucose, and is strongly inhibited by D-glucono-1,5-lactone, nojirimycin and 1-deoxynojirimycin.

Most cellulolytic fungi have similar cellulase systems containing one to several ß-glucosidases, endo-ß-glucanases and exo-ß-glucanases that act synergistically to hydrolyze insoluble cellulose (36). Synergism resulting from the concerted action of endoglucanases and exoglucanases has been explained by the production by endoglucanases of free polymer chain ends which serve as substrates for exoglucanases. Recently, strong exo-exo synergism has been reported for CBH I(D) and CBH II from T. reesei acting on crystalline

cellulose (7). Fagerstam and Pettersson (7) offered two possible explanations for exo-exo synergism: (1) the synergism may reflect a structural asymmetry in the substrate or (2) a change in the mode of action resulting from the formation of a complex between the two enzymes. However, no evidence for complex formation has been reported.

Subsite Mapping of Enzymes

Studies of the action pattern of polysaccharide hydrolases using their natural polymeric substrates led to the concept that glycosyl residues distant from the point of catalysis interact with the enzyme (37). Thus, the substrate binding region of the enzyme is considered to be an array of tandem subsites, each of which interacts independently with a specific glycosyl residue and with a certain affinity. The location of catalytic groups between two of the subsites, the number of subsites, the subsite affinity and the change in the unitary binding free energy at a subsite are characteristic features of polysaccharide hydrolases. Subsite models have been described to account for the enzymic properties of proteinases (38), nucleases (39) and carbohydrases (40-43).

The literature offers three methods to determine experimentally the number of subsites comprising the binding region, the energetics of interaction of each subsite with a glycosyl residue and the hydrolytic rate coefficients (37,43-45). A synopsis of equations most relevant to each

subsite-mapping procedure is found in Appendix A. Presented below is a brief desription of each method.

Hiromi and coworkers (44,46) applied the subsite model to exo-enzymes by using the first-order rate constant (V_{max}/K_m) and Km for each of a series of oligosaccharides. A substrate can be bound to an exoenzyme in a variety of binding modes; however, only one mode is productive. Since hydrolytic rate coefficients for each oligosaccharide are assumed equal, V_{max}/K_m values are directly proportional to the association constant of the single productive complex. Michaelis constants are assumed to approximate association constants. Thus, the ratios of V_{max}/K_m values for n-mer and n+1-mer substrates permit the estimation of the n+1-th subsite affinity. Using this method, the substrate binding region of glucoamylase from Rhizopus sp. was shown to consist of seven subsites, of which subsite II contributes the greatest proportion of the binding energy. Recently, Koyama et al. (47) applied Hiromi's method to glucoamylase from Aspergillus saito. This enzyme was also shown to consist of seven subsites, of which subsite II is the major contributor to the binding energy.

Although the method of Hiromi (46) is suitable for mapping exo-enzymes having one productive complex, it is not applicable to enzymes, such as endoenzymes, having more than one productive complex. Thoma and coworkers (43,48) have proposed a method to evaluate subsite affinities of endo-enzymes from product distribution ratios of end-labeled

oligosaccharides. Enzymic processes are separated into microscopic and macroscopic events. A microscopic coefficient characterizes one particular binding mode of a substrate. Each binding mode has a microscopic association constant, and each productive complex has a microscopic hydrolytic rate coefficient. Although microscopic constants are difficult to measure, they are related to measurable macroscopic parameters, which are a function of all binding modes of the substrate. The experimentally accessible parameters that are useful in subsite mapping are Km, Vmax, first order rate constant and bond cleavage frequencies measured as a function of chain length. Ratios of bond cleavage frequencies can be used to measure the size of the binding region, to locate the catalytic groups between two of the subsites and to calculate the apparent binding energies for some of the subsites. Allen and Thoma (49) using bond cleavage frequency analysis reported that the substrate binding region of Bacillus amyloliquefaciens α-amylase is composed of 10 subsites with catalytic groups located between subsites VI and VII.

Suganuma et al. (45) have proposed a method for evaluating subsite affinities that retains the advantages of Hiromi's and Thoma's methods. Suganuma et al. (45) reported that the substrate binding region of Taka-amylase A consists of 9 subsites with catalytic groups located between subsites 4 and 5. The subsite binding region of an endo-1,4-ß-xylanase from Cryptococcus albidus was examined using the

method of Suganuma et al. (45). The enzyme was shown to consist of 4 subsites with the catalytic groups located in the center (42).

Assessment

The mechanisms by which cellulolytic enzymes attack cellulose remain poorly understood, because the substrate, cellulose, is insoluble and heterogeneous. To define the mode of attack of cellulolytic enzymes, soluble substrates, such as cellooligosaccharides, should be used in enzymic studies. Although previous studies of cellulolytic enzymes using cellooligosaccharides as substrates provide information regarding rates of hydrolysis, quantitative estimates of the affinity of the enzymes for these substrates were not possible due to low sensitivity of the assays. In addition, the symmetric nature of cellooligosaccharides precludes identification of the precise glycosidic bonds cleaved by the enzymes.

In this report, the synthesis of reducing end-labeled cellooligosaccharides and a thin-layer chromatographic method for separating and quantitating these substrates are described. Reducing end-labeled cellooligosaccharides were used to identify the precise glycosidic bond(s) cleaved by ß-glucosidase, CBH I(D) and CBH II of T. reesei. These substrates were also used in initial rate studies to determine the affinity and maximal rates of hydrolysis by cellulolytic enzymes. Cellooligosaccharides uniformly labeled with carbon-14 were used in combination with reducing

end-labeled cellooligosaccharides to determine the direction from which cellulolytic enzymes attack. A subsite map for each enzyme was constructed from bond cleavage frequencies, Km and Vmax for the series of cellooligosaccharides. The results are discussed in terms of the role of each enzyme in the conversion of cellulose to glucose. A mechanism by which CBH I(D) and CBH II may exert exo-exo synergism is proposed.

CHAPTER 2
EXPERIMENTAL PROCEDURES

Materials

Enzymes

Cellobiohydrolase I(D) and CBH II, from extracellular culture filtrates of T. reesei QM 9414, were purified by Gritzali (6). Extracellular ß-glucosidase was purified from T. reesei as described previously (8).

Statzyme-Glucose 16 was purchased from Worthington Biochemical Corporation, Freehold, NJ.

Substrates

Cellobiose was obtained from Schwartz/Mann, Orangeburg, NY.

Sophorose was obtained from Adams Chemical Co., Round Lake, IL.

Laminaribiose was prepared by hydrolysis of laminarin and separated on a column of Bio-Gel P-2 by B. Greenberg in this laboratory.

The 4-methylumbelliferyl-ß-D-glucopyranoside (lot 86-50263), p-nitrophenyl-ß-D-glucopyranoside (lot 88C-5039), p-nitrophenyl-ß-D-galactopyranoside (lot 58C-5063), p-nitrophenyl-ß-D-xylopyranoside (lot 117C-0369), p-nitrophenyl-α-D-glucopyranoside (lot 59B-0100), p-nitrophenyl-1-thio-ß-D-glucopyranoside and gentiobiose (lot 35C-0173) were obtained from Sigma Chemical Company, St. Louis, MO.

Chemicals

Sodium boro[^{3}H]hydride (18.1 Ci/mmol, lot 25 and 12.1 Ci/mmol, lot 26) was obtained from Amersham, Arlington Heights, IL. The [^{14}C-U]cellulose (Nicotiana Tobacum L., 34.5 μCi/mg, lot 1396-151) and Aquasol were purchased from New England Nuclear, Boston, MA. Cellulose (SIGMACELL Type 100, lot 129C-0079) was obtained from Sigma Chemical Co., St. Louis, MO. Dextrose was obtained from the National Bureau of Standards, Washington, DC. Bromine (lot 22460) and Celite 545 were obtained from J.T. Baker Chemical Co., Phillipsburg, NJ. Calcium cellobionate (lot 101207) was obtained from ICN Pharmaceuticals, Inc., Cleveland, OH. Lactobionic acid (calcium salt) was obtained from Nutritional Biochemicals Corp., Cleveland, OH. The 2-propanol (certified ACS), acetonitrile (HPLC grade), ethyl acetate (certified ACS), methanol (HPLC grade), dimethyl sulfoxide (certified ACS), glucono-1,5-lactone (lot 793699) and p-anisaldehyde were obtained from Fisher Scientific, Fair Lawn, NJ.

All other chemicals were reagent grade.

Chromatographic Supplies

The LK5 (5 x 20 cm), LK6 (5 x 20 cm) and LK5D (20 x 20 cm, 250 μm) (lot 002431) Silica Gel TLC plates, Whatman 3 MM paper and Whatman Partisil PXS 10/25 PAC column (bonded cyano-amino type, polar phase) were obtained from Whatman Chemical Separations Division, Clifton, NJ.

Silica Gel IB2 Baker-flex (20 x 20 cm) TLC plates were purchased from J.T. Baker Chemical Co., Phillipsburg, NJ.

Cellulose (20 x 20 cm) (lot 6214) TLC plates were obtained from Eastman Kodak Company, Rochester, NY.

Polyamide Layer Sheets (15 x 15 cm, 50 μm) were obtained from Accurate Chemical and Scientific Corp., Hicksville, NY.

Amberlite IRA-45 (-OH) Anion Exchange Resin was obtained from Sigma Chemical Co., St. Louis, MO.

Amberlite IR-120 (H+) Cation Exchange Resin was obtained from Fisher Scientific, Fair Lawn, NJ.

Amberlite MB-3 Mixed Cation-Anion Exchange Resin was obtained from Mallinckrodt, Inc., Paris, KY.

Bio-Gel P-2 (200-400 mesh) and Bio-Gel P-2 (-400) mesh were purchased from BioRad Laboratories, Richmond, CA.

Millipore filters (0.22 μ) were purchased from Millipore Corp., Bedford, MA.

Molecular sieves (3 ^{o}A) were obtained from Davison Chemical, Baltimore, MD.

Methods

Carbohydrate Determination

Total neutral carbohydrate was determined by the phenol-sulfuric acid method of Dubois et al. (50). Alternatively, carbohydrate was determined by HPLC using differential refractometry. Reducing sugar was determined using the method of Nelson (51) and Somogyi (52). Glucose was used as a standard.

Protein Determination

Protein content was determined according to the method of Lowry et al. (53) as described by Bailey (54). Bovine serum albumin was used as a standard. Protein concentration of CBH I(D) was determined from the extinction coefficient, 13.8 (24).

High Performance Liquid Chromatography (HPLC)

Instrumentation. Cellooligosaccharides were separated and purity assessed using a Waters Association Model ALC 202/401 Liquid Chromatograph supplemented with a Model 6000 Solvent Delivery System (Waters Associates, Inc., Milford, MA). Column effluents were monitored using a differential refractometer and a Spectra-Physics Autolab System I integrator (Spectra-Physics, Santa Clara, CA) computed relative area of chromatographic peaks.

Reverse phase chromatography. Cellooligosaccharides were separated by reverse phase chromatography using a Whatman Partisil PXS 10/25 PAC column with an acetonitrile:water (75:25; v:v) solvent system (55). Cellooligosaccharides were eluted isocratically from the column at a flow rate of 1.5 ml/min at room temperature.

Bio-Gel P-2 chromatography. Cellooligosaccharides were also separated by gel permeation chromatography using a Bio-Gel P-2 (-400 mesh) column (0.75 x 240 cm). Cellooligosaccharides were eluted with water at a flow rate of 0.7 ml/min at 60°C.

Preparation of Cellooligosaccharides

Cellulose powder (15 g) was dissolved at 4°C in 200 ml of concentrated HCl (-30°C) (56). The slurry was stirred for 20 min at 4°C and then for 2 h at room temperature. After the hydrolysate was added to 600 ml of water (4°C), insoluble cellulose was removed by centrifugation (Sorvall RC-5B Centrifuge, Du Pont, Co., Newtown, CT) and the pellet was washed with 2 aliquots (100 ml) of water. The supernatants were combined, filtered (Whatman No. 1 paper) and neutralized using anion exchange resin (Amberlite IR-45 [-OH]). Cellooligosaccharides were concentrated in a rotary evaporator (Buchler Instruments, Fort Lee, NJ) and then fractionated on a Bio-Gel P-2 (200-400 mesh) column (4.4 x 115 cm). Approximately 200 g of cellulose powder yielded at least 500 mg of cellotriose through cellohexaose. Carbohydrates in column effluents were monitored using the method of Dubois et al. (50).

Oxidation of Cellooligosaccharides

Bromine oxidation. The method of Diehl et al. (57) was modified as described below and used to oxidize purified cellotriose through cellohexaose. Cadmium carbonate (0.45 g, 2.7 mmoles) was added to a solution of purified cellotriose (0.449 g, 0.89 mmoles) in water (19 ml). Bromine (0.028 ml, 1.1 mmoles) was added and the suspension was stirred in a stoppered flask in the dark for 24 h at room temperature. After the mixture was filtered through Celite, silver carbonate (0.32 g, 1.2 mmoles) was added to the

filtrate and the suspension was stirred for 20 min. The reaction mixture was filtered through Celite and the filtrate treated with an excess of hydrogen sulfide. The precipitate was removed by filtration through Celite and the filtrate freed of residual hydrogen sulfide by aeration. The filtrate was neutralized with calcium carbonate (58), concentrated to approximately 3 ml and filtered through a Millipore filter. The calcium salt of cellotrionic acid was separated from cellotriose and by-products of the reaction using Bio-Gel P-2 chromatography. Fractions containing calcium cellotrionate were combined, concentrated to a syrup and the product precipitated and washed with 2-methoxyethanol. Alternatively, isolation of calcium salts of cellooligosaccharide aldonic acids may be omitted and aldonic acids may be lactonized directly.

Oxidation with Adams' catalyst. Cellobiose (1 g, 1.5 mmoles) was oxidized in the presence of Adams' platinum oxide catalyst (0.5 g) and gaseous oxygen in aqueous solution (10 ml) at pH 3.7 as described by Conchie et al. (59) for oxidation of monosaccharides.

Lactonization of Cellooligosaccharides Aldonic Acids

Calcium cellotrionate (0.357 g) in 2 ml of water (4°C) was passed through a column containing 3 ml of cation exchange resin (Amberlite IR-120 [+H]) and the column washed with 30 ml of cold water (60). The effluent was concentrated to a thin syrup at 50°C under reduced pressure in a rotary evaporator and dried by successive evaporation in 6

ml of a mixture of dry 2-methoxyethanol and toluene (2:1) followed by evaporation to a syrup. The drying procedure was repeated three times. During the synthesis of cellotetranolactone, cellopentanolactone and cellohexanolactone precipitation of product before removal of water was prevented by using dimethyl sulfoxide in place of 2-methoxyethanol. After 5 ml of 2-methoxyethanol was added, cellotrionolactone precipitated from the syrup and the resulting suspension was centrifuged. Filtration was avoided, because precipitated lactones were hygroscopic at this stage of the synthesis. The pellet was washed with 3 aliquots (5 ml) of 2-methoxyethanol and then dried under reduced pressure at room temperature.

Reduction of Aldonic Lactones with Sodium Borohydride

Several procedures for reducing aldonic lactones to aldoses were evaluated using glucono-1,5-lactone, lactobionolactone or cellobionolactone as the starting compound. The procedures included reduction of lactones in the presence of cation exchange resin, boric acid, carbon dioxide or sodium acid oxalate as described by Frush and Isbell (61). Alternatively, 1.0 N H_2SO_4 was added to reaction mixtures to maintain weakly acidic conditions during reductions as described by Wolfrom and Wood (62).

Reduction of Lactones of Cellooligosaccharides with Sodium Boro[^{3}H]hydride

Reduction in the presence of carbon dioxide. Under an efficient hood, 10 ml of water was cooled to 4°C and a stream of carbon dioxide was bubbled through the solution. After the hydrogen ion concentration of the solution was adjusted to pH 6-7 (pH paper) with 1.0 N NaOH, 100 mg of cellotrionolactone was added and the solution was stirred. Immediately after cellotrionolactone was dissolved, 250 µl (5 mCi) of sodium boro[^{3}H]hydride (12.1-18.1 Ci/mmole) was added dropwise during 15 minutes. After an additional 15 minutes, the hydrogen ion concentration was adjusted to pH 2.5 with 1.0 N sulfuric acid and the solution stirred for 15 minutes. The solution was passed through a column containing 3 ml of cation exchange resin (Amberlite IR120 [+H]) and the effluent was concentrated to a syrup under reduced pressure in a rotary evaporator. The syrup was evaporated three times from 5 ml of water followed by evaporation of three 5 ml aliquots of methanol to remove borate esters. The resulting powder was dissolved in 1 ml of water and the [1-^{3}H]cellootriose was separated from unreacted lactone and by-products of the reaction using Bio-Gel P-2 HPLC. To prevent radiochemical decomposition, column effluents containing radioactive cellooligosaccharide were adjusted immediately to 10 percent ethanol and stored at -70°C. Unreacted lactone was converted to the corresponding calcium

salt and reused for future reductions. Chemical and radiochemical purity of [1-^{3}H]cellooligosaccharides were determined using thin-layer chromatography, reverse phase HPLC and Bio-Gel P-2 HPLC. Specific radioactivity was determined by measuring radioactivity by scintillation counting and carbohydrate by Bio-Gel P-2 HPLC, reverse phase HPLC or the method of Dubois et al. (50).

Reduction in the presence of sodium acid oxalate. Glucono-1,5-lactone (100 mg, 0.56 mmoles) was added to 20 ml of water (4°C) containing 7.3 mg (0.56 mmoles) of sodium acid oxalate. Under an efficient hood, 250 µl (5 mCi) of sodium boro[^{3}H]hydride (16.4 Ci/mmole) and then sodium borohydride (4.2 mg, 1.1 mmoles) were added dropwise to the solution. After 0.5 h, the hydrogen ion concentration was adjusted to pH 2.5 with 1.0 N H_2SO_4. The solution was stirred for 15 min and then neutralized with mixed-bed ion exchange resin (Amberlite MB-3). After removing ion exchange resin by filtration, the filtrate was concentrated to a syrup using a rotary evaporator. The syrup was dissolved in 75 ml of water and concentrated to remove tritiated water. Volatile and nonvolatile radioactivity was measured by scintillation counting.

Specificity of Radiolabeling

To determine the location of tritium in [^{3}H]cellooligosaccharides, [^{3}H]cellotriose (0.28 µCi) was diluted with cold cellotriose to a total of 4.1 mg (8.1 µmoles) and oxidized with an excess of bromine (20 µl, 390 µmoles).

After the solution was stirred at room temperature for 24 h, water was removed using a rotary evaporator. Radioactivity in water and oxidized products was measured by scintillation counting.

Measurement of Radioactivity

Radioactive samples were dissolved in 5 ml of Aquasol and counted using a Beckman LS-9000 liquid scintillation counter (Beckman Instruments, Inc., Palo Alto, CA). All radioactive measurements were automatically corrected for quenching. Aquasol was acidified (0.4 percent) with glacial acetic acid to retard chemiluminescence.

Preparation of [^{14}C-U]Cellooligosaccharides

Batch method. The [^{14}C-U]cellulose (750 µCi, 34.5 µCi/mg) was added to concentrated HCl (3 ml), which had been stored at -30°C. After the slurry was stirred at room temperature for 3 h, 3 ml of cold water (4°C) was added and the solution was neutralized with sodium bicarbonate. The reaction mixture was centrifuged and the supernatant was filtered through a Millipore filter. The [^{14}C-U]cellooligosaccharides were separated on a Bio-Gel P-2 (200-400 mesh) column (4.4 x 115 cm). Isolated [^{14}C-U]cellooligosaccharides were rechromatographed on the same column or using Bio-Gel P-2 HPLC until each [^{14}C-U]cellooligosaccharide was greater than 99 percent pure as judged by scintillation counting. Specific radioactivity of [^{14}C-U]cellooligosaccharides was assumed equal to that of the

[^{14}C-U]cellulose. Purified [^{14}C-U]cellooligosaccharides were stored in aqueous solution at -30°C.

Column method. The following procedure was used to increase the yield of [^{14}C-U]cellooligosaccharides of longer chain length (4-6) from acid hydrolysis of [^{14}C-U]cellulose. During a 3 h period, 90 ml of concentrated HCl (4°C) were passed through a column (0.6 x 7 cm) containing a mixture of [^{14}C-U]cellulose (250 µCi, 34.5 µCi/mg) and fine glass beads. The effluent was collected in a flask containing 50 ml saturated sodium bicarbonate solution. The hydrogen ion concentration of the solution in the collection flask was maintained at approximately pH 7 with the addition of sodium bicarbonate. The effluent was desalted and the [^{14}C-U]cellooligosaccharides were separated on a Bio-Gel P-2 (200-400 mesh) column (4.4 x 115 cm). Fractions containing soluble cellooligosaccharides of chain length greater than two were combined and rechromatographed through the same column. Radioactivity in column effluents was measured by liquid scintillation counting.

Thin-Layer Chromatography (TLC)

Separation of cellooligosaccharides. Aqueous samples (5-15 µg) of cellooligosaccharides in 1-2 µl aliquots were applied to TLC plates. To a developing tank (7 x 27 x 25 cm) lined with two sheets of Whatman 3 MM paper (25 x 30 cm), 50-100 ml of the appropriate solvent was added; the paper was saturated with the same solvent and the tank equilibrated for 0.5 h. Plates were developed twice with

solvent A (ethyl acetate:water:isopropanol; 2:1:2; v:v:v) (63), solvent B (ethyl acetate:water:isopropanol; 40:25:27; v:v:v), solvent C (ethyl acetate:water:n-propanol; 40:30:34; v:v:v), solvent D (ethyl acetate:methanol:acetic acid:water; 2:1:1:1; v:v:v:v), solvent E (acetonitrile:water; 70:30; v:v), solvent F (ethyl acetate:dimethyl sulfoxide:water: isopropanol; 60:40:20:20; v:v:v:v), solvent H (ethyl acetate:water:methanol; 1:2:1; v:v:v) or I (ethyl acetate:water:methanol; 2:1:1; v:v:v). Plates were developed until the solvent front migrated to 0.5 cm from the top of the plate and then dried at 110°C for 5 min between developments. Carbohydrates were stained with potassium dichromate reagent or silver nitrate reagent (64). In some instances, before applying samples silica gel plates were immersed in 0.03 M sodium borate, sodium meta-bisulfite, sodium acetate or 0.2 M sodium phosphate for 5 min and then dried for 1 h at 110°C (65).

Separation of [1-^{3}H]cellooligosaccharides. Aqueous samples (20-30 µl) of [1-^{3}H]cellooligosaccharides were applied to preadsorbent zones of Whatman LK5D silica gel plates. After samples were applied, the plate was dried in an efficient hood with cool, dry air for 45 min. To remove traces of water, the preadsorbent zone was saturated with several drops of acetone and the plates were dried for an additional 15 min. On humid days, plates were dried at room temperature under reduced pressure for an additional 30 min. After the developing tank was lined with two sheets of

Whatman 3 MM paper, 30 ml of solvent G (ethyl acetate: water:methanol; 40:15:20; v:v:v) were added to the tank. Whatman 3 MM paper was saturated with solvent G and the tank equilibrated for 0.5 h. Plates (maximum of 2 per tank) were developed until the solvent front migrated to 0.5 cm from the top of the plate (1.5 h). The plates were removed from the tank and dried in an efficient hood with dry, cool air or under reduced pressure at room temperature for 0.5 h. While the plates were drying, solvent in the tank was replenished. The plates usually were developed 3 times, after which they were dried at 110°C for 5 min. However, when initial rates of enzymic hydrolysis of [1-^{3}H]cellohexaose were to be determined, plates were developed a total of 4 times to assure baseline separation between [1-^{3}H]cellopentaose and [1-^{3}H]cellohexaose. After channels containing radioactive cellooligosaccharides were covered with Whatman 3 MM paper, channels containing cellooligosaccharide standards were stained with p-anisaldehyde reagent (64).

Extraction of a mixture of [1-^{3}H]cellooligosaccharides from thin-layer chromatographic plates. A mixture containing equal amounts of radioactivity of [1-^{3}H]glucose through [1-^{3}H]cellohexaose was applied to Whatman LK5 TLC plates. The plates were dried under an efficient hood for 1 h with dry, cool air or in an oven at 110°C for 15 min. Areas containing radioactive samples were scraped with a single-edged razor blade onto weighing paper and then transferred into 7 ml scintillation vials. The following

procedures for extracting [1-^{3}H]cellooligosaccharides from scrapings were evaluated.

Method A: Water (0.5 ml) was added to vials and then vials were placed in boiling water for 15 min.

Method B: Dimethyl sulfoxide:water (1:1; v:v) (0.5 ml) was added to vials and then vials were placed in boiling water for 15 min.

Method C: Water (0.5 ml) was added to vials and then vials were sonicated for 0.5 h.

Method D: Aquasol (5 ml) and 20 µl of glacial acetic acid were added directly to vials containing scrapings.

Aquasol (5 ml) and 20 µl of glacial acetic acid were added to each sample and the vials were shaken vigorously. Radioactivity was measured using a scintillation counter to 2 percent sigma error or for a maximum of 2 min.

Extraction of individual [1-^{3}H]cellooligosaccharides. Samples (2.5-10 µl) of each [1-^{3}H]cellooligosaccharide containing equal amounts of radioactivity were applied to Whatman LK5D TLC plates and then the plates were dried at 110°C for 0.5 h. Areas containing individual [1-^{3}H]cellooligosaccharides were scraped with a single-edged razor blade onto weighing paper and then transferred to a 7 ml scintillation vial. For Method A, water (0.5 ml) was added to the vial and the vial was then vortexed for 30 s. For Method B, water (1.5 ml) was added to the vial and then the

vial was vortexed for 30 s. For Method C, water (0.5 ml) was added to the vial and then the vial was sonicated for 15 min. After samples were treated as described above, Aquasol (5 ml) and 20 µl of glacial acetic acid were added to the slurry and the vials were shaken vigorously. A gel formed when samples treated according to Method B were shaken. Samples were counted in a scintillation counter to 2 percent sigma error or a maximum of 2 min.

Enzymic Assays

ß-Glucosidase. Aryl-ß-D-glycosidase activity was determined by measuring the release of p-nitrophenol from p-nitrophenyl-D-glycosides after incubation with purified ß-glucosidase (66). Samples were incubated at 40°C for 20 or 30 min in 2.5 ml of 50 mM sodium acetate buffer, pH 5.0, which contained 3 mM sodium azide and 2.4 mM p-nitrophenyl-D-glycosides. The reactions were terminated by immersing the tubes containing the assay mixture in a boiling water bath for 5 min. After the addition of 1.0 ml of 7.5 percent (w/v) potassium phosphate (K_2HPO_4), the absorbance of p-nitrophenol at 400 nm was measured. Specific activity was expressed as µmoles of p-nitrophenol released/min/mg of protein. The absorbance was linear from 5 to 60 µg of p-nitrophenol.

Activity of the ß-glucosidase on ß-linked glucose disaccharides was determined by measuring the production of glucose from sophorose, laminaribiose and gentiobiose. Samples were incubated at 40°C for 30 min in 0.5 ml of

sodium acetate buffer, pH 5.0, which contained 3 mM sodium azide and various concentrations of substrate. The reaction was stopped by immersing tubes containing the assay mixture in a boiling water bath for 5 min. Glucose was measured by a modification of the Statzyme Glucose Reagent method as described by Worthington Biochemical Corporation (67). The absorbance of NADH at 340 nm was measured after the addition of 100 µl of assay mixture to 1.0 ml of Statzyme Glucose Reagent. The absorbance measured was linear from 5 to 50 µg of D-glucose. Specific activity was expressed as µmoles of disaccharide hydrolyzed/min/mg of protein.

Initial rates of hydrolysis of 4-methylumbelliferyl-ß-D-glucopyranoside catalyzed by ß-glucosidase were measured by continuously monitoring the formation of 4-methylumbelliferone. Samples were incubated at 40°C in 1.0 ml of 50 mM sodium acetate buffer, pH 5.0, which contained 3 mM sodium azide and various concentrations of 4-methylumbelliferyl-ß-D-glucopyranoside. The absorbance due to 4-methylumbelliferone at 346 nm was measured continuously as described by Rosenthal and Saifer (68). The absorbance response was linear in the range of 0.05 to 0.50 µmole of 4-methylumbelliferone. Specific activity was expressed as µmoles of 4-methylumbelliferone released/min/mg of protein.

Hydrolysis of labeled cellooligosaccharides. Activities of ß-glucosidase, CBH I(D) and CBH II on [1-^{3}H]cellooligosaccharides were determined by measuring the change in the distribution of radioactive products and substrates

during the time course of reactions. The ß-glucosidase, CBH I(D) or CBH II were incubated at 40°C in 100 µl of 5 mM sodium acetate buffer, pH 5.0, which contained 0.3 mM sodium azide and 0.1-0.5 µCi of [1-^{3}H]cellooligosaccharide. When activities of exoglucanases on [1-^{3}H]cellooligosaccharides and [^{14}C-U]cellooligosaccharides were determined, 0.19-0.22 µCi of [^{14}C-U]cellooligosaccharide were included in the assay mixture. Total concentration of cellooligosaccharide in assay mixtures was adjusted with corresponding unlabeled cellooligosaccharide. The concentration of enzyme in an assay was chosen to give approximately 50 percent degradation of substrate in 30 min. Assay mixtures were contained in 2 ml conical, glass centrifuge tubes. The reaction was stopped at various times by mixing a 10 µl sample of the assay mixture with 10 µl of 2 N HCl. The volume of sample removed from the assay mixture was chosen to give sufficient counts to detect 0.5 percent hydrolysis at a single bond of a labeled cellooligosaccharide. Labeled cellooligosaccharides in samples removed from assay mixtures were separated using thin-layer chromatography as described above. Labeled cellooligosaccharides were extracted routinely from silica gel scrapings by adding 1.5 ml of 2 percent glacial acetic acid and vortexing for 15 s. Aquasol (5 ml) was added and the mixture was shaken vigorously until a gel formed. Radioactivity was measured in a scintillation counter to 2 percent sigma error or a maximum of 5 min.

Kinetic Analysis of Hydrolysis Data

Allen (69) showed that bond cleavage frequencies are best evaluated by plotting product ratios (radioactivity of each product divided by total radioactivity of the sample) vs. extent of reaction (total radioactivity of the products divided by total radioactivity of the sample). Bond cleavage frequencies were determined from the slope of product ratio vs. extent of reaction plots. Subtraction of sample background is unnecessary, because zero-time sample background affects only the intercept of the plot.

Initial rates of hydrolysis of [1-^{3}H]cellooligosaccharides were estimated from the slope of a line through the linear, initial region of time course plots. Time course plots were constructed by plotting the amount of [1-^{3}H]cellooligosaccharides (moles) vs. time (min). The concentration of a [1-^{3}H]cellooligosaccharide was determined by multiplying the product ratio by the initial concentration of substrate. Specific activities were expressed as μmoles of [1-^{3}H]cellooligosaccharide hydrolyzed/min/mg of protein. Sample calculations for determining bond cleavage frequencies and initial rates of hydrolysis are provided in Appendix B.

Determination of Kinetic Constants

Values of K_m, V_{max} and V_{max}/K_m for activity of exoglucanases were estimated from initial rates of hydrolysis using HYPER Fortran program described by Cleland (70). The HYPER program was also used to determine apparent values of

K_m and V_{max} for competitive inhibition plots. The activity of CBH I(D) on [1-^{3}H]cellotriose was analyzed using Program Two/One kindly provided by W.W. Cleland. Kinetic equations used in the analyses are listed in Appendix C.

Evaluation of Subsite Affinities

Subsite affinities of the ß-glucosidase were determined in part from the values of V_{max}/K_m obtained for cleavage of [1-^{3}H]cellotriose through [1-^{3}H]cellohexaose as described by Hiromi et al. (44). Subsite affinities of the ß-glucosidase were also determined using competitive inhibition constants for glucose through cellohexaose as described by Roeser and Legler (71). Subsite affinities of CBH I(D) and CBH II were determined from bond cleavage frequencies, K_m and V_{max} for [1-^{3}H]cellotriose through [1-^{3}H]cellohexaose using the method of Allen and Thoma (48) and the method of Suganuma et al. (45). Dr. J. Allen kindly provided a copy of the depolymerase computer model and sample input/output data. A brief description of each method is provided in Appendix A.

CHAPTER 3
PREPARATION OF [1-^{3}H]CELLOOLIGOSACCHARIDES AND [^{14}C-U]CELLOOLIGOSACCHARIDES

Introduction

Cellooligosaccharides have been used as substrates to investigate the mode of action and to estimate steady state kinetic parameters of cellulolytic enzymes (5,29). However, some glycosidic bonds of cellooligosaccharides that are susceptible to attack cannot be identified precisely, because identical products are formed from hydrolysis at different glycosidic bonds. Furthermore, low sensitivity of high performance liquid chromatographic analysis (HPLC) of cellooligosaccharides limits the substrate concentration at which initial rates of enzymic reactions can be measured. To overcome these limitations, cellooligosaccharides which are asymmetrically and radioactively labeled are required.

Although the enzymic methods for synthesizing oligosaccharides radioactively labeled at either the reducing or nonreducing end have been reported (42,72-74), similar methods have not been developed for synthesizing end-labeled cellooligosaccharides. Carbohydrates can be labeled chemically with tritium at carbon one of the reducing end glucosyl residue by catalytic exchange of unlabeled compounds in the presence of tritium gas and $PdO/BaSO_4$ catalyst (75). Alternatively, carbon one-labeled aldoses can be prepared by

the reduction of aldonolactones with sodium boro[^{3}H]hydride (76) or lithium boro[^{3}H]hydride (77) in weakly acidic solutions. The formation of alditols is prevented under these conditions, because the hydroxyl group at carbon one in its hemiacetal form is not readily displaced by hydride (78). The reduction of aldonolactones with sodium amalgam in tritiated water resulted in lower yields of products than reduction with lithium boro[^{3}H]hydride (77). A practical synthesis of cellooligosaccharides based on the Koenigs-Knor type of reaction has recently been reported by Takeo et al. (79) and may be adapted to the synthesis of nonreducing end-labeled cellooligosaccharides.

Although catalytic exchange is a straightforward, rapid method and affords products with high specific radioactivities, the necessity of using large amounts of tritium gas (10 Ci per reaction) makes this procedure potentially more hazardous and less economical than reduction of lactones with sodium boro[^{3}H]hydride. The synthesis of lactones of cellooligosaccharides is a prerequisite for their subsequent reduction with sodium boro[^{3}H]hydride. However, these lactones may serve as inhibitors in mechanistic studies of cellulolytic enzymes. The synthesis of reducing end-labeled cellooligosaccharides using sodium boro[^{3}H]hydride and the preparation of [^{14}C-U]cellooligosaccharides from [^{14}C-U]cellulose are described in this report.

Results and Discussion

A flowchart of the synthesis of [1-^{3}H]cellooligosaccharides is shown in Fig. 3-1. Purified cellooligosaccharides, which were prepared from acid hydrolysis of cellulose, were oxidized specifically at carbon 1 of the reducing glucosyl residue with mild bromine oxidation. The resulting aldonic acids of cellooligosaccharides were converted to calcium salts with calcium carbonate and then purified using Bio-Gel P-2 chromatography. Calcium salts of cellooligosaccharide aldonic acids facilitated purification of oxidized products and subsequent lactonization. Cellooligosaccharide lactones were formed from the corresponding calcium salts by first removing calcium with anion exchange resin and then shifting the equilibrium from acid to lactone by removing water. After sodium boro[^{3}H]hydride was used to reduce cellooligosaccharide lactones specifically at carbon 1, [1-^{3}H]cellooligosaccharides were purified using Bio-Gel P-2 chromatography.

Preparation of Cellooligosaccharides

Cellooligosaccharides used in synthesis of [1-^{3}H]cellooligosaccharides and in enzymic assays as substrates or inhibitors were generated from cellulose by acid hydrolysis. Soluble cellooligosaccharides were separated on a Bio-Gel P-2 column as shown in Fig. 3-2. Cellotriose through cellohexaose were rechromatographed on the same column until they were >99 percent pure as determined by reverse-phase

Figure 3-1 Synthesis of [1-^{3}H]cellooligosaccharides

In this scheme, purified cellooligosaccharides are oxidized at carbon 1 of the reducing end glycosyl residue with bromine. The resulting cellooligosaccharide aldonic acids are converted to calcium salts, which are then separated from unoxidized cellooligosaccharides using Bio-Gel P-2 chromatography. After calcium is removed from purified calcium salts of cellooligosaccharide aldonic acids using cation exchange resin, lactones of cellooligosaccharides are formed by evaporating water from a solution containing cellooligosaccharide aldonic acids and 2-methoxyethanol (or dimethylsulfoxide). Reduction of lactones of cellooligosaccharide aldonic acids with sodium boro[^{2}H]hydride in the presence of CO_2 yields [1-^{3}H]cellooligosaccharides.

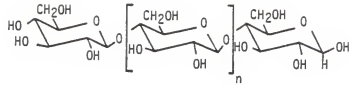

1. Br_2, $CdCO_3$, H_2O
2. $AgCO_3$
3. H_2S

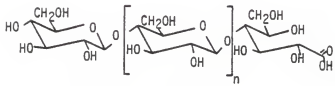

$\frac{1}{2}CaCO_3$

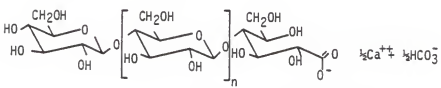

2-methoxyethanol, toluene

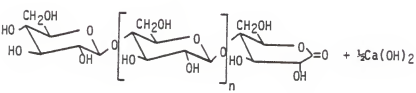

1. NaB^3H_4
2. H_2O

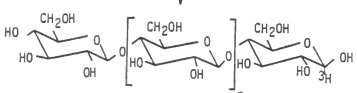

Figure 3-2 Elution pattern from Bio-Gel P-2 column chromatography of cellooligosaccharides generated from acid hydrolysis of cellulose

Cellooligosaccharides were eluted with water from a Bio-Gel P-2 (200-400 mesh) column (4.4x115 cm). Carbohydrate in column effluents was measured using the phenol-sulfuric acid method of Dubois (50). Peaks represent from right to left glucose, cellobiose, cellotriose, cellotetraose, cellopentaose, and cellohexaose. Each fraction contained 6.8 ml.

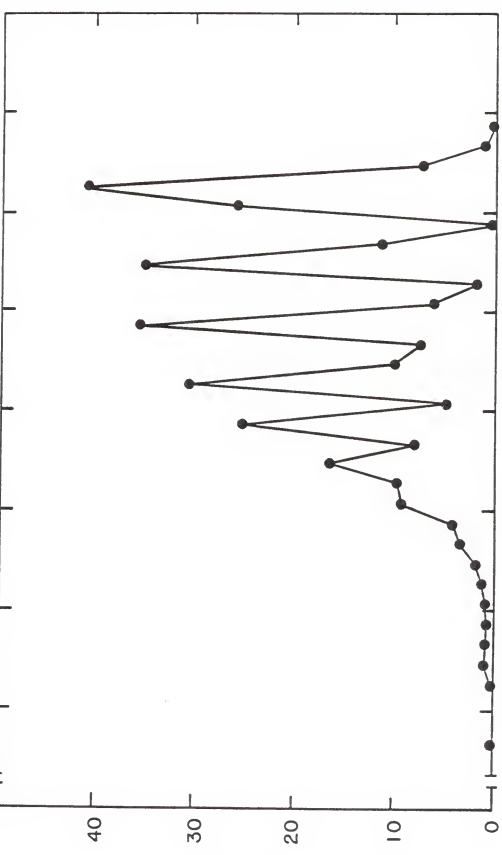
GLUCOSE (μMOL / FRACTION)
0
10
20
30
40
0
80
100
120
140
160
180
200
FRACTION

HPLC. Cellooligosaccharides of chain length greater than 6 precipitated from solution.

Preparation of cellooligosaccharides using Bio-Gel P-2 chromatography avoids the disadvantages of slow flow rates and necessity of repacking columns associated with the charcoal-Celite column method described by Miller et al. (56). Bio-Gel P-2 chromatography has also been used to prepare maltooligosaccharides as described by John et al. (80). Hsu et al. (29) prepared cellotriose and cellotetraose using a Bio-Gel P-2 (-400 mesh) column (1.5 x 200 cm).

Oxidation of Cellooligosaccharides

The results of oxidizing purified cellobiose through cellohexaose with bromine using a modification of the method of Diehl et al. (57) are presented in Table 3-1. Although on a weight basis, oxidation yielded greater than 100 percent of crude calcium cellooligosaccharide aldonic acids, reducing sugar assay indicated that yields ranged from 79-95 percent. The general decrease in yield as chain length increases may have resulted from the corresponding decrease in concentration of groups available for oxidation.

Diehl et al. (57) isolated cellobiono-1,5-lactone in 54 percent yield (weight) from oxidation of cellobiose, whereas cellobiose was oxidized in 93 percent yield using the method described in this report. At different steps in the synthesis, Diehl et al. (57) filtered the reaction mixture through a bed of decolorizing carbon overlaid with Celite. When the method of Diehl et al. (57) was modified by using

Table 3-1

Oxidation of Cellooligosaccharides

Cellooligosaccharides were oxidized with bromine using a modification of a method described by Diehl et al. (57). Oxidized cellooligosaccharides were converted to their calcium salts with calcium carbonate.

Oligo-saccharide	Weight of Cellooligosaccharide (g)	Weight of Crude Calcium Salt (g)	% Yield[a]
Cellobiose	0.50	0.56	93
Cellotriose	0.45	0.49	95
Cellotetraose	0.50	0.54	93
Cellopentaose	0.50	0.52	90
Cellohexaose	0.36	0.44	79

[a] Yields were determined by measuring loss of reducing sugar.

only Celite as a filtering aid, cellobiose was oxidized in 93 percent yield. The affinity of cellooligosaccharides for charcoal has been used as the basis for separating cello-oligosaccharides on charcoal-Celite columns (56).

Cellobiose was also oxidized using Adam's platinum oxide catalyst as described by Conchie et al. (59). However, the resulting product was reduced with sodium borohydride in 12 percent yield. Since higher yields of reducible products were obtained from oxidation with bromine, oxidation in the presence of Adam's catalyst was not used to oxidize cellooligosaccharides.

Unoxidized cellooligosaccharides significantly reduce the specific radioactivity of [1-^{3}H]cellooligosaccharides, if they are not removed before cellooligosaccharide lactones are reacted with sodium boro[^{3}H]hydride. Since oxidized cellooligosaccharides contained 5-21 percent of contaminating cellooligosaccharides, oxidized cellooligosaccharides were converted to their calcium salts and separated using Bio-Gel P-2 chromatography. The separation of calcium salts of cellooligosaccharide aldonic acids from cellooligosaccharides was more reproducible than that of the corresponding aldonic acids. Although cellooligosaccharide aldonic acids and calcium salts eluted before cellooligosaccharides, cellooligosaccharide aldonic acids eluted as 2 peaks. The relative size of the peaks may represent the equilibrium between the aldonic acid and aldonolactone. Occasionally, cellooligosaccharide aldonic acids appeared to adhere to the

column matrix necessitating repacking the column. Thus, oxidized cellooligosaccharides were purified from cello-oligosaccharides as their calcium salts. Furthermore, cellooligosaccharide lactones obtained from calcium salts of cellooligosaccharide aldonic acids were reduced with sodium borohydride in higher yields than cellooligosaccharide lactones obtained directly from aldonic acids as described below.

Lactonization of Cellooligosaccharide Aldonic Acids

The method of Diehl et al. (57) affords cellobiono-1,5-lactone directly from oxidation of cellobiose. In preliminary experiments, cellobiono-1,5-lactone prepared using the method of Diehl et al. (57) was reduced with sodium borohydride in <25 percent yield. However, commercially available glucono-1,5-lactone was reduced in >80 percent yield suggesting that cellobiono-1,5-lactone synthesized using the method of Diehl et al. (57) may contain significant amounts of cellobionic acid.

Isbell and Frush (60) reported the lactonization of calcium lactobionate in 87 percent yield. Cellobiono-1,5-lactone prepared from calcium cellobionate using the method of Isbell and Frush (60) was reduced with sodium borohydride in >80 percent yield. Thus, cellooligosaccharide aldonic acids were converted to corresponding calcium salts and then lactonized using the method of Isbell and Frush (60).

The results of converting purified calcium salts of cellooligosaccharide aldonic acids to corresponding lactones

are presented in Table 3-2. The yields of cellooligosaccharide lactones are comparable to those obtained for glucono-1,5-lactone and lactobionolactone reported by Isbell and Frush (60). The low yield of cellobiono-1,5-lactone may be due to its higher solubility in 2-methoxyethanol. Samples of cellobiono-1,5-lactone and cellopentano-1,5-lactone were reduced with sodium borohydride to cellobiose and cellopentaose, respectively, in >50 percent yield.

When calcium salts of cellotetranoic acid, cellopentanoic acid or cellohexanoic acid were lactonized in the presence of 2-methoxyethanol, the resulting lactones were reduced with sodium boro[^{3}H]hydride in <0.1 percent yield of radioactivity. Furthermore, products of the lactonization precipitated from 2-methoxyethanol before water was completely removed suggesting that aldonic acids formed instead of aldonolactones. Isolated products were slightly soluble in water. However, when 2-methoxyethanol was substituted with dimethyl sulfoxide, lactones, which were very soluble in water and were reduced with sodium borohydride in >50 percent yield of carbohydrate, were obtained.

Calcium salts of cellooligosaccharides served as an aid to purify oxidized cellooligosaccharides from contaminating cellooligosaccharides using Bio-Gel P-2 chromatography. Precipitation of these calcium salts with 2-methoxyethanol may be omitted and lactones may be obtained directly after removal of calcium by anion exchange resin.

Table 3-2

Lactonization of Calcium Salts of Cellooligosaccharide Aldonic Acids

Calcium salts of cellooligosaccharide aldonic acids were converted to their corresponding lactones, after removal of calcium by anion exchange resin and removal of water using a rotary evaporator as described in Experimental Procedures.

Calcium Salt	Weight of Calcium Salt (g)	Weight of Cellooligo-saccharide Lactone (g)	% Yield[a]
Calcium Cellobionate	1.0	0.54	60
Calcium Cellotrionate	0.36	0.33	98
Calcium Cellotetranate	0.017	0.015	94
Calcium Cellopentanate	0.016	0.013	90
Calcium Cellohexanate	0.020	0.017	89

[a] Yields are based on the measured weights of lactones and calcium salts assuming anhydrous molecular weights.

The identification of synthesized products as calcium salts of cellooligosaccharide aldonic acids and corresponding 1,5-lactones is supported by characteristic infrared bands for C-O asymmetric stretch of CO_2^- carboxylate and C=O stretch of 1,5-lactone groups listed in Table 3-3. Whereas 1,5-lactones have characteristic C=O stretch at 1760-1725 cm^{-1}, 1,4-lactones have characteristic C=O stretch at 1790-1765 cm^{-1} (81). The formation of 1,4-lactones is unlikely, because oxygen of carbon 4 contributes to the glycosidic bond of the next residue.

Reduction of Lactones of Cellooligosaccharide Aldonic Acids with Sodium Boro[^{3}H]hydride

Procedures for reduction of aldonolactones in the presence of cation exchange resin, boric acid, carbon dioxide, sodium acid oxalate or dilute H_2SO_4 were evaluated on the basis of yields and stability of pH of the solution during the reaction. Although lactobionolactone or cellobiono-1,5-lactone prepared by the method of Diehl et al. (57) was reduced in the presence of each of the above buffering systems to the corresponding sugar in 15-25 percent yield, carbon dioxide and sodium acid oxalate provided more stable pH's. The results of reduction of cellooligosaccharide lactones in the presence of carbon dioxide or sodium acid oxalate with sodium boro[^{3}H]hydride are described below.

The results of reducing cellooligosaccharide lactones in the presence of carbon dioxide with sodium

Table 3-3

Major Infrared Bands of Calcium Salts of Cellooligosaccharide Aldonic Acids and Cellooligosaccharides Lactones

Cellooligosaccharide	Wavenumber (cm^{-1})
	C-O Asymmetric Stretch of CO_2^- Carboxylate[a]
Calcium Cellobionate	1557
Calcium Cellotrionate	1565
Calcium Cellotetranate	1585
Calcium Cellopentanate	1590
Calcium Cellohexanate	1598
	C=O Stretch of 1,5-Lactone[a]
Cellobiono-1,5-lactone	1719
Cellotriono-1,5-lactone	1720
Cellotetrano-1,5-lactone	1722
Cellopentano-1,5-lactone	1728
Cellohexano-1,5-lactone	1736

[a] Assignments were based on characteristic infrared bands shown by various carboxylate and 1,5-lactone groups reported by Tipson and Parker (81).

Table 3-4

Reduction of Cellooligosaccharide Lactones with Sodium Boro[^{3}H]hydride

Cellooligosaccharide lactones were dissolved in water while the hydrogen ion concentration was maintained at pH 6-7 with a continuous stream of CO_2. Sodium boro[^{3}H]hydride was added dropwise during a 15 min period and then tritiated water was removed using a rotary evaporator. [1-^{3}H]Cellooligosaccharides were purified using Bio-Gel P-2 chromatography.

Lactone	Weight of Lactone (g)	Sodium Boro[^{3}H]hyride (mCi)	[1-^{3}H]Cello-oligosaccharide (mCi)	Specific Radioactivity (Ci/mole)	% Yield of Radio-activity
Glucono-1,5-lactone[a]	0.10	5	0.580	1.33[b]	12
Cellobiono-1,5-lactone[a]	0.10	5	0.47	2.50[b]	9.5
Cellotriono-1,5-lactone	0.10	10	0.46	3700[c]	4.6
Cellotetrano-1,5-lactone	0.010	5	0.068	3750[c]	1.4
Cellopentano-1,5-lactone	0.10	17.4	5.1	2707[c]	29
Cellohexano-1,5-lactone	0.077	7.6	1.2	3109[c]	16

[a] Sodium borohydride was also added to reductions.
[b] Carbohydrate determined using method of Dubois et al. (50).
[c] Carbohydrate determined using Bio-Gel P-2 HPLC.

boro[^{3}H]hydride at pH 6-7 are shown in Table 3-4. Highly radioactive cellooligosaccharides (2707-3750 Ci/mole) were obtained in sufficient quantities for enzymic analysis of cellulases. The specific radioactivities of [1-^{3}H]glucose and [1-^{3}H]cellobiose are lower than those of [1-^{3}H]cellotriose through [1-^{3}H]cellohexaose, because after the addition of sodium boro[^{3}H]hydride more lactone was converted to sugar with sodium borohydride. Two factors may have contributed to the low yield of [1-^{3}H]cellotetraose: (1) 10-fold less carbohydrate was present initially, although on a weight basis the concentration was similar to the other reductions and (2) the pH was lower, approximately 6. Preliminary experiments indicated that using 100 mg of lactone significantly improves yields of incorporation of tritium. The yields of [1-^{3}H]cellopentaose and [1-^{3}H]cellohexaose are higher, because the pH of the reaction mixtures was approximately 7. The initial concentration of sodium hydroxide was 0.017 M during the synthesis of [1-^{3}H]cellopentaose and [1-^{3}H]cellohexaose. This seemed to stabilize the pH during the addition of sodium boro[^{3}H]hydride which is stored in 0.1-0.3 M sodium hydroxide.

The initial pH of the reaction mixture strongly influences the reduction of aldonolactones with sodium boro-[^{3}H]hydride. At alkaline pH's, lactones hydrolyze to aldonic acids (60), whereas at acidic pH's sodium boro[^{3}H]hydride hydrolyzes. In addition, lactones are more readily converted to alditols at alkaline pH's. Thus, the

pH must be sufficiently high to stabilize sodium boro[^{3}H]hydride, but sufficiently low to prevent hydrolysis of lactones and formation of alditols.

Specific radioactivities of [1-^{3}H]cellotetraose through [1-^{3}H]cellohexaose are comparable to those obtained for [1-^{3}H]glucose (3900 mCi/mmol) and [1-^{3}H]lactose (3000 mCi/mmol) using PdO/$BaSO_4$ catalyst as described by Evans et al. (75). Specific radioactivities of [1-^{3}H]cellooligosaccharides are 10-fold higher than those reported by Biely et al. (82) for [1-^{3}H]xylooligosaccharides. Biely et al. (82) used PdO/$BaSO_4$ catalyst and tritium gas to label xylooligosaccharides.

Reduction of glucono-1,5-lactone in the presence of sodium acid oxalate with sodium boro[^{3}H]hydride produced [^{3}H]glucose in 0.65 percent yield. Since the initial pH of the solution was 3.8, sodium boro[^{3}H]hydride may have hydrolyzed before reacting with glucono-1,5-lactone. Although Frush and Isbell (61) reduced aldonolactones to aldoses in >95 percent yield with excess sodium borohydride, the initial pH of the reaction is not suited for reductions with sodium boro[^{3}H]hydride.

Purity and Stability of [1-^{3}H]Cellooligosaccharides

The [1-^{3}H]cellooligosaccharides were purified on a Bio-Gel P-2 column (4.4 x 115 cm) and using Bio-Gel P-2 HPLC. The [1-^{3}H]cellooligosaccharides were shown to be >99 percent pure using thin-layer chromatography, reverse-phase HPLC and Bio-Gel P-2 HPLC. Alditols of

cellooligosaccharides were not detected by refractive index or scintillation counting. Reducing end-labeled cellooligosaccharides of specific radioactivity >250 Ci/mole were stored in 10 percent ethanol at -70°C. Reducing end-labeled cellohexaose (3109 Ci/mole) is extremely labile and produced several decomposition products (approximately 80 percent of total radioactivity) after 24 h in 10 percent ethanol at 4°C. Reducing end-labeled cellooligosaccharides of specific radioactivity <250 Ci/mole were stored in aqueous solution at -30°C.

Specificity of Radiolabeling

To confirm that tritium was incorporated at carbon 1 of [^{3}H]cellooligosaccharides, 0.28 μCi of [^{3}H]cellotriose was oxidized with an excess of bromine for 24 h. After removal of tritiated water using a rotary evaporator, 92 percent of the initial radioactivity was accounted for, of which 99.1 percent was in tritiated water and 0.9 percent was in residue of oxidized products. Thus, 99.1 percent of recovered tritium was located at carbon 1.

Although catalytic tritiation yields sugars specifically labeled at carbon 1 (>98 percent) (75), reduction of lactones with lithium boro[^{3}H]hydride in some cases yields significant quantities of labeled alditols (77).

Preparation of [^{14}C-U]Cellooligosaccharides

Batch method. The [^{14}C-U]cellooligosaccharides, which were used in conjunction with [1-^{3}H]cellooligosaccharides to investigate the action patterns of cellulolytic enzymes,

were generated from [^{14}C-U]cellulose during hydrolysis with concentrated HCl. The distribution of [^{14}C-U]cellooligosaccharides resulting from acid hydrolysis of [^{14}C-U]cellulose using the batch method and subsequent separation using Bio-Gel P-2 chromatography is shown in Table 3-5. Hydrolysis yielded 39 percent soluble cellooligosaccharides ranging from [^{14}C-U]glucose to [^{14}C-U]celloheptaose. Preliminary experiments, in which the hydrolysis time was varied from 1 to 21.5 h, indicated that the greatest proportion of [^{14}C-U]cellopentaose and [^{14}C-U]cellohexaose was obtained after 3 h of hydrolysis. Labeled [^{14}C-U]cellopentaose and [^{14}C-U]cellohexaose are the most useful for double-label experiments with corresponding [1-^{3}H]cellooligosaccharides. Labeled [^{14}C-U]cellotriose through [^{14}C-U]cellohexaose were purified using Bio-Gel P-2 HPLC until each eluted as a single symmetric peak of radioactivity. Purified [^{14}C-U]cellooligosaccharides were stored safely in aqueous solution at -30°C.

Column method. To promote formation of [^{14}C-U]cellooligosaccharides of chain length 4-6, [^{14}C-U]cellulose was hydrolyzed by pouring concentrated HCl through a column containing a mixture of glass beads and [^{14}C-U]cellulose. The eluant was collected in a flask containing a saturated solution of sodium bicarbonate. Hydrolysis yielded 24 percent soluble cellooligosaccharides, of which predominantly [^{14}C-U]cellopentaose (36 percent) and [^{14}C-U]cellotriose (12 percent) were obtained. The column method did not provide

Table 3-5

Preparation of [^{14}C-U]Cellooligosaccharides

[^{14}C-U]Cellulose (750 μCi) was hydrolyzed with 3 ml of concentrated HCl for 3 h. Soluble [^{14}C-U]cellooligosaccharides were separated on a Bio-Gel P-2 column (4.4x115 cm).

[^{14}C-U]Cello-oligosaccharide	Radioactivity (μCi)		Percent of Recovered Cellooligosaccharides
Glucose	100		34
Cellobiose	52		18
Cellotriose	40		14
Cellotetraose	52		18
Cellopentaose	22		7.6
Cellohexaose	18		6.0
Celloheptaose	11		3.6
	295	(39% of initial [^{14}C-U]cellulose hydrolyzed)	

[^{14}C-U]cellooligosaccharides of chain length 4-6 in high yield.

Conclusions

Several [^{3}H]cellooligosaccharides have been synthesized by sodium boro[^{3}H]hydride reduction of cellooligosaccharide lactones. The [^{3}H]cellooligosaccharides were shown to be specifically labeled at carbon 1 of the reducing end glucosyl residue. The specific radioactivities of [1-^{3}H]cellooligosaccharides are sufficiently high to measure initial rates of hydrolysis of cellulolytic enzymes at micromolar substrate concentrations. Purified [^{14}C-U]cello-oligosaccharides have also been prepared and can be used in conjunction with [1-^{3}H]cellooligosaccharides to study the action patterns of cellulolytic enzymes.

CHAPTER 4
SEPARATION OF [1-^{3}H]CELLOOLIGOSACCHARIDES BY THIN-LAYER CHROMATOGRAPHY

Introduction

Soluble cellooligosaccharides have been used to investigate kinetics and action patterns of cellulolytic enzymes (5,14,29) and have been separated using high performance liquid chromatography (HPLC)(55,83-85), paper chromatography (PC)(20), and thin-layer chromatography (TLC)(19,63,86). Sensitivity afforded by HPLC detection methods limits substrate concentrations at which cellulolytic enzymes may be assayed to values greater than 1 mM. Furthermore, long elution times for cellooligosaccharides makes HPLC impractical for processing large numbers of samples. Previously reported TLC techniques provide limited resolution and quantitation of cellooligosaccharides has not been demonstrated.

The synthesis of [1-^{3}H]cellooligosaccharides of high specific radioactivity affords a detection sensitivity not previously possible with cellooligosaccharides. A TLC technique which is quantitative, reliable and provides excellent resolution of cellooligosaccharides is required to take advantage of this sensitivity in analyzing enzymic digests of low concentrations of cellooligosaccharides.

A compilation of methods for separating cellooligosaccharides using HPLC has been reported recently (87). Ladisch and Tsao (83) separated glucose through cellohexaose using an Aminex 50W-X4 (Ca^{2+}) column; however, elution times exceeded 25 min. Although Vratny et al. (84) reported the separation of glucose through cellohexaose, glucose through cellotriose were resolved poorly. The method of Chen and McGinnis (85) requires that cellooligosaccharides be converted to oximes before separation on silica gel columns containing polar-bonded alkylamino groups. Excellent resolution was reported by Gum and Brown (55) using a Whatman PXS-1025 PAC column; however, elution times exceeded 25 min for baseline separation.

Kanda et al. (20) separated cellooligosaccharides on Whatman No. 1 paper using 1-butanol:pyridine:water (6:4:3, v/v) solvent. Although glucose through cellotriose were well separated, cellotetraose through cellohexaose comigrated even after 100 h of development.

Cellooligosaccharides have been separated using thin-layer chromatography on Kieselgel G or Kieselguhr G adsorbents with ethyl acetate:water:isopropanol solvents. Saif-ur-Rahman et al. (63) separated glucose through cellohexaose on Kieselgel G plates (20x60 cm) using ethyl acetate:water:isopropanol (2:1:2, v/v) solvent. The disadvantages of this method are the commercial unavailability of such plates and the limited resolution of cellopentaose and cellohexaose. Brown and Andersson (86) separated

cellooligosaccharides on Kieselguhr G plates (20x20 cm) buffered with 0.02 M sodium acetate using 65 percent aqueous isopropanol:ethyl acetate (1:1). Although R_F values for individual sugars indicated good separation, quality of resolution of mixtures was not reported. The ß-glucosidase from T. koningii was assayed using cellooligosaccharides as substrates; the products then were separated on Kieselgel G using 2 ascents of ethyl acetate:isopropanol:water (18:13:9; v:v:v)(19). The quality of the separation was not reported. None of the above methods reviewed have been shown to permit quantitative recovery of the compounds.

Here is reported a TLC method for the separation with high resolution and the quantitative extraction of [1-^{3}H]cellooligosaccharides from silica gel. The silica gel plates employed are readily available commercially and separation of carbohydrates is similar to that on Kieselgel G or Kieselguhr G (65) without the requirements for impregnation with salts. This method facilitated the study of kinetics and action patterns of cellulolytic enzymes.

Results and Discussion

Separation of [1-^{3}H]Cellooligosaccharides

Silica gel, cellulose and polyamide adsorbents were evaluated for their ability to separate cellooligosaccharides with a variety of solvents and impregnants (Table 4-1). Glucose through cellopentaose were separated well on silica gel with solvent A; however, cellopentaose and cellohexaose were poorly separated. Although Saif-ur-Rahman et

Table 4-1

Resolution of Cellooligosaccharides With Different Adsorbents, Impregnants and Solvents

Adsorbent	Impregnant[a]	Solvent[b]	Develop-ments	Resolution
IB2	none	A	2	G1-G5 fair;G6 poor
Cellulose	none	H	2	G1-G2 poor;G2-G5 fair;G5-G6 poor
IB2	none	H	2	G1-G6 poor
Polyamide	none	A	2	G1-G6 poor
IB2	none	E	1	G1-G3 fair;G4-G6 poor
IB2	none	F	1	G1-G6 fair (DMSO good solvent)
IB2	borate	A	2	G1-G3 fair;G4-G6 poor
IB2	borate	D	2	G1-G4 good;G5-G6 poor
IB2	metabisulfite	A	2	G1-G3 excellent; G4-G6 poor
IB2	metabisulfite	D	2	G1-G4 good;G5-G6 poor
IB2	acetate	A	2	G1-G4 fair;G5-G6 poor
IB2	acetate	D	2	G1-G5 good;G5-G6 fair
LK5	phosphate	A	3	G1-G4 good;G5-G6 poor
LK5	none	B	3	G1-G5 good;G5-G6 poor
LK5D	none	B	6	G1-G5 good;G5-G6 fair
LK5	none	C	3	G1-G5 good;G5-G6 poor
LK5/LK5D	none	G	3	G1-G6 excellent
K5	none	I	3	G1-G4 excellent; G5-G6 poor
K6	none	I	3	G1-G4 excellent; G5-G6 poor

[a] Impregnants were 0.03 M sodium borate, sodium metabisulfite, sodium acetate or 0.2 M sodium phosphate.

[b] Solvent compositions were A (ethyl acetate:water:isopropanol; 2:1:2), B (ethyl acetate:water:isopropanol; 40:25:27), C (ethyl acetate:water:n-propanol; 40:30:34), D (ethyl acetate:methanol: acetic acid:water; 2:1:1:1), E (acetonitrile:water; 70:30), F (ethyl acetate:dimethyl sulfoxide:water:isopropanol; 60:40:20:20), G (ethyl acetate:water:methanol; 40:15:20) or H (ethyl acetate:water:methanol; 1:2:1), or I (ethyl acetate:water:methanol; 2:1:1).

al. (63) reported good separation of cellooligosaccharides using solvent A, we observed negligible migration of cellohexaose. Separation of cellooligosaccharides on cellulose TLC plates was fair; however, migration of cellohexaose was negligible. Furthermore, the cellulose adsorbent easily flaked, thereby eliminating this adsorbant for use with radioactive cellooligosaccharides. Polyamide adsorbent poorly separated cellooligosaccharides.

Separation of sugars on silica gel is improved by impregnating silica gel with inorganic salts, such as bisulfite, boric acid, mono- and dibasic phosphate and sodium acetate (65). Although impregnating silica gel with salts typically improved resolution of glucose through cellopentaose, cellopentaose and cellohexaose were poorly resolved. Sodium acetate and sodium metabisulfite increased resolution more than did boric acid and sodium phosphate. The use of impregnants, especially boric acid, lowered R_F values for cellooligosaccharides.

Isopropanol, n-propanol, methanol and dimethyl sulfoxide each characteristically influenced the migration of cellooligosaccharides. Isopropanol and n-propanol typically separated glucose through cellotetraose with excellent resolution, whereas longer cellooligosaccharides were poorly separated. Dimethyl sulfoxide served as an excellent solvent for cellooligosaccharides, yielding high R_F values with decreasing resolution of longer cellooligosaccharides. Methanol also yielded high R_F values; however,

resolution between adjacent cellooligosaccharides was similar regardless of chain length. Concentrations of methanol higher than those in solvent G increased the spreading of bands. Lower concentrations of methanol increased the sharpness of bands, but decreased the difference between R_F values.

Although Baker-flex IB2 silica gel plates were used to evaluate most solvents and impregnants, Whatman K5 and K6 series plates provided higher resolution of cellooligosaccharides. The LK5D series is especially suited for separation of [1-^{3}H]cellooligosaccharides, because (1) plates contain a preadsorbent zone which increases resolution, (2) preadsorbent zone allows addition of up to 50 µl of sample, (3) prechanneled plates prevent contamination of samples and (4) 150 Å pore size provides excellent separation of polar compounds.

The best separation of cellooligosaccharides was obtained using Whatman LK5D silica gel plates with three ascents of solvent G and is shown in Fig. 4-1. The ability of preadsorbent zone to focus cellooligosaccharides is reflected in the sharpness of the bands. Similarly, [1-^{3}H]glucose and through [1-^{3}H]cellohexaose were separated with high resolution as shown by the distribution of radioactivity in Fig. 4-2. The R_F values are listed in Table 4-2.

Preliminary experiments indicated that approximately 5-10 percent of [1-^{3}H]cellooligosaccharides adsorbed

Figure 4-1 Thin-layer chromatographic pattern of cello-oligosaccharides

Cellooligosaccharides were separated on Whatman LK5D TLC plates using 3 ascents of solvent G (ethyl acetate:water:methanol; 40:15:20; v:v:v). The TLC plate was stained for carbohydrate using p-anisaldehyde reagent as described in Experimental Procedures. Lanes, from left to right, contain 1 µg of glucose, cellobiose, cellotriose, cellotetraose, cellopentaose, cellohexaose and a mixture of glucose-cellohexaose (1 µg each).

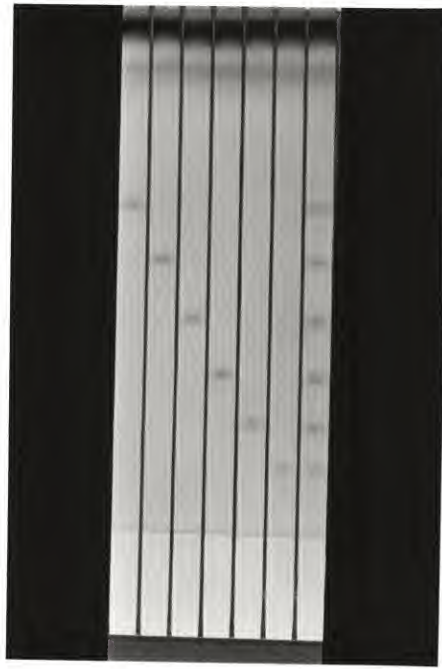

Figure 4-2 Thin-layer chromatographic pattern of [1-^{3}H]cellooligosaccharides

Reducing end-labeled cellooligosaccharides were separated on Whatman LK5D TLC plates using 3 ascents of solvent G (ethyl acetate:water: methanol; 40:15:20; v:v:v). The lane was divided into 2 mm zones from which [1-^{3}H]cellooligosaccharides were eluted and quantitated by scintillation counting as described in Experimental Procedures. The mixture applied contained 8300 dpm of each [1-^{3}H]cellooligosaccharide. The peaks represent, from left to right, [1-^{3}H]cellohexaose, [1-^{3}H]cellopentaose, [1-^{3}H]cellotetraose, [1-^{3}H]cellotriose, [1-^{3}H]cellobiose and [1-^{3}H]glucose. The arrow represents the end of the preadsorbent zone.

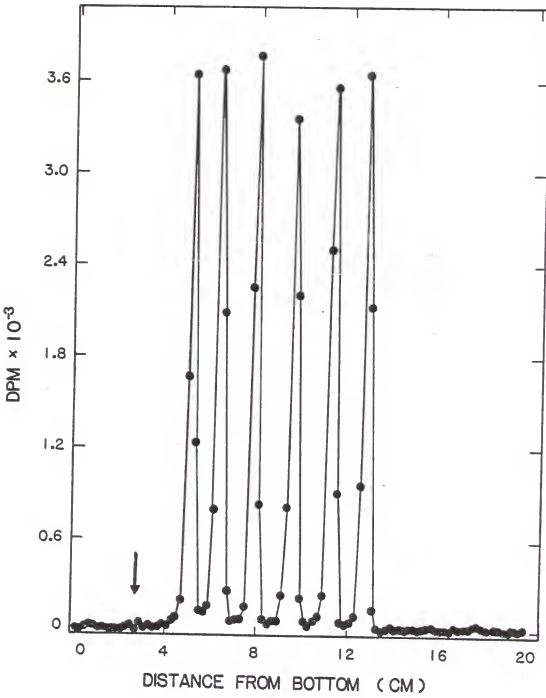
3.6
3.0
2.4
1.8
1.2
0.6
0
DPM x 10-3
0
4
8
12
16
20
DISTANCE FROM BOTTOM (CM)

Table 4-2

Values of the Migration Parameter, R_F

[1-^{3}H]Cellooligosaccharides were separated using Whatman LK5D TLC plates with 3 developments in solvent G (ethyl acetate:water:methanol; 40:15:20; v:v:v).

[1-^{3}H]Cellooligosaccharide	R_F[a]
Glucose	0.59
Cellobiose	0.50
Cellotriose	0.39
Cellotetraose	0.30
Cellopentaose	0.20
Cellohexaose	0.13

[a] R_F values were based on distance migrated by cellooligosaccharides and solvent from top of preadsorbent zone.

irreversibly, when plates were dried at 110°C after application [1-^{3}H]cellooligosaccharides. To avoid irreversible adsorption at the origin or at intermediate positions of migration, plates must be dried at room temperature instead of at 110°C.

Extraction of [1-^{3}H]Cellooligosaccharides

Four methods of extracting a mixture containing equal amounts of radioactivity of [1-^{3}H]glucose through [1-^{3}H]cellohexaose from Whatman LK5 TLC plates were evaluated and the results are shown in Table 4-3. When plates were dried at room temperature before extraction, cellooligosaccharides were recovered 10-14 percent more efficiently than when plates were dried at 110°C. Extracting cellooligosaccharides before adding Aquasol improved recoveries by 42-45 percent with plates dried at room temperature and 32-37 percent with plates dried at 110°C. Percent recovery of cellooligosaccharides was approximately equal for each extraction procedure, when plates were dried at room temperature. However, extraction using dimethyl sulfoxide:water solvent yielded slightly lower recoveries than other extraction procedures when plates were dried at 110°C.

Low recoveries of radioactivity from silica gel suspended in Aquasol may result from physical quenching elicited by silica gel. Aqueous solvents may serve to desorb cellooligosaccharides and disperse silica gel, thereby promoting contact of [1-^{3}H]cellooligosaccharides with

Table 4-3

Extraction of a Mixture of [1-^{3}H]Cellooligosaccharides From Thin-layer Chromatographic Plates

A mixture containing equal amounts of radioactivity of [1-^{3}H]glucose through [1-^{3}H]cellohexaose was applied to Whatman LK5 TLC plates. After drying the plates at room temperature for 1 h or at 110°C for 15 min, [1-^{3}H]cellooligosaccharides were extracted using the following methods: A, water (0.5 ml) was added to vials and then vials were placed in boiling water for 15 min; B, dimethyl sulfoxide:water (1:1, v:v) (0.5 ml) was added to vials and then vials were placed in boiling water for 15 min; C, water (0.5 ml) was added to vials and then vials were sonicated for 0.5 h; O, Aquasol (5 ml) and 20 µl of glacial acetic acid were added directly to vials containing scrapings.

	Drying Temperature			
	Room Temperature		110°C	
Extraction Procedure	Total DPM	% Recovered[a]	Total DPM	% Recovered[a]
A	41500± 400	94±2	36800±500	84±2
B	40700± 800	93±3	34700±500	79±2
C	42000±1400	96±4	36800±800	84±2
D	22200± 100	51±1	20800±400	47±1

[a] Recoveries were based on total radioactivity added to plate: 43970±840 DPM.

scintillation cocktail. Scott (88) eluted glucose, mannose, galactose, arabinose, xylose and sucrose from silica gel with 95 percent recovery.

To assure equal recoveries of [1-^{3}H]cellooligosaccharides from silica gel, methods for extracting individual [1-^{3}H]cellooligosaccharides from Whatman LK5D plates were evaluated. The results are shown in Table 4-4. Although recoveries of [1-^{3}H]cellooligosaccharides using methods A, B and C were similar, the range of recoveries for method B was less than those of methods A and C. Thus, method B, by which [1-^{3}H]cellooligosaccharides are counted with an efficiency of 88±3, was chosen as the extraction procedure. The efficiency of extraction varies slightly from plate to plate and with length of heating at 110°C. To efficiently stain cellooligosaccharide standards, plates were heated at 110°C after the final development.

Conclusions

A thin-layer chromatographic method for quantitating and separating [1-^{3}H]cellooligosaccharides with high resolution on silica gel has been developed. Although TLC methods for separating cellooligosaccharides have been reported (19,63,86), resolution and quantitation of cellooligosaccharides comparable to that reported here have not been demonstrated. The separation of [1-^{3}H]cellooligosaccharides on Whatman LK5D silica gel plates with 3 ascents of ethyl acetate:water:methanol (40:15:20; v:v:v) will facilitate the analysis of products formed from the action of cellulolytic enzymes on radioactive cellooligosaccharides.

Table 4-4

Extraction of Individual [1-^{3}H]Cellooligosaccharides From Thin-layer Chromatographic Plates

Samples of each [1-^{3}H]cellooligosaccharide were added to Whatman LK5D TLC plates. After drying plates at 110°C for 30 min, [1-^{3}H]cellooligosaccharides were extracted using the following methods: A, water (0.5 ml) was added to vials and then vials vortexed for 30 s; B, water (1.5 ml) was added to vials and then vials vortexed for 30 s; C, water (0.5 ml) was added to vials and then vials sonicated for 15 min.

[1-^{3}H]Cello-oligosaccharide	DPM Applied	Extraction Method A DPM	A % Recovered	B DPM	B % Recovered	C DPM	C % Recovered
Glucose	37800±400	31500±700	84±2	32000± 400	85±2	32600±600	86±2
Cellobiose	26000±400	24300±400	93±2	23100±1000	89±4	24400±200	94±1
Cellotriose	12100±200	10600±300	88±3	10300± 300	85±3	10900±200	89±2
Cellotetraose	28300±600	24400±900	86±4	25000± 400	88±2	26400±500	93±3
Cellopentaose	36100±200	32200±300	89±3	32000± 900	89±2	33200±100	92±2
Cellohexaose	15000±300	13500±400	90±3	13400± 100	89±2	13700±400	91±3
			88±3		88±3		91±2

CHAPTER 5
MODE OF ACTION OF ß-GLUCOSIDASE

Introduction

The cellulase system of T. reesei is comprised of endoglucanases, cellobiohydrolase I (D), cellobiohydrolase II and ß-glucosidases. Cellulolytic enzymes act sequentially and cooperatively to degrade crystalline cellulose to glucose. The role of the ß-glucosidase in saccharification of cellulose is to degrade cellobiose, an inhibitor of the depolymerizing enzymes, and cellooligosaccharides to glucose (5,21,36). Although extracellular ß-glucosidases have been purified and partially characterized from Trichoderma reesei (8), Trichoderma viride (16,34,35), Trichoderma koningii (19), Irpex lacteus (20) and Botryodiplodia theobromae (89), little information is available regarding the direction from which ß-glucosidases remove glucosyl residues, mode of attack (repetitive or multiple attack), kinetic constants governing the binding of cellooligosaccharides and topography of active sites.

A variety of aglycones linked through ß-glycosidic bonds are hydrolyzed by ß-glucosidases (32). The nature of the aglycone influences rates of hydrolysis. Cellulolytic ß-glucosidases are specific for the C-4 hydroxyl group and do not hydrolyze ß-galactosides (90). In general, as cellooligosaccharide chain length increases, K_m decreases

indicating that cellooligosaccharides are good substrates for ß-glucosidases (90). Rates of hydrolysis of cellooligosaccharides correspondingly increase with increasing chain length. The dependence of rates of hydrolysis and K_m on chain length suggested to Shewale (90) that in saccharification of cellulose, ß-glucosidases are engaged more in hydrolysis of cellooligosaccharides than in hydrolysis of cellobiose. Hydrolysis of reduced cellooligosaccharides by ß-glucosidases indicates that glycosyl residues are sequentially removed from the nonreducing end; however, the effects of modifying the reducing glucosyl residue on enzymic activity have not been investigated (91).

Although the arrangement of subsites in the active site of ß-glucosidases is poorly understood, subsite affinities have been evaluated for glucoamylase from Rhizopus delemar (44) and Aspergillus saito (47). The subsite maps, which were constructed using the method of Hiromi et al. (44), show that the active site of each enzyme consists of 7 subsites. Subsite II (numbered from the nonreducing end) contributes the greatest proportion of binding energy, whereas the affinity of subsite I is negligible. Subsite affinities decrease in order from subsites III through VII. Since only one productive complex is possible with glucoamylases, the catalytic groups are positioned between subsites I and II.

To determine the mode of action, topography of the active site and to more clearly define the role of the

ß-glucosidase in the cellulase system of T. reesei, the activity of the ß-glucosidases on [1-^{3}H]cellooligosaccharides is examined in this report. The use of [1-^{3}H]cellooligosaccharides permits measurement of initial rates of hydrolysis at micromolar substrate concentrations. In addition, these asymmetrically labeled cellooligosaccharides permit identification of glycosidic bonds susceptible to enzymic hydrolysis. The ß-glucosidase was shown to remove glucosyl residues from the nonreducing end of cellooligosaccharides in a multi-chain mode of attack. Maximum velocities were determined to be independent of chain length, whereas K_m's decrease as chain length increases. Cellooligosaccharides were also used as inhibitors of ß-glucosidase-catalyzed hydrolysis of methylumbelliferyl-ß-D-glucopyranoside (MUG). Inhibition constants of cellooligosaccharides were shown to be similar to the corresponding Michaelis constants. Two approaches were used to evaluate subsite affinities of the ß-glucosidase and revealed that the active site consists primarily of 3 subsites. The results are discussed in terms of the role of the ß-glucosidase in saccharification of cellulose.

Results and Discussion

Hydrolysis of [1-^{3}H]Cellooligosaccharides

To determine initial rates and to identify products formed from ß-glucosidase-catalyzed hydrolysis of [1-^{3}H]cellooligosaccharides, samples were removed from assay mixtures at various times and products separated using

TLC. Michaelis parameters were obtained by measuring initial rates of hydrolysis at various concentrations of [1-^{3}H]cello-oligosaccharides.

The activity of ß-glucosidase on [1-^{3}H]cellobiose is shown in Fig. 5-1. Reducing end-labeled cellobiose was hydrolyzed with a corresponding increase of [1-^{3}H]glucose. Since only reducing end-labeled products were monitored in the assay, glucose at the nonreducing end was not observed. Initial bond cleavage frequencies were determined from the slopes of product ratios versus extent of reaction plots. Deviation from linearity of the slope indicates a change in mode of action. Bond cleavage frequency analysis of ß-glucosidase catalyzed hydrolysis of [1-^{3}H]cellobiose indicated that only one bond was cleaved since the slope of [1-^{3}H]glucose product ratio versus extent of reaction curve is equal to 1.0 (Fig. 5-2). Recovery of [1-^{3}H]cellobiose and [1-^{3}H]glucose from TLC plates was constant for each time point and at each concentration of substrate assayed indicating that transfer reactions are unlikely to occur from 0.25 to 10.0 mM [1-^{3}H]cellobiose.

Linear Lineweaver-Burk and Eadie-Hofstee plots were obtained using initial rates of hydrolysis from 0.25 to 10.0 mM [1-^{3}H]cellobiose (Fig. 5-3). Values of K_m and V_{max} were determined to be 880±40 µM and 17.7±0.2 µmol/min/mg, respectively (Table 5-1).

Reducing end-labeled cellobiose and [1-^{3}H]glucose were formed during ß-glucosidase hydrolysis of [1-^{3}H]cellotriose (Fig. 5-4). The initial appearance of only [1-^{3}H]cellobiose

Figure 5-1 Time course hydrolysis of [1-^{3}H]cellobiose by β-glucosidase

The β-glucosidase (1.05×10^{-4} mg) was incubated in 100 µl of 5 mM sodium acetate buffer, pH 5.0, containing 250 µM [1-^{3}H]cellobiose. Samples were removed from the reaction mixture after various intervals and analyzed using TLC as described in Experimental Procedures. The early, linear region of [1-^{3}H]cellobiose degradation curve yielded the initial velocity. The curves represent the distribution of [1-^{3}H]glucose (o) and [1-^{3}H]cellobiose (●).

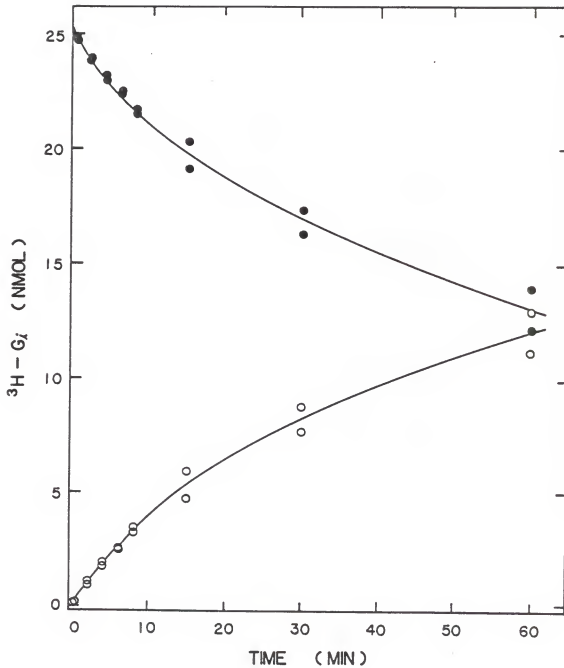
25
20
15
10
5
0
$^3H - G_i$ (NMOL)
0
10
20
30
40
50
60
TIME (MIN)

Figure 5-2 Bond cleavage frequency plot for hydrolysis of [1-^{2}H]cellobiose by β-glucosidase

The β-glucosidase (1.05×10^{-4} mg) was incubated in 100 µl of 5 mM sodium acetate buffer, pH 5.0, containing 250 µM [1-^{2}H]cellobiose. Samples were removed from the reaction mixture and analyzed using TLC as described in Experimental Procedures. The initial slope of each line is the bond cleavage frequency of the substrate bond yielding the product (Gi). The curves represent the product ratio of [1-^{2}H]glucose (o) and substrate ratio of [1-^{2}H]cellobiose (●).

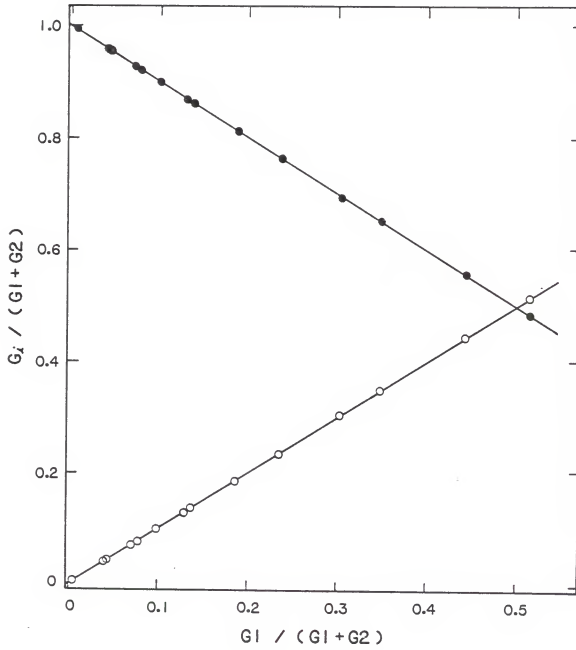
1.0
0.8
0.6
0.4
0.2
0
0
0.1
0.2
0.3
0.4
0.5
Gi / (G1+G2)
G1 / (G1+G2)

Figure 5-3 Lineweaver-Burk and Eadie-Hofstee plots for hydrolysis of [1-^{3}H]cellobiose by β-glucosidase

Initial rates for hydrolysis of [1-^{3}H]cellobiose (0.25-10 mM) by β-glucosidase were used to construct Lineweaver-Burk (A) and Eadie-Hofstee (B) plots.

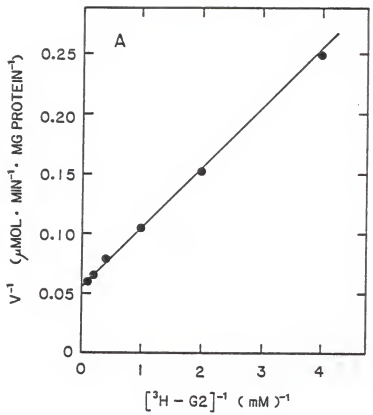
A
0.25
0.20
0.15
0.10
0.05
0
0
1
2
3
4
V⁻¹ (μMOL • MIN⁻¹• MG PROTEIN⁻¹)
[³H – G2]⁻¹ (mM)⁻¹

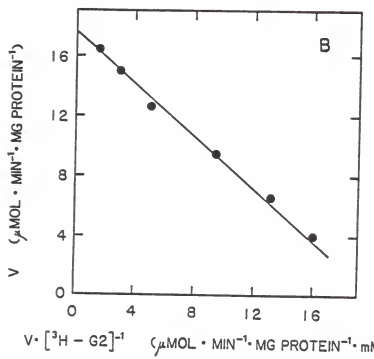
B
16
12
8
4
0
0
4
8
12
16
V (μMOL • MIN⁻¹• MG PROTEIN⁻¹)
V• [³H – G2]⁻¹ (μMOL • MIN⁻¹• MG PROTEIN⁻¹• mM⁻¹)

Table 5-1

Kinetic Constants for [1-^{3}H]Cellooligosaccharide Hydrolysis of β-Glucosidase of T. reesei

Activity of β-glucosidase was assayed at various concentrations of [1-^{3}H]cellooligosaccharides (0.1 → 0.5 μCi) in the presence of 5 mM sodium acetate buffer, pH 5.0, containing 0.3 mM sodium azide. Kinetic constants were determined from initial rates of hydrolysis using Celand's HYPER program (70).

[1-^{3}H]Cellooligo-saccharide	V_{max}/K_m	K_m (μM)	V_{max} (μ mole/min mg of protein)
Cellobiose	0.0200± 0.0001	880 ± 40	17.7 ± 0.2
Cellotriose	0.22 ± 0.02	74 ± 11	16.2 ± 0.9
Cellotetraose	0.60 ± 0.06	35 ± 5	21 ± 1
Cellopentaose	0.52 ± 0.04	35 ± 4	18.2 ± 0.8
Cellohexaose	0.50 ± 0.09	37 ± 10	18 ± 2

Figure 5-4 Time course hydrolysis of [1-^{3}H]cellotriose by β-glucosidase

The β-glucosidase (8.6×10^{-6} mg) was incubated in 100 μl of 5 mM sodium acetate buffer, pH 5.0, containing 55 μM [1-^{3}H]cellotriose. Samples were removed from the reaction mixture after various intervals and analyzed using TLC as described in Experimental Procedures. The early, linear region of [1-^{3}H]cellotriose degradation curve yielded the initial velocity. The curves represent the distribution of [1-^{3}H]glucose (o), [1-^{3}H]cellobiose (●) and [1-^{3}H]cellotriose (□).

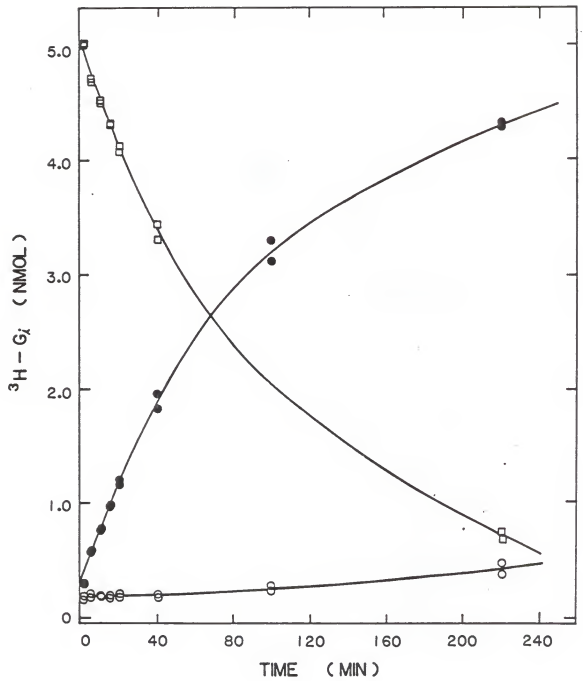
5.0
4.0
3.0
2.0
1.0
0
$^3H - G_i$ (NMOL)
0
40
80
120
160
200
240
TIME (MIN)

indicated that β-glucosidase removes glucosyl residues from the nonreducing end. The lag in the appearance of [1-^{3}H]glucose indicated that [1-^{3}H]cellobiose must accumulate before it is hydrolyzed. Reducing end-labeled glucose appeared after approximately 80% hydrolysis of [1-^{3}H]cellotriose, where [1-^{3}H]cellobiose concentration has reached 200 μM. Bond cleavage frequency analysis showed that hydrolysis occurs exclusively at bond 1 (numbered from the nonreducing end) resulting in the initial formation of only [1-^{3}H]cellobiose (Fig. 5-5). Deviation from linearity of the slopes of [1-^{3}H]cellobiose and [1-^{3}H]glucose after approximately 80 percent hydrolysis of [1-^{3}H]cellotriose indicates that [1-^{3}H]glucose is formed from hydrolysis of [1-^{3}H]cellobiose, instead of cleavage at bond 2 of [1-^{3}H]cellotriose.

When initial rates of hydrolysis were determined from 10 to 300 μM [1-^{3}H]cellotriose, linear Lineweaver-Burk and Eadie-Hofstee plots were obtained (Fig. 5-6). Values of K_m and V_{max} for hydrolysis of [1-^{3}H]cellotriose were determined to be 74±11 μM and 16.2±0.9 μmol/min/mg, respectively (Table 5-1).

The time course of β-glucosidase hydrolysis of [1-^{3}H]cellotetraose is shown in Fig. 5-7. Initially, [1-^{3}H]cellotriose was the only product formed indicating that hydrolysis occurred at the nonreducing end. Reducing end-labeled cellobiose appeared after approximately 13 percent degradation of [1-^{3}H]cellotetraose. Bond cleavage

Figure 5-5 Bond cleavage frequency plot for hydrolysis of [1-^{3}H]cellotriose by ß-glucosidase

The ß-glucosidase (8.6×10^{-6} mg) was incubated in 100 µl of 5 mM sodium acetate buffer, pH 5.0, containing 55 µM [1-^{3}H]cellotriose. Samples were removed from the reaction mixture after various intervals and analyzed using TLC as described in Experimental Procedures. The initial slope of each line is the bond cleavage frequency of the substrate bond yielding the product (Gi). The curves represent the product ratio of [1-^{3}H]glucose (o) and [1-^{3}H]cellobiose (•) and the substrate ratio of [1-^{3}H]cellotriose (□).

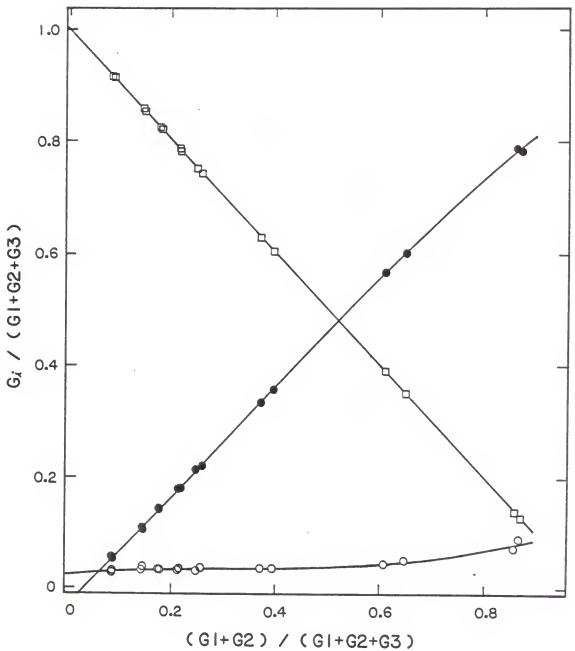
1.0
0.8
0.6
0.4
0.2
0
0
0.2
0.4
0.6
0.8
Gi / (G1+G2+G3)
(G1+G2) / (G1+G2+G3)

Figure 5-6 Lineweaver-Burk and Eadie-Hofstee plots for hydrolysis of [1-^{3}H]cellotriose by ß-glucosidase

Initial rates for hydrolysis of [1-^{3}H]cellotriose (10-300 µM) by ß-glucosidase were used to construct Lineweaver-Burk (A) and Eadie-Hofstee (B) plots.

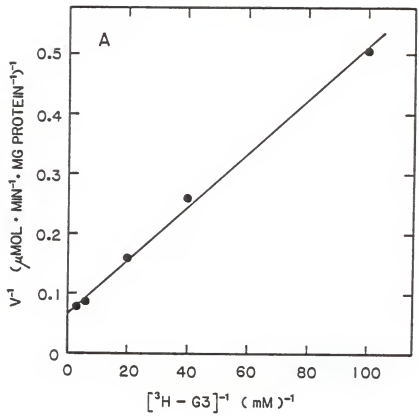
A
0.5
0.4
0.3
0.2
0.1
0
20
40
60
80
100
V^{-1} (μMOL • MIN^{-1}• MG PROTEIN^{-1})$^{-1}$
[^{3}H – G3]$^{-1}$ (mM)$^{-1}$

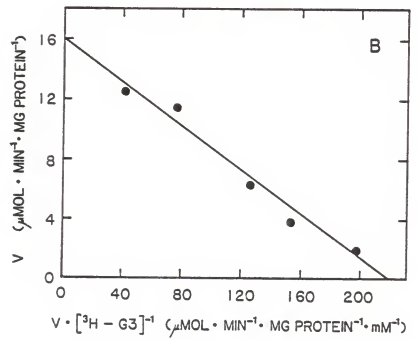
B
16
12
8
4
0
40
80
120
160
200
V (μMOL • MIN^{-1}• MG PROTEIN^{-1})
V • [^{3}H – G3]$^{-1}$ (μMOL • MIN^{-1}• MG PROTEIN^{-1}• mM^{-1})

Figure 5-7 Time course hydrolysis of [1-^{3}H]cellotetraose by β-glucosidase

The β-glucosidase (7.08×10^{-6} mg) was incubated in 100 µl of 5 mM sodium acetate buffer, pH 5.0, containing 40 µM [1-^{3}H]cellotetraose. Samples were removed from the reaction mixture after various intervals and analyzed using TLC as described in Experimental Procedures. The early, linear region of [1-^{3}H]cellotetraose degradation curve yielded the initial velocity. The curves represent the distribution of [1-^{3}H]glucose (o), [1-^{3}H]cellobiose (●), [1-^{3}H]cellotriose (□) and [1-^{3}H]cellotetraose (■).

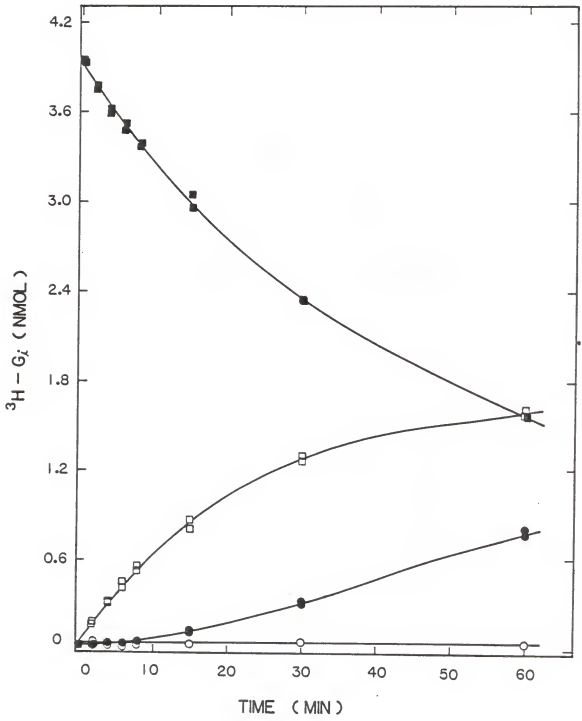
4.2
3.6
3.0
2.4
1.8
1.2
0.6
0
$^3H - G_i$ (NMOL)
0
10
20
30
40
50
60
TIME (MIN)

frequency analysis confirmed that bond 1 was exclusively hydrolyzed; however, deviation from linearity after approximately 13 percent degradation of [1-^{3}H]cellotetraose indicated that [1-^{3}H]cellotriose is hydrolyzed to [1-^{3}H]cellobiose and glucose (Fig. 5-8). No [1-^{3}H]glucose was produced by 60 percent hydrolysis of substrate.

Initial velocities of [1-^{3}H]cellotetraose hydrolysis obtained from the early, linear portion of time course plots were used to construct linear Lineweaver-Burk and Eadie-Hofstee plots (Fig. 5-9). Values of K_m and V_{max} for hydrolysis of [1-^{3}H]cellotetraose were determined to be 35±5 μM and 21±1 μmol/min/mg, respectively (Table 5-1).

Products formed during hydrolysis of [1-^{3}H]cellopentaose catalyzed by ß-glucosidase are shown in Fig. 5-10. Consistent with the pattern established by [1-^{3}H]cellotriose and [1-^{3}H]cellotetraose degradation, ß-glucosidase initiated attack at the nonreducing end of [1-^{3}H]cellopentaose yielding [1-^{3}H]cellotetraose. After approximately 8 percent degradation of [1-^{3}H]cellopentaose, [1-^{3}H]cellotriose appeared. Reducing end-labeled cellobiose appeared after 25 percent degradation of [1-^{3}H]cellopentaose, whereas no [1-^{3}H]glucose is produced after 80 percent hydrolysis of [1-^{3}H]cellopentaose. Bond cleavage frequency analysis showed a linear decrease of [1-^{3}H]cellopentaose with a corresponding initial, linear increase of [1-^{3}H]cellotetraose (Fig. 5-11). Deviation from linearity of [1-^{3}H]cellotetraose curve indicated that [1-^{3}H]cellotetraose

Figure 5-8 Bond cleavage frequency plot for hydrolysis of [1-^{3}H]cellotetraose by ß-glucosidase

The ß-glucosidase (7.08×10^{-6} mg) was incubated in 100 µl of 5 mM sodium acetate buffer, pH 5.0, containing 40 µM [1-^{3}H]cellotetraose. Samples were removed from the reaction mixture after various intervals and analyzed using TLC as described in Experimental Procedures. The initial slope of each line is the bond cleavage frequency of the substrate bond yielding the product (Gi). The curves represent the product ratios of [1-^{3}H]glucose (o), [1-^{3}H]cellobiose (●) and [1-^{3}H]cellotriose (□) and the substrate ratio of [1-^{3}H]cellotetraose (■).

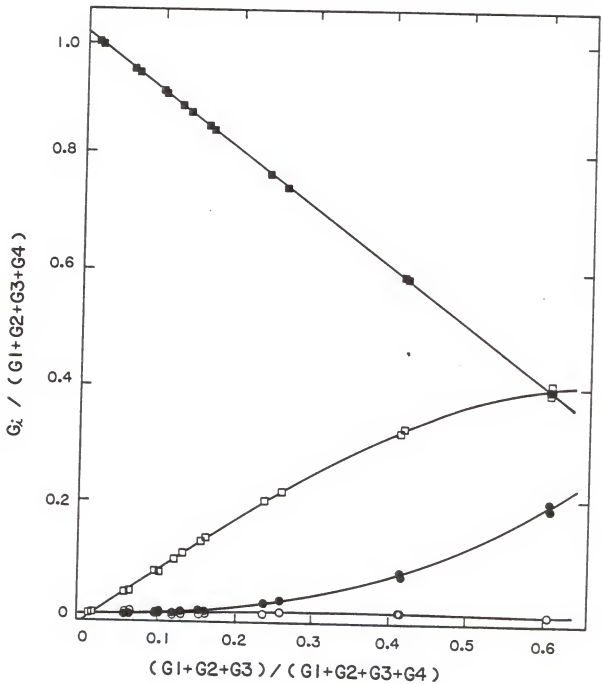
1.0
0.8
0.6
0.4
0.2
0
0
0.1
0.2
0.3
0.4
0.5
0.6
Gi / (G1+G2+G3+G4)
(G1+G2+G3) / (G1+G2+G3+G4)

Figure 5-9 Lineweaver-Burk and Eadie-Hofstee plots for hydrolysis of [1-^{3}H]cellotetraose by β-glucosidase

Initial rates for hydrolysis of [1-^{3}H]cellotetraose (10-250 μM) were used to construct Lineweaver-Burk (A) and Eadie-Hofstee (B) plots.

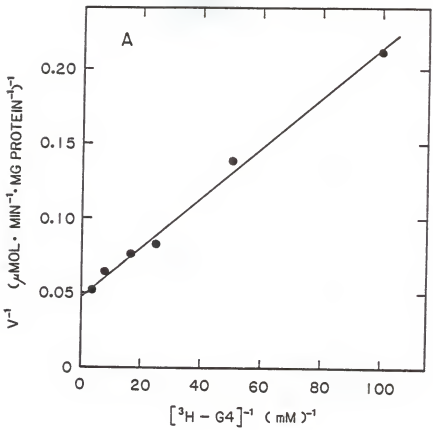
A
0.20
0.15
0.10
0.05
0
0
20
40
60
80
100
V^{-1} (μMOL · MIN^{-1}· MG PROTEIN^{-1})$^{-1}$
[^{3}H – G4]$^{-1}$ (mM)$^{-1}$

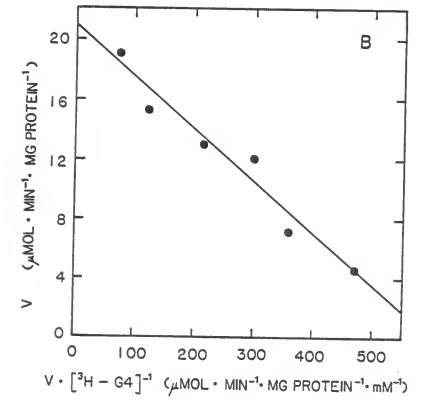
B
20
16
12
8
4
0
0
100
200
300
400
500
V (μMOL · MIN^{-1}· MG PROTEIN^{-1})
V · [^{3}H – G4]$^{-1}$ (μMOL · MIN^{-1}· MG PROTEIN^{-1}· mM^{-1})

Figure 5-10 Time course hydrolysis of [1-^{3}H]cellopentaose by ß-glucosidase

The ß-glucosidase (8.33×10^{-6} mg) was incubated in 100 µl of 5 mM sodium acetate buffer, pH 5.0, containing 30 µM [1-^{3}H]cellopentaose. Samples were removed from the reaction mixture after various intervals and analyzed using TLC as described in Experimental Procedures. The early, linear region of the [1-^{3}H]cellopentaose degradation curve yielded the initial velocity. The curves represent the distribution of [1-^{3}H]glucose (o), [1-^{3}H]cellobiose (●), [1-^{3}H]cellotriose (□), [1-^{3}H]cellotetraose (■) and [1-^{3}H]cellopentaose (Δ).

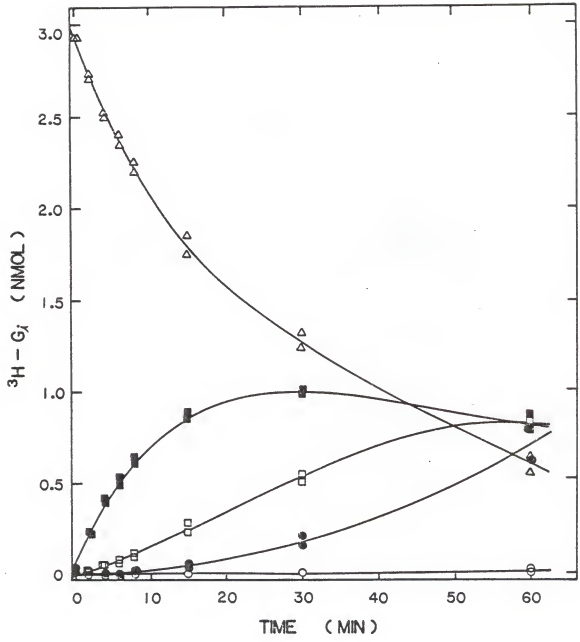
3.0
2.5
2.0
1.5
1.0
0.5
0
0
10
20
30
40
50
60
TIME (MIN)
$^3H - G_i$ (NMOL)

Figure 5-11 Bond cleavage frequency plot for hydrolysis of [1-^{3}H]cellopentaose by β-glucosidase

The β-glucosidase (8.33×10^{-6} mg) was incubated in 100 µl of 5 mM sodium acetate buffer, pH 5.0, containing 30 µM [1-^{3}H]cellopentaose. Samples were removed from the reaction mixture and analyzed using TLC as described in Experimental Procedures. The initial slope of each line is the bond cleavage frequency of the substrate yielding the product (Gi). The curves represent the product ratios of [1-^{3}H]glucose (o), [1-^{3}H]cellobiose (●) and [1-^{3}H]cellotriose (□) and [1-^{3}H]cellotetraose (■) and the substrate ratio of [1-^{3}H]cellopentaose (Δ).

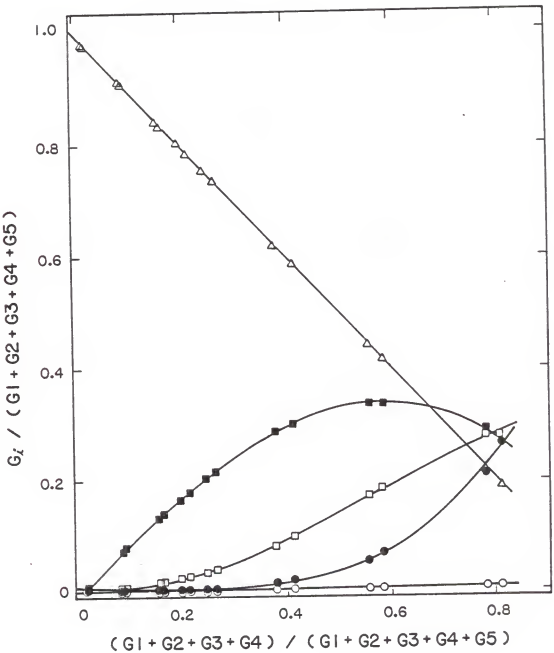
1.0
0.8
0.6
0.4
0.2
0
0
0.2
0.4
0.6
0.8
G_i / (G1 + G2 + G3 + G4 + G5)
(G1 + G2 + G3 + G4) / (G1 + G2 + G3 + G4 + G5)

serves as substrate for β-glucosidase forming [1-^{3}H]cellotriose. Similarly, [1-^{3}H]cellotriose served as a substrate forming [1-^{3}H]cellobiose. No [1-^{3}H]glucose was detected after 80 percent hydrolysis of [1-^{3}H]cellopentaose.

The initial, linear region of the decrease in [1-^{3}H]cellopentaose concentration was used to determine initial rates of hydrolysis. Lineweaver-Burk and Eadie-Hofstee plots constructed using initial rates are linear (Fig. 5-12). Values of K_m and V_{max} for hydrolysis of [1-^{3}H]cellopentaose were determined to be 35±4 μM and 18.2±0.8 μmol/min/mg, respectively (Table 5-1).

The β-glucosidase also catalyzed the hydrolysis of [1-^{3}H]cellohexaose producing [1-^{3}H]cellopentaose as the first detectable product (Fig. 5-13). After approximately 6 percent hydrolysis of [1-^{3}H]cellohexaose, [1-^{3}H]cellotetraose appeared. Reducing end-labeled cellotriose and [1-^{3}H]cellobiose appeared after 16 percent and 50 percent disappearance of cellohexaose, respectively. No detectable [1-^{3}H]glucose was detected after 50 percent hydrolysis of [1-^{3}H]cellohexaose. Bond cleavage frequency analysis confirmed that [1-^{3}H]cellopentaose was the first product formed from hydrolysis of [1-^{3}H]cellohexaose (Fig. 5-14). Deviation from linearity of the bond cleavage frequency curve of [1-^{3}H]cellopentaose after 6 percent hydrolysis of [1-^{3}H]cellohexaose indicated that [1-^{3}H]cellopentaose serves as a substrate for β-glucosidase. Similarly,

Figure 5-12 Lineweaver-Burk and Eadie-Hofstee plots for hydrolysis of [1-^{3}H]cellopentaose by ß-glucosidase

Initial rates for hydrolysis of [1-^{3}H]cellopentaose (7.5-150 µM) by ß-glucosidase were used to construct Lineweaver-Burk (A) and Eadie-Hofstee (B) plots.

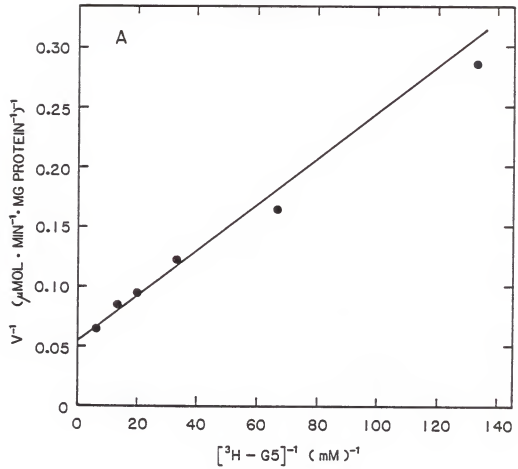
A
0.30
0.25
0.20
0.15
0.10
0.05
0
0
20
40
60
80
100
120
140
V⁻¹ (μMOL · MIN⁻¹· MG PROTEIN⁻¹)⁻¹
[³H – G5]⁻¹ (mM)⁻¹

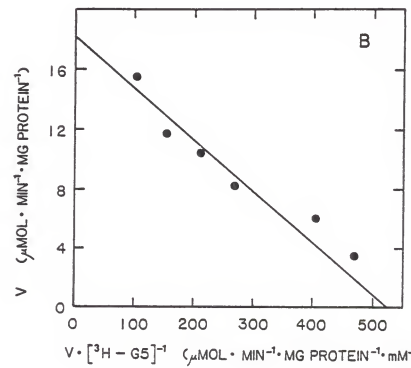
B
16
12
8
4
0
0
100
200
300
400
500
V
(μMOL · MIN⁻¹· MG PROTEIN⁻¹)
V · [³H – G5]⁻¹ (μMOL · MIN⁻¹· MG PROTEIN⁻¹· mM⁻¹)

Figure 5-13 Time course hydrolysis of [1-^{3}H]cellohexaose by ß-glucosidase

The ß-glucosidase (3.17×10^{-5} mg) was incubated in 100 µl of 5 mM sodium acetate buffer, pH 5.0, containing 250 µM [1-^{3}H]cellohexaose. Samples were removed from the reaction mixture after various intervals and analyzed using TLC as described in Experimental Procedures. The early, linear region of the [1-^{3}H]cellohexaose degradation curve yielded the initial velocity. The curves represent the distribution of [1-^{3}H]glucose (o), [1-^{3}H]cellobiose (●), [1-^{3}H]cellotriose (□), [1-^{3}H]cellotetraose (■), [1-^{3}H]cellopentaose (Δ) and [1-^{3}H]cellohexaose (▲).

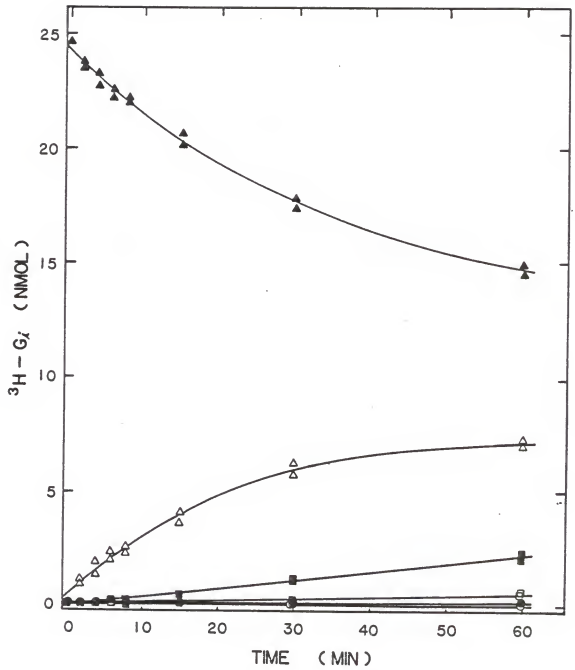
25
20
15
10
5
0
$^3H - G_i$ (NMOL)
0
10
20
30
40
50
60
TIME (MIN)

Figure 5-14 Bond cleavage frequency plot for hydrolysis of [1-^{3}H]cellohexaose by β-glucosidase

The β-glucosidase (3.17×10^{-5} mg) was incubated in 100 μl of 5 mM sodium acetate buffer, pH 5.0, containing 250 μM [1-^{3}H]cellohexaose. Samples were removed from the reaction mixture after various intervals and analyzed using TLC as described in Experimental Procedures. The initial slope of each line is the bond cleavage frequency of the substrate yielding the product (Gi). The curves represent the product ratios of [1-^{3}H]glucose (o), [1-^{3}H]cellobiose (●) and [1-^{3}H]cellotriose (□), [1-^{3}H]cellotetraose (■) and [1-^{3}H]cellopentaose (△) and the substrate ratio of [1-^{3}H]cellohexaose (▲).

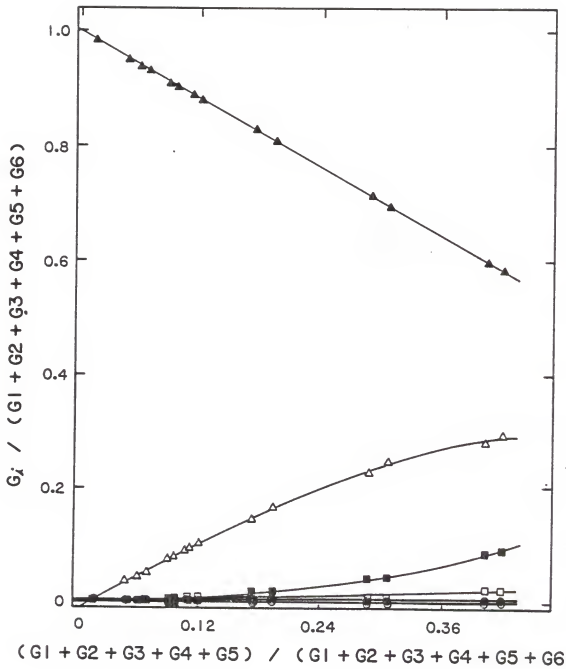
1.0
0.8
0.6
0.4
0.2
0
0
0.12
0.24
0.36
Gi / (G1 + G2 + G3 + G4 + G5 + G6)
(G1 + G2 + G3 + G4 + G5) / (G1 + G2 + G3 + G4 + G5 + G6)

[1-^{3}H]cellotetraose and [1-^{3}H]cellotriose also serve as substrates for β-glucosidase.

Linear Lineweaver-Burk and Eadie-Hofstee plots constructed using initial velocities derived from time course plots of [1-^{3}H]cellohexaose hydrolysis are shown in Fig. 5-15. Values of K_m and V_{max} were determined to be 37±11 μM and 18±2 μmol/min/mg, respectively (Table 5-1).

The action patterns of β-glucosidase from T. reesei on [1-^{3}H]cellooligosaccharides indicate that the β-glucosidase removes glucosyl residues from the nonreducing end. Furthermore, products are released from the enzyme after hydrolysis of substrate indicating multi-chain attack. The β-glucosidase exhibited little tendency to repetitively attack [1-^{3}H]cellooligosaccharides .

Hirayama et al. (92) and Cole and King (91) reported that β-glucosidases from P. oryzae and A. niger, respectively, sequentially remove glucosyl residues from the nonreducing end of reduced cellooligosaccharides. Whether modifying the reducing end glucosyl residue of cellooligosaccharides affects the mode of action of β-glucosidases has not been demonstrated. Glucoamylase from R. delemar has also been shown to remove glucosyl residues from nonreducing ends of oligosaccharides (93); however, whether mode of action is repetitive or multi-chain was not determined.

Kinetic constants determined from initial rates of hydrolysis of β-glucosidase-catalyzed hydrolysis of [1-^{3}H]cellobiose through [1-^{3}H]cellohexaose are summarized

Figure 5-15 Lineweaver-Burk and Eadie-Hofstee plots for hydrolysis of [1-^{3}H]cellohexaose by β-glucosidase

Initial rates for hydrolysis of [1-^{3}H]cellohexaose (7.5-150 μM) by β-glucosidase were used to construct Lineweaver-Burk (A) and Eadie-Hofstee (B) plots.

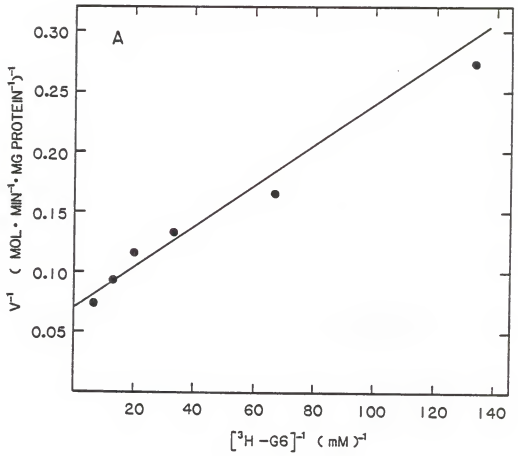
A
0.30
0.25
0.20
0.15
0.10
0.05
20
40
60
80
100
120
140
V⁻¹ (MOL. • MIN⁻¹• MG PROTEIN⁻¹)⁻¹
[³H -G6]⁻¹ (mM)⁻¹

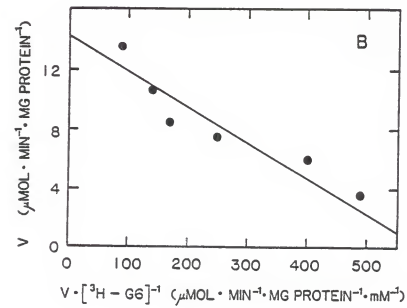
B
12
8
4
0
100
200
300
400
500
V (μMOL • MIN⁻¹• MG PROTEIN⁻¹)
V • [³H – G6]⁻¹ (μMOL • MIN⁻¹• MG PROTEIN⁻¹• mM⁻¹)

in Table 5-1. Maximal rates of [1-^{3}H]cellooligosaccharide hydrolysis vary by less than 25 percent with chain length; however, K_m decreases approximately 25-fold from [1-^{3}H]cellobiose to [1-^{3}H]cellohexaose. The decrease in K_m as chain length increases is reflected in V/K values, which are approximately 25- to 30-fold greater for [1-^{3}H]cellotriose through [1-^{3}H]cellohexaose than for [1-^{3}H]cellobiose.

Michaelis constants for cellooligosaccharide hydrolysis by ß-glucosidases from A. niger (94) and S. rolfsii (95) decrease from 4- to 20-fold as chain length increases. In contrast, Michaelis constants determined for two ß-glucosidases purified from T. koningii by Wood and McCrae (19) increase as chain length increases. The dependence of Michaelis constants on chain length of cellooligosaccharides suggested to Shewale (90) that the role of ß-glucosidases in saccharification of cellulose is to hydrolyze cellooligosaccharides instead of cellobiose. However, the role of the ß-glucosidases in cellulase systems should be assessed in terms of the roles of other cellulolytic components-not exclusively by kinetic parameters of one component.

Although the decrease in Michaelis constants with increasing chain length for [1-^{3}H]cellooligosaccharides hydrolyzed by ß-glucosidase of T. reesei is similar to those reported for other fungal ß-glucosidases, values of Michaelis constants for [1-^{3}H]cellotriose through [1-^{3}H]cellohexaose are approximately 3- to 20-fold less. For example, the K_m's for hydrolysis of cellobiose

through cellohexaose by ß-glucosidase BG-2 from S. rolfsii were determined to be 3.07, 1.23, 0.85, 0.40, and 0.37 mM, respectively (95). When hydrolysis of cellotriose was monitored using Statzyme glucose assay, K_m was determined to be 760 µM (data not shown). However, initial rates of glucose production from cellotriose were not measured accurately, because the amount of glucose in assay mixtures before 10 percent hydrolysis of cellotriose was below the sensitivity of the Statzyme assay. Therefore, the 760 µM K_m for cellotriose is a poor estimate. Since the extent of cellooligosaccharide hydrolysis by ß-glucosidases from A. niger (91), S. rolfsii (95) and T. koningii (19) were not reported, the accuracy and comparability of those Michaelis constants can not be evaluated.

Hydrolysis of [^{14}C-U]Cellooligosaccharides and [1-^{3}H]Cellooligosaccharides

Since experiments using reducing-end labeled cello-oligosaccharides provide little information regarding the fate of unlabeled products, [^{14}C-U]cellooligosaccharides, which were generated from [^{14}C-U]cellulose, were used in conjunction with [1-^{3}H]cellooligosaccharides. Products formed during the hydrolysis of [1-^{3}H]cellopentaose and [^{14}C-U]cellopentaose are listed in Table 5-2. Although the amount of [1-^{3}H]cellooligosaccharides is similar to that of the corresponding [^{14}C-U]cellooligosaccharides at each time interval, glucose is almost exclusively labeled with ^{14}C confirming that all glucose arises from hydrolysis at

Table 5-2

Hydrolysis of [1-^{3}H]Cellopentaose and [^{14}C-U]Cellopentaose by β-Glucosidase

The β-glucosidase (1.1×10^{-5} mg) was incubated at 40°C in 100 µl of 5 mM sodium acetate buffer, pH 5.0, containing 0.55 µCi of [1-^{3}H]cellopentaose and 0.22 µCi of [^{14}C-U]cellopentaose. Total concentration of cellopentaose was 83 µM.

	Pmol			
	Time (min)			
Cellooligosaccharide	0	4	8	30
[1-^{3}H]Glucose	0	4.9± 0.2	14 ± 5	20± 11
[^{14}C-U]Glucose	0	660 ±80	1100 ±100	3400±800
[1-^{3}H]Cellobiose	0	0.9± 0.3	3.3± 0.5	96± 60
[^{14}C-U]Cellobiose	0	8 ± 8	23 ± 9	180± 60
[1-^{3}H]Cellotriose	0	32 ± 7	81 ± 18	560±190
[^{14}C-U]Cellotriose	0	30 ± 4	73 ± 5	500±130
[1-^{3}H]Cellotetraose	0	590 ±30	960 ± 90	2100±240
[^{14}C-U]Cellotetraose	0	540 ±60	830 ± 90	1870±200
[1-^{3}H]Cellopentaose	8116± 9	7490 ±90	7060 ±120	5320±500
[^{14}C-U]Cellopentaose	7640±10	7060 ±70	6700 ±100	5090±430

bond 1. The predominant reducing end-labeled product is [1-^{3}H]cellotetraose.

Initial rates of formation of products and hydrolysis of cellopentaose for ß-glucosidase are listed in Table 5-3. The hydrolysis of [1-^{3}H]cellopentaose and [^{14}C-U]cellopentaose are within experimental error indicating absence of a detectable kinetic isotope effect. The rate of formation of glucose is dominated by [^{14}C-U]glucose confirming that ß-glucosidase removes glucose from the nonreducing end of cellopentaose. Initial rates of formation of [1-^{3}H]cellooligosaccharides are dominated by that of [1-^{3}H]cellotetraose.

Products formed during hydrolysis of [1-^{3}H]cellohexaose and [^{14}C-U]cellohexaose are shown in Table 5-4. Consistent with the pattern established by hydrolysis of cellopentaose, glucose is almost exclusively labeled with ^{14}C indicating that the ß-glucosidase removes glucosyl residues from the nonreducing end of cellohexaose. In contrast, the predominant reducing end-labeled product is [1-^{3}H]cellopentaose.

Initial rates of formation of products and hydrolysis of [1-^{3}H]cellohexaose and [^{14}C-U]cellohexaose are listed in Table 5-5. The initial rates of hydrolysis of [1-^{3}H]cellohexaose and [^{14}C-U]cellohexaose are within experimental error indicating the absence of a detectable kinetic isotope effect. The rate of formation of [^{14}C-U]glucose is similar to the rates of hydrolysis of [1-^{3}H]cellohexaose and

Table 5-3

Initial Rates for ß-Glucosidase Activity on [1-^{3}H]Cellopentaose and [^{14}C-U]Cellopentaose

The ß-glucosidase (1.1×10^{-5} mg) was incubated at 40°C in 100 µl of 5 mM sodium acetate buffer, pH 5.0, containing 0.55 µCi of [1-^{3}H]cellopentaose and 0.22 µCi of [^{14}C-U]cellopentaose. Total concentration of cellopentaose was 83 µM.

Cellooligosaccharide	Initial Velocity (pmol/min)	
	^{3}H	^{14}C
Glucose	1.2 ± 0.8	165 ± 8
Cellobiose	0.3 ± 0.2	2 ± 2
Cellotriose	9 ± 1	8 ± 3
Cellotetraose	144 ± 4	133 ± 7
Cellopentaose	-154 ± 6	-146 ± 10

Table 5-4

Hydrolysis of [1-^{3}H]Cellohexaose and [^{14}C-U]Cellohexaose by ß-Glucosidase

The ß-glucosidase (8.7×10^{-6} mg) was incubated at 40°C in 100 µl of 5 mM sodium acetate buffer, pH 5.0, containing 0.55 µCi of [1-^{3}H]cellohexaose and 0.19 µCi of [^{14}C-U]cellohexaose. Total concentration of cellohexaose was 59.5 µM.

	Pmol			
	Time (min)			
Cellooligosaccharide	0	4	8	30
[1-^{3}H]Glucose	0	4 ± 2	5 ± 4	14 ± 2
[^{14}C-U]Glucose	0	350 ±10	600 ±200	1290 ± 60
[1-^{3}H]Cellobiose	0	0.3± 3	0.1± 1	2 ± 2
[^{14}C-U]Cellobiose	0	3 ± 1	10 ± 7	35 ± 5
[1-^{3}H]Cellotriose	0	<0.1	8 ± 3	12.6± 0.5
[^{14}C-U]Cellotriose	0	13 ±10	25 ± 4	50 ± 10
[1-^{3}H]Cellotetraose	0	30.2± 0.8	70 ± 10	170 ± 30
[^{14}C-U]Cellotetraose	0	30 ±10	60 ± 20	140 ± 30
[1-^{3}H]Cellopentaose	0	305 ± 3	440 ± 20	870 ± 70
[^{14}C-U]Cellopentaose	0	274 ± 5	350 ± 20	750 ± 50
[1-^{3}H]Cellohexaose	5630±60	5290 ±60	5100 ± 90	4600 ±200
[^{14}C-U]Cellohexaose	5035±30	4720 ±50	4600 ± 90	4100 ±100

Table 5-5

Initial Rates for ß-Glucosidase Activity on [1-^{3}H] Cellohexaose and [^{14}C-U]Cellohexaose

The ß-glucosidase(8.7×10^{-6} mg) was incubated at 40°C in 100 µl of 5 mM sodium acetate buffer, pH 5.0, containing 0.55 µCi of [1-^{3}H]cellohexaose and 0.19 µCi of [^{14}C-U]cellohexaose. Total concentration of cellohexaose was 59.5 µM.

Cellooligosaccharide	Initial Velocity (pmol/min)	
	^{3}H	^{14}C
Glucose	1.2 ± 0.4	88 ± 7
Cellobiose	0.07 ± 0.69	0.7 ± 1
Cellotriose	-0.2 ± 0.4	3.2 ± 0.9
Cellotetraose	7.6 ± 0.8	6 ± 2
Cellopentaose	76 ± 10	68 ± 15
Cellohexaose	-84 ± 10	-77 ± 13

[^{14}C-U]cellohexaose. The negligible rate formation of [1-^{3}H]glucose supports that cleavage occurs from the non-reducing end of cellohexaose. Rates of reducing end-labeled product formation are dominated by that of [1-^{3}H]cellopentaose.

Inhibition of Methylumbelliferylglucoside (MUG) Hydrolysis by Cellooligosaccharides

To determine the affinity of ß-glucosidase for each cellooligosaccharide, purified cellobiose through cellohexaose were used to inhibit ß-glucosidase-catalyzed hydrolysis of MUG in separate experiments. Figures 5-16, 5-17, 5-18, 5-19 and 5-20 illustrate the inhibition patterns obtained for cellobiose, cellotriose, cellotetraose and cellopentaose and cellohexaose, respectively, during hydrolysis of MUG. Lineweaver-Burk and Dixon plots indicate that each cellooligosaccharide competitively inhibits the ß-glucosidase. Straight lines whose intercepts approach the origin were obtained when Dixon replots were constructed for cellobiose, cellotriose and cellotetraose (Fig. 5-21) and for cellopentaose and cellohexaose (Fig. 5-22). A straight line through the origin of a Dixon replot indicates purely competitive inhibition. Competitive inhibition constants determined for each cellooligosaccharide are listed in Table 5-6. The affinity of ß-glucosidase for cellooligosaccharides increases from cellobiose through cellohexaose. In contrast, the ß-glucosidase has a higher affinity for the product glucose than for cellobiose as substrate. Since

Figure 5-16 Inhibition of β-glucosidase by cellobiose using 4-methylumbelliferyl-β-D-glucopyranoside as the substrate

The reaction mixture contained 0.17 μg of β-glucosidase with 4-methylumbelliferyl-β-D-glucopyranoside as the substrate in 50 mM sodium acetate buffer, pH 5.0, as described in Experimental Procedures. A. Lineweaver-Burk plot: the fixed levels of inhibitor were 0 (○), 0.64 (●), 13 (□) and 3.8 mM (■). B. Dixon plot: the levels of substrate were 12 (▲), 19 (△), 24 (■), 48 (□), 59 (●) and 95 μM (○).

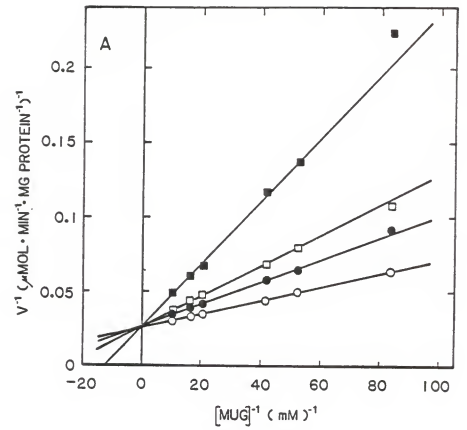
A
0.2
0.15
0.1
0.05
0
−20
0
20
40
60
80
100
V⁻¹ (μMOL · MIN⁻¹ · MG PROTEIN⁻¹)⁻¹
[MUG]⁻¹ (mM)⁻¹

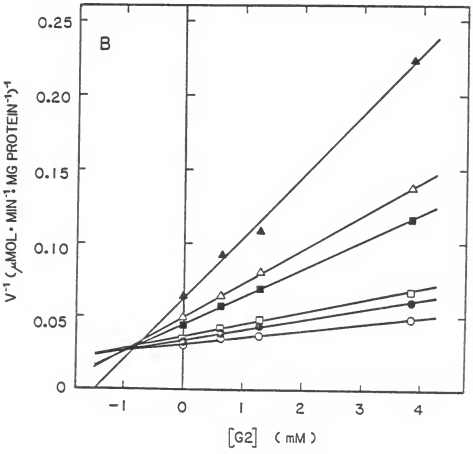
B
0.25
0.20
0.15
0.10
0.05
0
−1
0
1
2
3
4
V⁻¹ (μMOL · MIN⁻¹ · MG PROTEIN⁻¹)⁻¹
[G2] (mM)

Figure 5-17 Inhibition of β-glucosidase by cellotriose using 4-methylumbelliferyl-β-D-glucopyranoside as the substrate

The reaction mixture contained 0.17 μg of β-glucosidase with 4-methylumbelliferyl-β-D-glucopyranoside as the substrate in 50 mM sodium acetate buffer, pH 5.0, as described in Experimental Procedures. A. Lineweaver-Burk plot: the fixed levels of inhibitor were 0 (○), 26 (●), 53 (□) and 130 μM (■). B. Dixon plot: the levels of substrate were 12 (▲), 19 (△), 24 (■), 48 (□), 59 (●) and 95 μM (○).

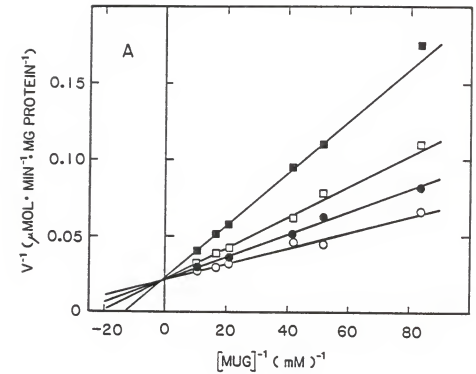
A
0.15
0.10
0.05
0
-20
0
20
40
60
80
V⁻¹ (μMOL• MIN⁻¹• MG PROTEIN⁻¹)
[MUG]⁻¹ (mM)⁻¹

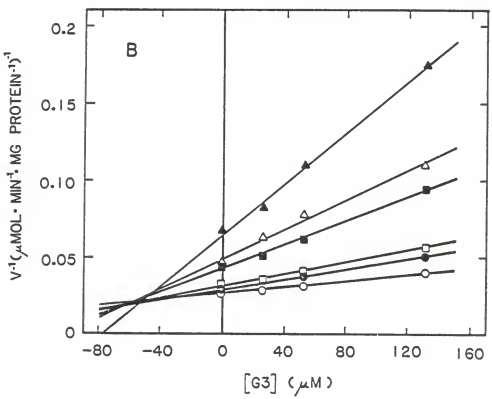
B
0.2
0.15
0.10
0.05
0
-80
-40
0
40
80
120
160
V⁻¹(μMOL• MIN⁻¹• MG PROTEIN⁻¹)⁻¹
[G3] (μM)

Figure 5-18 Inhibition of β-glucosidase by cellotetraose using 4-methylumbelliferyl-β-D-glucopyranoside as the substrate

The reaction mixture contained 0.17 μg of β-glucosidase with 4-methylumbelliferyl-β-D-glucopyranoside as the substrate in 50 mM sodium acetate buffer, pH 5.0, as described in Experimental Procedures. A. Lineweaver-Burk plot: the fixed levels of inhibitor were 0 (○), 25 (●), 49 (□) and 120 μM (■). B. Dixon plot: the levels of substrate were 12 (▲), 19 (△), 24 (■), 48 (□), 59 (●) and 95 μM (○).

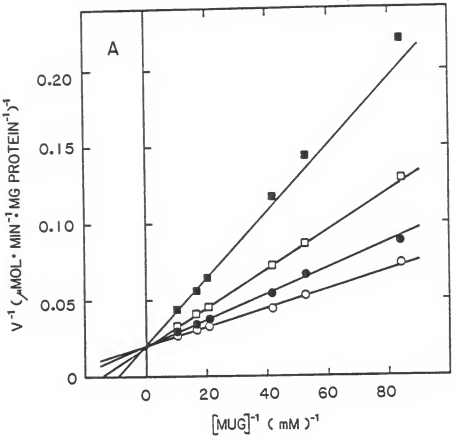
A
0.20
0.15
0.10
0.05
0
0
20
40
60
80
V⁻¹ (μMOL · MIN⁻¹ · MG PROTEIN⁻¹)⁻¹
[MUG]⁻¹ (mM)⁻¹

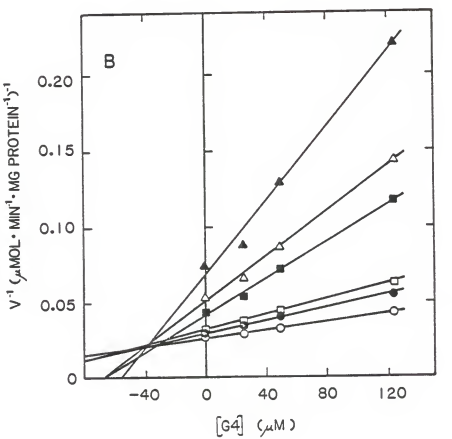
B
0.20
0.15
0.10
0.05
0
-40
0
40
80
120
V⁻¹ (μMOL · MIN⁻¹ · MG PROTEIN⁻¹)⁻¹
[G4] (μM)

Figure 5-19 Inhibition of β-glucosidase by cellopentaose using 4-methylumbelliferyl-β-D-glucopyranoside as the substrate

The reaction mixture contained 0.17 μg of β-glucosidase with 4-methylumbelliferyl-β-D-glucopyranoside as the substrate in 50 mM sodium acetate buffer, pH 5.0, as described in Experimental Procedures. A. Lineweaver-Burk plot: the fixed levels of inhibitor were 0 (○), 9.2 (●), 18 (□) and 56 μM (■). B. Dixon plot: the levels of substrate were 12 (▲), 19 (△), 24 (■), 48 (□), 59 (●) and 95 μM (○).

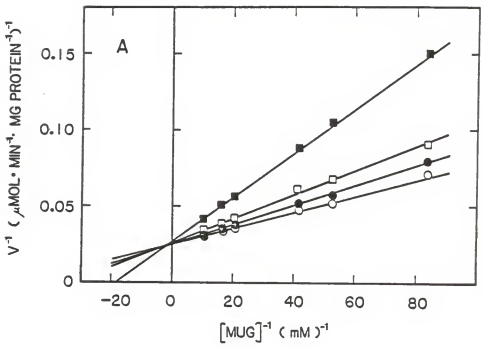
A
0.15
0.10
0.05
0
−20
0
20
40
60
80
V⁻¹ (μMOL • MIN⁻¹ • MG PROTEIN⁻¹)⁻¹
[MUG]⁻¹ (mM)⁻¹

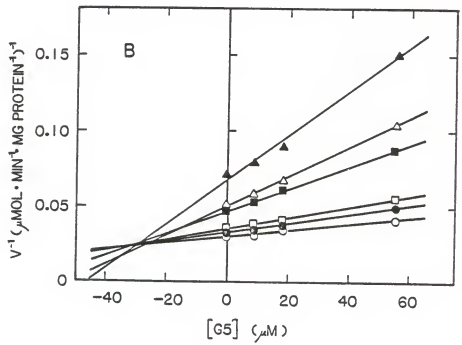
B
0.15
0.10
0.05
0
−40
−20
0
20
40
60
V⁻¹ (μMOL • MIN⁻¹ • MG PROTEIN⁻¹)⁻¹
[G5] (μM)

Figure 5-20 Inhibition of β-glucosidase by cellohexaose using 4-methylumbelliferyl-β-D-glucopyranoside as the substrate

The reaction mixture contained 0.17 μg of β-glucosidase with 4-methylumbelliferyl-β-D-glucopyranoside as the substrate in 50 mM sodium acetate buffer, pH 5.0, as described in Experimental Procedures. A. Lineweaver-Burk plot: the fixed levels of inhibitor were 0 (○), 15 (●), 30 (□) and 64 μM (■). B. Dixon plot: the levels of substrate were 12 (▲), 18 (△), 23 (■), 46 (□), 58 (●) and 93 μM (○).

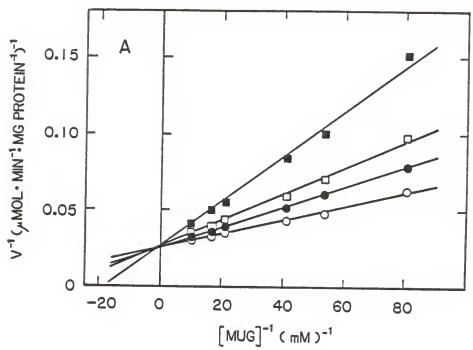
A
0.15
0.10
0.05
0
−20
0
20
40
60
80
V⁻¹ (μMOL • MIN⁻¹ • MG PROTEIN⁻¹)⁻¹
[MUG]⁻¹ (mM)⁻¹

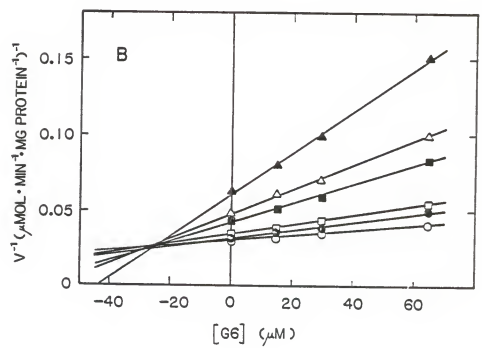
B
0.15
0.10
0.05
0
−40
−20
0
20
40
60
V⁻¹ (μMOL • MIN⁻¹ • MG PROTEIN⁻¹)⁻¹
[G6] (μM)

Figure 5-21 Dixon replots of inhibition of β-glucosidase by cellobiose, cellotriose and cellotetraose

Dixon replots were obtained using (A) cellobiose, (B) cellotriose and (C) cellotetraose as inhibitors with 4-methylumbelliferyl-β-D-glucopyranoside as the substrate.

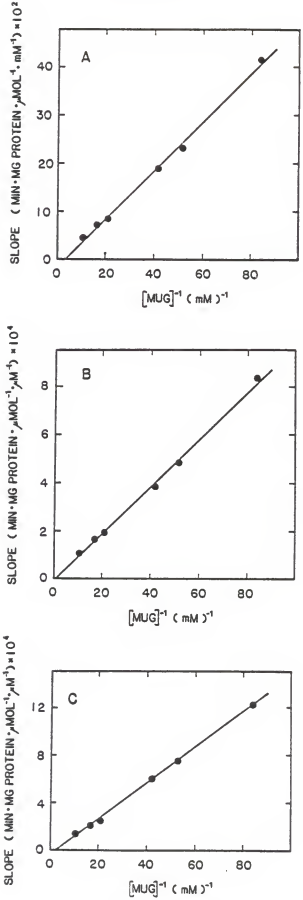
A
SLOPE (MIN • MG PROTEIN • μMOL⁻¹ • mM⁻¹) • 10²
[MUG]⁻¹ (mM)⁻¹
B
SLOPE (MIN • MG PROTEIN • μMOL⁻¹ • μM⁻¹) • 10⁴
[MUG]⁻¹ (mM)⁻¹
C
SLOPE (MIN • MG PROTEIN • μMOL⁻¹ • μM⁻¹) • 10⁴
[MUG]⁻¹ (mM)⁻¹

Figure 5-22 Dixon replots of inhibition of β-glucosidase by cellopentaose and cellohexaose

Dixon replots were obtained using (A) cellopentaose and (B) cellohexaose as inhibitors with 4-methylumbelliferyl-β-D-glucopyranoside as the substrate.

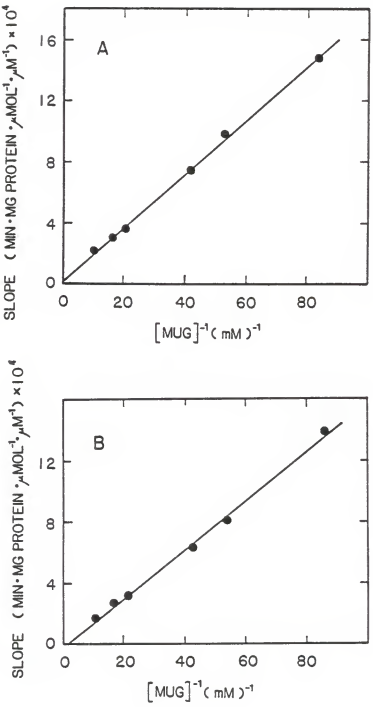
A
B
SLOPE (MIN·MG PROTEIN·μMOL⁻¹·μM⁻¹) ×10⁴
[MUG]⁻¹(mM)⁻¹
0
4
8
12
16
20
40
60
80

Table 5-6

Inhibition of ß-Glucosidase by Cellooligosaccharides

Cellooligosaccharides were used to inhibit the ß-glucosidase hydrolysis of methylumbelliferylglucoside (MUG). Competitive inhibition constants were determined using computer analysis as described in Experimental Procedures.

Cellooligosaccharide	K_i (μM)
Glucose[a]	700 ± 60
Cellobiose	1040 ± 10
Cellotriose	58 ± 3
Cellotetraose	46 ± 2
Cellopentaose	35 ± 3
Cellohexaose	31 ± 2

[a] Reference (8).

the major role of the β-glucosidase in saccharification of cellulose is to convert cellobiose, an inhibitor of the depolymerizing enzymes, to glucose, the relative affinities of the β-glucosidase for glucose and cellobiose serve as a sensitive point of control. The inhibition constants for cellobiose through cellohexaose are similar to Michaelis constants for [1-^{3}H]cellobiose through [1-^{3}H]cellohexaose, suggesting that Michaelis constants are good approximations of dissociation constants for cellooligosaccharides.

Subsite Mapping of β-Glucosidase

The decrease in K_m and K_i for cellooligosaccharides as well as the dependence of K_m and V_{max}/K_m for cellooligosaccharide hydrolysis by β-glucosidase on chain length suggests that the active site of the β-glucosidase is composed of subsites which specifically interact with glucosyl residues of cellooligosaccharides. Hiromi et al. (44) formulated a theory by which the binding affinities of subsites of glucoamylase from R. delemar were estimated from the dependence of V_{max}/K_m on chain length. If hydrolytic rate coefficients for all bonds are independent of chain length, V_{max}/K_m values are directly proportional to the association constant of the single productive complex. Similar to glucoamylase, the activity of the β-glucosidase from T. reesei on [1-^{3}H]cellooligosaccharides indicates that the β-glucosidase binds cellooligosaccharides in one productive complex and cleaves glucosyl residues from the

nonreducing end. Therefore, the method of Hiromi et al. (44) was used to construct a subsite map from values of V_{max}/K_m listed in Table 5-1 for the β-glucosidase. Equations relevant to the subsite mapping theory of Hiromi et al. (44) are outlined in Appendix A.

Affinities for subsites III-VII of glucamylase were evaluated by comparing the V_{max}/K_m values for (n+1)-mer and n-mer substrates. The affinity of subsite I and k_{+2} (hydrolytic rate coefficient) for glucoamylase were obtained from the vertical and horizontal intercepts, respectively, of a plot of $\exp(A_{n+1}/RT)$ versus $(1/V_{max})_n$. The linearity of their plot indicates that k_{+2} is independent of chain length (n). The affinity of subsite II for glucoamylases was then calculated from the known affinities of subsites I and III-VII. However, a plot of $\exp(A_{n+1}/RT)$ versus $(1/V_{max})_n$ using V_{max} values for the β-glucosidase (Table 5-1) was not linear. Thus, affinity of subsite 1 could not be evaluated. Since determination of the affinity of subsite 2 requires values for affinities of subsites 1 and 3-6, the affinity of subsite 2 could not be evaluated. Therefore, only the summation affinities of subsites 1 and 2 can be determined.

The subsite map for the β-glucosidase indicates that the active site is composed primarily of 4 subsites (subsites 1-4)(Fig. 5-23). The affinities of subsites 5 and 6 are negligible. The β-glucosidase binds cellooligosaccharides in one productive complex and cleaves glucosyl

Figure 5-23 Subsite map for ß-glucosidase constructed using values of V_{max}/K_m for cellooligosaccharides

Subsite affinities were estimated using the method of Hiromi et al. (44) and values of V_{max}/K_m for [1-^{2}H]cellooligosaccharide hydrolysis by ß-glucosidase. The arrow shows the position of the catalytic groups. Since individual affinities of subsites 1 and 2 could not be evaluated using the method of Hiromi et al. (44), the sum of affinities of subsites 1 and 2 is shown.

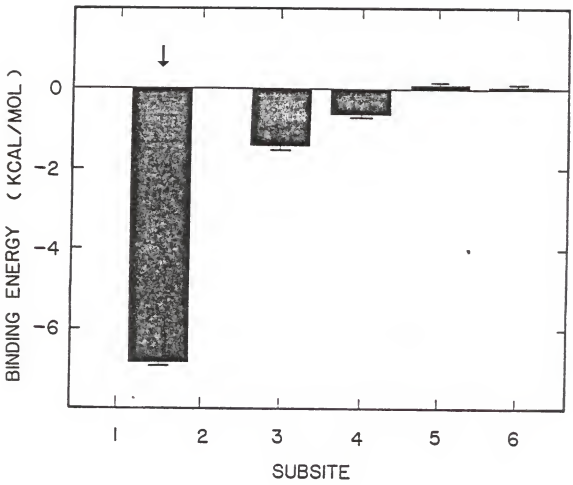
BINDING ENERGY (KCAL/MOL)
0
-2
-4
-6
1
2
3
4
5
6
SUBSITE

residues from the nonreducing end indicating that the catalytic groups are located between subsites 1 and 2. Although subsites 1 and 2 provide the greatest proportion of binding energy, the individual contributions of subsites 1 and 2 cannot be determined using the method of Hiromi et al. (44).

Although Michaelis constants of [1-^{3}H]cellooligosaccharide hydrolysis by the β-glucosidase decrease with increasing chain length, the subsite map indicates that the β-glucosidase preferentially binds glucose through cellotetraose. If -0.8 kcal/mol is taken as the average free energy decrease caused by formation of one hydrogen bond (96), then subsites 1 and 2 could involve the formation of approximately 9 hydrogen bonds (Appendix D). Subsites 3 and 4 could contribute 2 and 1 hydrogen bonds, respectively. The affinities of subsites 5 and 6 are negligible.

An alternative method for evaluating subsite binding affinities of the β-glucosidase is to calculate the contribution of glucosyl residues to the free energy of binding from the ratio of inhibition constants for a series of cellooligosaccharides. Roeser and Legler (71) estimated the contribution of hydroxyl groups of β-glucopyranosides to hydrolysis by β-glucosidase A_3 of Aspergillus wentii by a similar comparison of inhibition constants. A subsite map constructed from the competitive inhibition constants of cellooligosaccharides (Table 5-2), using the method of Roeser and Legler (71), is shown in Fig. 5-24. The active

Figure 5-24 Subsite map for β-glucosidase constructed using values of inhibition constants for cellooligosaccharides

Subsite affinities were estimated using the method of Roeser and Legler (71) and values of inhibition constants for cellooligosaccharides. The arrow shows the position of the catalytic groups.

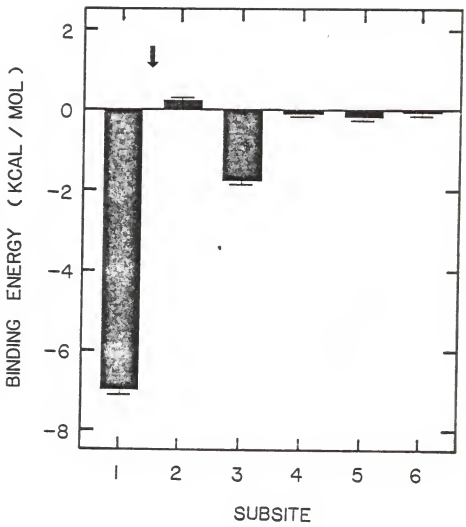
BINDING ENERGY (KCAL / MOL)
2
0
-2
-4
-6
-8
1
2
3
4
5
6
SUBSITE

site of ß-glucosidase comprises primarily 3 subsites, with subsite 1 contributing the greatest proportion of binding energy. Binding at subsite 2 is slightly unfavorable, whereas binding at subsites 4-6 is negligible. Subsite 3 contributes significant binding suggesting that the ß-glucosidase scavenges cellotriose formed from the action of the depolymerizing enzymes on cellulose. Subsites 1 and 3 could provide approximately 9 and 2 hydrogen bonds, respectively, for binding of glucosyl residues of cellooligosaccharides (Appendix D).

To construct the subsite map using the method of Roeser and Legler (71), the assumption that glucose binds predominantly at subsite 1 was made. Glucose is believed to bind predominantly at subsite 1, because (1) substrate specificity studies yielded Michaelis constants for ß-linked glucosyl disaccharides (Appendix E) that are similar to the K_i determined for glucose (8), whereas Michaelis constants for ß-glucosides containing hydrophobic aglycones, such as p-nitrophenyl-ß-D-glucoside and 4-methylumbelliferyl-ß-D-glucoside (8), are 10-fold lower than K_i for glucose, and (2) the ß-glucosidase catalyzes the formation of transfer products (8). The formation of transfer products indicates that binding of glucose is sufficiently strong at subsite 1 to maintain a glucosyl-enzyme intermediate. The relative affinities of glucose, ß-linked glucosyl disaccharides and ß-glucosides containing hydrophobic aglycones suggests that

subsite 1 is specific for glucose, whereas subsite 2 prefers hydrophobic compounds.

The subsite map (Fig. 5-23) constructed using the method of Hiromi et al. (44) is incomplete, because the individual contributions of subsites 1 and 2 cannot be evaluated. However, the method of Roeser and Legler (71) provides a complete subsite map. Both subsite maps indicate that binding at subsites 5 and 6 is negligible and that binding at subsite 3 could contribute to the binding of cellooligosaccharides. Although significant affinity of subsite 4 for glucosyl residues was determined using the method of Hiromi et al. (44), binding at subsite 4 was determined to be negligible using the method of Roser and Legler (71). The V_{max} of [1-^{3}H]cellotetraose is approximately 13 percent higher than that of [1-^{3}H]cellopentaose whereas the corresponding values of K_m are indistinguishable. Since the method of Hiromi et al. (44) uses values of V_{max}/K_m for evaluating subsite affinities, the V_{max} will significantly alter apparent subsite affinities. Nevertheless, the contribution of subsite 4 to binding of cellooligosaccharides is minor.

Subsites affinities have been evaluated for several glucoamylases (41). The subsite adjacent to the catalytic groups and toward the reducing end contributes the greatest proportion of binding energy. The subsite to the left of catalytic groups provides, in general, unfavorable binding energy. In contrast, the corresponding subsites in the

active site of the ß-glucosidase of T. reesei. exhibit the opposite pattern: subsite to the right of catalytic groups provides unfavorable binding energy, whereas the subsite to the left contributes the greatest proportion of binding energy.

The affinities of subsites adjacent to catalytic groups of glucoamylase were evaluated from the linear relationship of $\exp(A_{n+1}/RT)$ versus $(1/V_{max})_n$. However, examination of this plot reported by Hiromi et al. (44) for glucoamylase of R. delemar shows that linearity is primarily dependent on the V_{max} for maltose. A linear dependence between these parameters is not obtained, if the value of V_{max} for maltose is omitted. Thus, determination of the binding affinity of the subsite to the left of the catalytic groups may be inaccurate using the method of Hiromi et al. (44). The subsite to which glucose primarily binds must be identified by other experimental approaches. Although fluorometric studies on the binding of gluconolactone and glucose to glucoamylase reportedly supports that gluconolactone and glucose bind to subsites 1 and 2, respectively, the displacement of gluconolactone from glucoamylase by glucose was partly competitive (97). This suggests that subsite 1 has significant affinity for a glucosyl residue.

Conclusions. The extracellular ß-glucosidase from T. reesei binds [1-^{3}H]cellooligosaccharides in one productive mode and removes glucosyl residues from the nonreducing end. Products are released from the ß-glucosidase after

hydrolysis indicating multi-chain mode of attack. No evidence for repetitive attack was obtained. Michaelis constants for cellooligosaccharide hydrolysis by the β-glucosidase decrease with increasing chain length. In contrast, values of V_{max} are essentially independent of chain length. Inhibition constants for cellooligosaccharides are similar to Michaelis constants indicating that K_m approximates K_s. A subsite map constructed using the method of Hiromi et al. (44) shows that the active site of the β-glucosidase is composed primarily of 3 subsites; however, a fourth subsite toward the reducing end (subsite 4) provides some affinity for glucosyl residues. Catalytic groups are located between subsites 1 and 2. The active site of the β-glucosidase was also shown to consist primarily of 3 subsites using the method of Roeser and Legler (71). The number of subsites and the relative binding affinities suggests that the role of this β-glucosidase is to convert cellobiose, an inhibitor of depolymerizing enzymes, and cellotriose to glucose. Additional subsites may be required to promote efficient hydrolysis of longer cellooligosaccharides.

CHAPTER 6
MODE OF ACTION OF CELLOBIOHYDROLASE I(D)

Introduction

Cellobiohydrolases have been purified from the extracellular matrix of several cellulolytic fungi including *T. reesei* (5,7), *T. viride* (13), *T. koningii* (18) and *I. lacteus* (20). The role of cellobiohydrolases in the saccharification of cellulose is thought to be the removal of cellobiosyl residues from nonreducing chain ends of cellulose (36). Chain ends are generated by endoglucanases which hydrolyze internal glycosidic bonds of cellulose. Cellobiose, an inhibitor of the depolymerizing enzymes, is converted to glucose by β-glucosidases. Component enzymes of cellulase systems act synergistically to convert native, crystalline cellulose to glucose (18). Although the role of cellobiohydrolases in saccharification of cellulose has been established, the mode of action, the topography of the active sites, the direction from which enzymes attack and the mechanism by which cellobiohydrolases synergistically degrade crystalline cellulose have not been described.

Two cellobiohydrolases have been purified and partially characterized from *T. reesei* (6,7). Hsu et al. (29) estimated values of K_m and V_{max} for cellotriose and cellotetraose hydrolysis catalyzed by a cellobiohydrolase

isolated from T. reesei. Hydrolysis of cellotetraose yielded predominantly cellobiose, whereas glucose and cellobiose were produced from hydrolysis of cellotriose. Glucose and cellobiose inhibited the enzyme. Hsu et al. (29) estimated kinetic constants from an analysis of the entire time course of the reaction. Initial rate studies were precluded due to low sensitivity of HPLC analysis of cellooligosaccharides. The action patterns of cellooligosaccharide hydrolysis by cellobiohydrolase I(D) [CBH I(D)] were investigated by Gritzali (6) using HPLC. Cellobiohydrolase I(D) produces cellobiose and increasing proportions of glucose and cellotriose as the chain length of the oligosaccharide substrate increases. Cellohexaose is hydrolyzed by CBH I(D) in a repetitive attack mode. The rate of hydrolysis of cellohexaose is 2-fold higher than that of cellotetraose and cellopentaose.

Since hydrolysis at different glycosidic bonds of cellooligosaccharides may yield identical action patterns, the precise bond hydrolyzed cannot be identified. To overcome this problem, reduced cellooligosaccharides have been used to investigate cellobiohydrolases (98). Cellobiohydrolase I(D) of T. viride showed little tendency to hydrolyze bonds linking the sorbityl residue at the former reducing end of the substrate. An alternative approach to introducing asymmetry into cellooligosaccharides is to convert cellooligosaccharides to 4-methylumbelliferyl glycosides (30). High performance liquid chromatographic analysis of

reaction products of series of 4-methylumbelliferyl glycosides from cellooligosaccharides indicated that CBH I(D) lacks specificity for glycosidic bonds of the glycosides.

Two cellobiohydrolases purified from T. reesei by Fagerstam and Pettersson (7) were shown to synergistically degrade crystalline cellulose. This type of synergism is referred to as exo-exo synergism. The mechanism by which CBH I(D) and CBH II exert exo-exo synergism is unknown.

In this report, [1-^{3}H]cellooligosaccharides are used as substrates to identify glycosidic bonds cleaved and to determine initial rates of cellooligosaccharide hydrolysis by CBH I(D). Michaelis constants were determined using the initial rates of [1-^{3}H]cellooligosaccharide hydrolysis. Subsite binding affinities for CBH I(D) were evaluated from bond cleavage frequencies, K_m and V_{max} for [1-^{3}H]cellooligosaccharides. Action patterns of CBH I(D) on [1-^{3}H]cellooligosaccharides and [^{14}C-U]cellooligosaccharides indicate that CBH I(D) repetitively attacks longer cellooligosaccharides and proceeds from the reducing terminus. The results are discussed in terms of the role of CBH I(D) in the saccharification of cellulose.

Results and Discussion

Hydrolysis of [1-^{3}H]Cellooligosaccharides

To determine initial rates of hydrolysis and to identify glycosidic bonds cleaved by CBH I(D) [1-^{3}H]cellooligosaccharides were used as substrates. Samples were removed from assay mixtures and products separated using TLC.

Reducing end-labeled products formed during hydrolysis of [1-^{3}H]cellotriose are shown in Fig. 6-1. Cellobiohydrolase I(D) cleaves both bonds of [1-^{3}H]cellotriose as shown by the formation of [1-^{3}H]glucose and [1-^{3}H]cellobiose. Bond cleavage frequency analysis indicates that bond 1 and 2 are cleaved with a frequency of 0.30 and 0.70 at 1 mM [1-^{3}H]cellotriose, respectively (Fig. 6-2). Furthermore, the ratio of [1-^{3}H]glucose to [1-^{3}H]cellobiose remains constant through 80 percent hydrolysis of [1-^{3}H]cellotriose. This indicates that [1-^{3}H]cellobiose is not further degraded by CBH I(D). However, the ratio of [1-^{3}H]glucose to [1-^{3}H]cellobiose changes as a function of concentration of [1-^{3}H]cellotriose. At 15 μM [1-^{3}H]cellotriose, the bond cleavage frequencies yielding [1-^{3}H]glucose and [1-^{3}H]cellobiose are 0.94 and 0.06, respectively; whereas at 50 mM [1-^{3}H]cellotriose, the corresponding frequencies are 0.67 and 0.33 (Fig. 6-3).

Initial rates of hydrolysis determined from 15 μM to 50 mM [1-^{3}H]cellotriose were used to construct the Eadie-Hofstee plot shown in Fig. 6-4. Values of K_m and V_{max} were determined to be 9.0 ± 4.5 μM and 0.016 ± 0.002 μmol/min/mg, respectively, for the high affinity site. Values of K_m and V_{max} for the low affinity site are 3400 ± 600 μM and 0.26 ± 0.02 μmol/min/mg, respectively.

The presence of high and low affinity sites may represent (1) the presence of two enzymes in the preparation, (2) two binding sites on CBH I(D) or (3) the formation of

Figure 6-1 Time course hydrolysis of [1-^{3}H]cellotriose by CBH I(D)

Cellobiohydrolase I(D) (13 μg) was incubated in 100 μl of 5 mM sodium acetate buffer, pH 5.0, containing 1 mM [1-^{3}H]cellotriose. Samples were removed from the reaction mixture after various intervals and analyzed using TLC as described in Experimental Procedures. The early, linear region of [1-^{3}H]cellotriose degradation curve yielded the initial velocity. The curves represent the distribution of [1-^{3}H]glucose (o), [1-^{3}H]cellobiose (•) and [1-^{3}H]cellotriose (□).

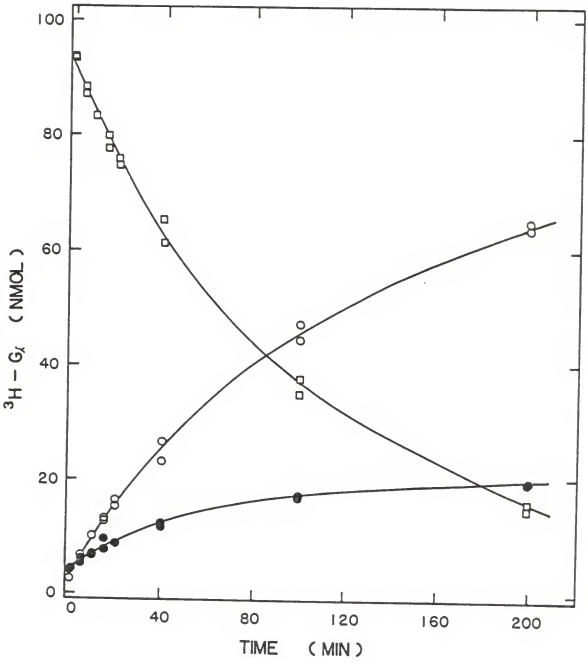
100
80
60
40
20
0
$^3H - G_\alpha$ (NMOL)
0
40
80
120
160
200
TIME (MIN)

Figure 6-2 Bond cleavage frequency plot for hydrolysis of [1-^{3}H]cellotriose by CBH I(D)

Cellobiohydrolase I(D) (13 µg) was incubated in 100 µl of 5 mM sodium acetate buffer, pH 5.0, containing 1 mM [1-^{3}H]cellotriose. Samples were removed from the reaction mixture after various intervals and analyzed using TLC as described in Experimental Procedures. The slope of each line is the bond cleavage frequency of the substrate bond yielding the product (Gi). The curves represent the product ratios of [1-^{3}H]glucose (o) and [1-^{3}H]cellobiose (●) and the substrate ratio of [1-^{3}H]cellotriose (□).

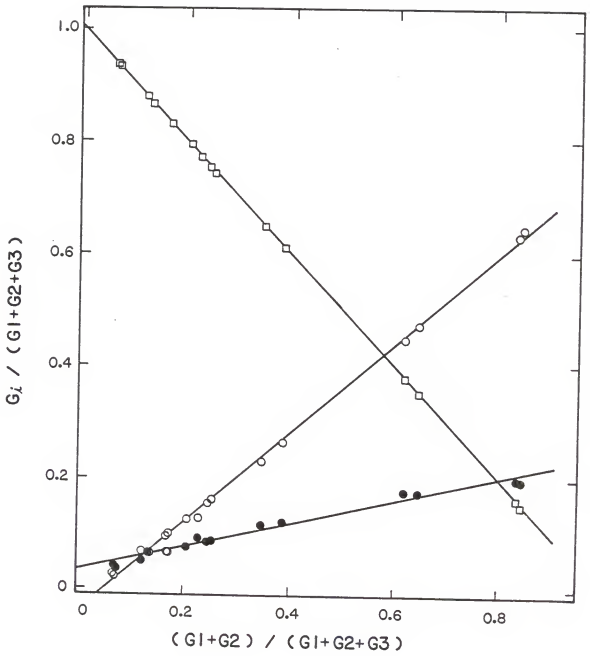
1.0
0.8
0.6
0.4
0.2
0
0
0.2
0.4
0.6
0.8
Gi / (G1+G2+G3)
(G1+G2) / (G1+G2+G3)

Figure 6-3 Effect of [1-^{3}H]cellotriose concentration on product ratios

The initial product ratios from [1-^{3}H]cellotriose degradation by CBH I(D) are shown as a function of initial [1-^{3}H]cellotriose concentration (0.015-50 mM). The curves represent the initial product ratios of [1-^{3}H]glucose (o) and [1-^{3}H]cellobiose (●).

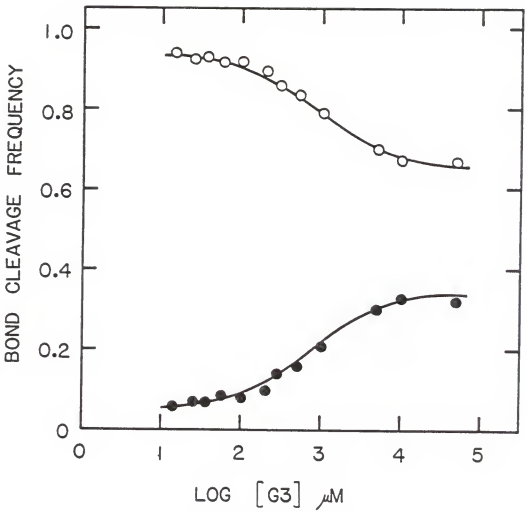
BOND CLEAVAGE FREQUENCY
1.0
0.8
0.6
0.4
0.2
0
0
1
2
3
4
5
LOG [G3] μM

Figure 6-4 Eadie-Hofstee plot for hydrolysis of [1-^{3}H]cellotriose hydrolysis by CBH I(D)

Initial rates for hydrolysis of [1-^{3}H]cellotriose (0.015-50 mM) by CBH I(D) were used to construct the Eadie-Hofstee plot.

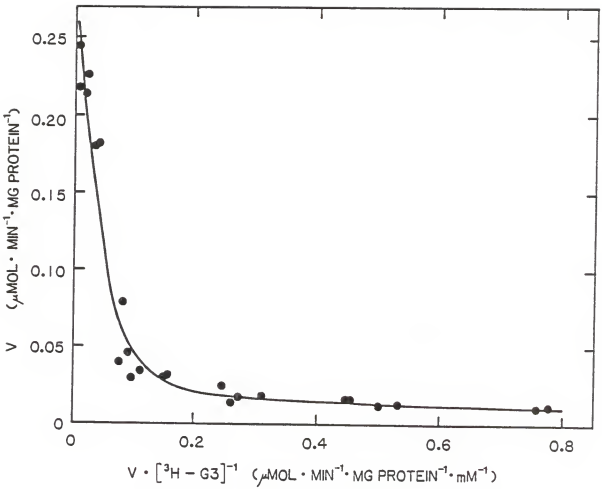
0.25
0.20
0.15
0.10
0.05
0
V (μMOL · MIN⁻¹ · MG PROTEIN⁻¹)
0
0.2
0.4
0.6
0.8
V · [³H – G3]⁻¹ (μMOL · MIN⁻¹ · MG PROTEIN⁻¹ · mM⁻¹)

transfer or condensation products at high concentrations of substrate. Cellobiohydrolase I(D) has been shown to be pure by polyacrylamide disc gel electrophoresis, sodium dodecyl sulfate polyacrylamide disc gel electrophoresis, isoelectric focusing and sedimentation equilibrium centrifugation (6). Cellobiohydrolase I(D) also migrates as a single, symmetric peak on a Sephadex G-100 gel filtration column (2.5x100 cm)(data not shown). Nevertheless, the presence of a contaminating enzyme is difficult to rule out completely. Since recovery of [1-^{3}H]cellooligosaccharides was constant at each time interval, the formation of transfer or condensation products is unlikely. However, the TLC method may not resolve putative transfer or condensation products. Transfer and condensation products have also not been detected during HPLC analysis of cellotriose hydrolysis catalyzed by CBH I(D). Since the active site of cellobiohydrolase I(D) may consist of a series of subsites, it is possible that at high concentrations of [1-^{3}H]cellotriose (>5 mM) another molecule of [1-^{3}H]cellotriose may bind nonproductively and influence both the rate of catalysis and bond cleavage frequencies. However, concentration of cellotriose during saccharification of cellulose has been estimated to be less than 1 mM (14). The binding of 2 molecules of trisaccharide has been proposed to explain similar dependence of bond cleavage frequencies on concentration of trisaccharide for A. oryzae α-amylase (99) and an endo-1,4-ß-xylanase from C. albidus (82).

Cellobiohydrolase I(D) primarily cleaves [1-^{3}H]cellotetraose at bonds 2 and 3 forming [1-^{3}H]cellobiose and [1-^{3}H]glucose (Fig. 6-5). Bond cleavage frequency analysis showing a linear relationship between product ratios and extent of reaction throughout the reaction demonstrates that the mode of action does not change with time (Fig. 6-6). Bond cleavage frequencies yielding [1-^{3}H]glucose, [1-^{3}H]cellobiose and [1-^{3}H]cellotriose were determined to be 0.19, 0.80 and 0.01, respectively. In contrast to the dependence of bond cleavage frequencies on concentration of [1-^{3}H]cellotriose, bond cleavage frequencies were independent of the concentration of [1-^{3}H]cellotretraose. This suggests that the active site of CBH I(D) comprises less than eight subsites, and may not accomodate 2 molecules of cellotetraose.

Linear Lineweaver-Burk and Eadie-Hofstee plots were constructed using initial rates of hydrolysis of [1-^{3}H]cellotetraose at concentrations from 0.5 to 15 μM (Fig. 6-7). Values of K_m and V_{max} for hydrolysis of [1-^{3}H]cellotetraose are 3.1 ± 0.2 μM and 1.51 ± 0.05 μmol/min/mg, respectively. In contrast to the high and low affinity sites evaluated during hydrolysis of [1-^{3}H]cellotriose, the binding of [1-^{3}H]cellotetraose is described by one set of K_m and V_{max} values. No evidence was obtained for a low affinity site at substrate concentration up to 1 mM.

The time course of CBH I(D) hydrolysis of [1-^{3}H]cellopentaose is shown in Fig. 6-8. Cellobiohydrolase I(D)

Figure 6-5 Time course hydrolysis of [1-^{3}H]cellotetraose by CBH I(D)

Cellobiohydrolase I(D) (4.5 ng) was incubated in 100 µl of 5 mM sodium acetate buffer, pH 5.0, containing 1 µM [1-^{3}H]cellotetraose. Samples were removed from the reaction mixture after various intervals and analyzed using TLC as described in Experimental Procedures. The early, linear region of [1-^{3}H]cellotetraose degradation curve yielded the initial velocity. The curves represent the distribution of [1-^{3}H]glucose (o), [1-^{3}H]cellobiose (●), [1-^{3}H]cellotriose (□) and [1-^{3}H]cellotetraose (■).

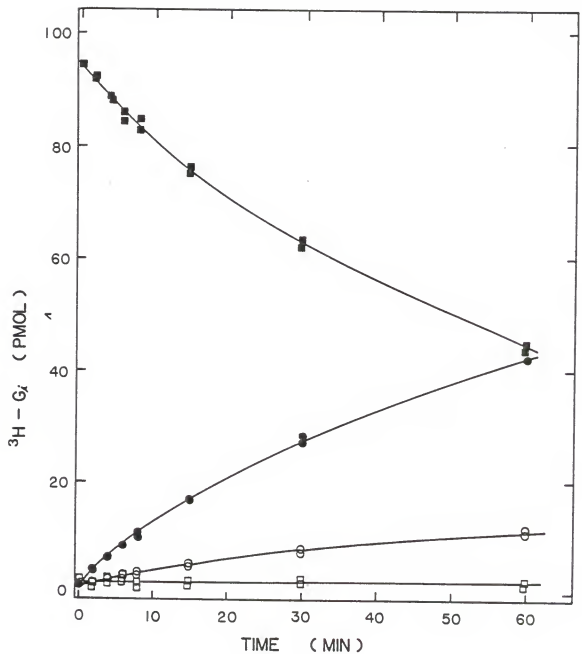
100
80
60
40
20
0
0
10
20
30
40
50
60
TIME (MIN)
$^3H - G_i$ (PMOL)

Figure 6-6 Bond cleavage frequency plot for hydrolysis of [1-^{3}H]cellotetraose by CBH I(D)

Cellobiohydrolase I(D) (4.5 ng) was incubated in 100 µl of 5 mM sodium acetate buffer, pH 5.0, containing 1 µM [1-^{3}H]cellotetraose. Samples were removed from the reaction mixture after various intervals and analyzed using TLC as described in Experimental Procedures. The slope of each line is the bond cleavage frequency of the substrate bond yielding the product (Gi). The curves represent the product ratios of [1-^{3}H]glucose (o), [1-^{3}H]cellobiose (●) and [1-^{3}H]cellotriose (□) and the substrate ratio of [1-^{3}H]cellotetraose (■).

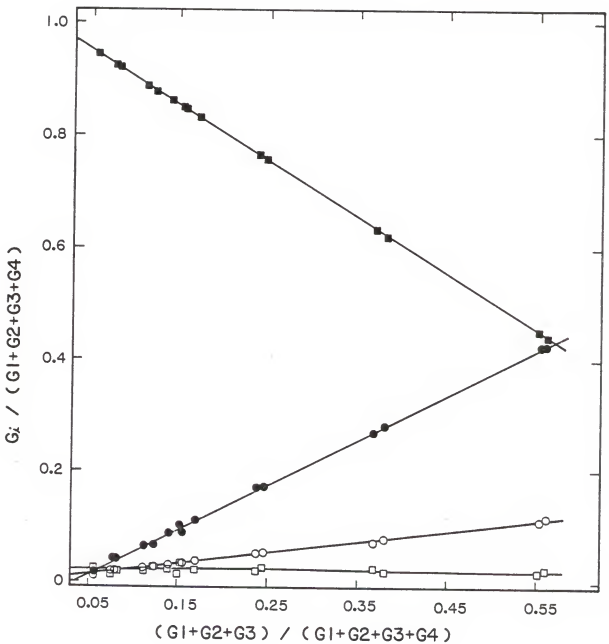
1.0
0.8
0.6
0.4
0.2
0
Gi / (G1+G2+G3+G4)
0.05
0.15
0.25
0.35
0.45
0.55
(G1+G2+G3) / (G1+G2+G3+G4)

Figure 6-7 Lineweaver-Burk and Eadie-Hofstee plots for hydrolysis of [1-^{3}H]cellotetraose by CBHI(D)

Initial rates for hydrolysis of [1-^{3}H]cellotetraose (0.5-15 μM) by CBH I(D) were used to construct Lineweaver-Burk (A) and Eadie-Hofstee (B) plots.

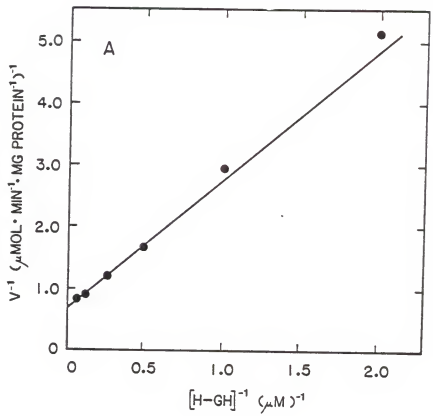
A
5.0
4.0
3.0
2.0
1.0
0
0.5
1.0
1.5
2.0
V⁻¹ (μMOL• MIN⁻¹• MG PROTEIN⁻¹)⁻¹
[H-GH]⁻¹ (μM)⁻¹

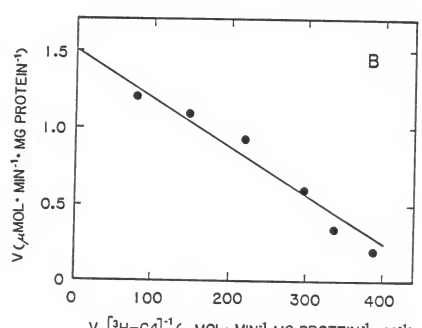
B
1.5
1.0
0.5
0
100
200
300
400
V (μMOL• MIN⁻¹• MG PROTEIN⁻¹)
V [³H-G4]⁻¹ (μMOL• MIN⁻¹• MG PROTEIN⁻¹• mM⁻¹)

Figure 6-8 Time course hydrolysis of [1-^{3}H]cellopentaose by CBH I(D)

Cellobiohydrolase I(D) (3.8 ng) was incubated in 100 µl of 5 mM sodium acetate buffer, pH 5.0, containing 2.5 µM [1-^{3}H]cellopentaose. Samples were removed from the reaction mixture after various intervals and analyzed using TLC as described in Experimental Procedures. The early, linear region of [1-^{3}H]cellopentaose degradation curve yielded the initial velocity. The curves represent the distribution of [1-^{3}H]glucose (o), [1-^{3}H]cellobiose (●), [1-^{3}H]cellotriose (□), [1-^{3}H]cellotetraose (■) and [1-^{3}H]cellopentaose (Δ).

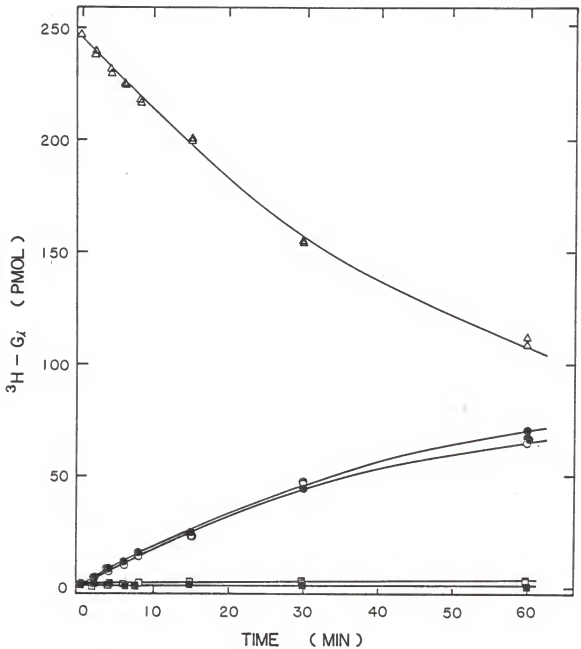
250
200
150
100
50
0
0
10
20
30
40
50
60
TIME (MIN)
$^3H - G_i$ (PMOL)

cleaves primarily bonds 3 and 4 forming [1-^{3}H]glucose and [1-^{3}H]cellobiose, respectively. Initial bond cleavage frequencies yielding [1-^{3}H]glucose, [1-^{3}H]cellobiose, [1-^{3}H]cellotriose and [1-^{3}H]cellotetraose were determined to be 0.480, 0.513, 0.02 and <0.005, respectively (Fig. 6-9). Bond cleavage frequencies were essentially constant during the time course of the reaction and did not change from 0.25 to 5.0 μM [1-^{3}H]cellopentaose.

Initial velocities obtained from the early, linear region of the time course of hydrolysis of [1-^{3}H]cellopentaose were used to construct linear Lineweaver-Burk and Eadie-Hofstee plots (Fig. 6-10). Values of K_m and V_{max} were determined to be 0.52 ± 0.04 μM and 1.26 ± 0.03 μmol/min/mg.

Products formed during CBH I(D)-catalyzed hydrolysis of [1-^{3}H]cellohexaose is shown in Fig. 6-11. This cellobiohydrolase preferentially cleaves bonds 4 and 5 producing [1-^{3}H]cellobiose and [1-^{3}H]glucose. Initial bond cleavage frequencies derived from the slopes of product ratios versus extent of reaction for [1-^{3}H]glucose, [1-^{3}H]cellobiose, [1-^{3}H]cellotriose, [1-^{3}H]cellotetraose and [1-^{3}H]cellopentaose are 0.62, 0.35, 0.025, 0.005 and <0.005, respectively (Fig. 6-12). Bond cleavage frequencies did not appreciably change during the time course of hydrolysis. Initial bond cleavage frequencies were also constant over a range of substrate concentration from 0.25 μM to 2.5 μM.

The early, linear region of the time course of [1-^{3}H]cellohexaose hydrolysis yielded initial rates used to

Figure 6-9 Bond cleavage frequency plot for hydrolysis of [1-^{3}H]cellopentaose by CBH I(D)

Cellobiohydrolase I(D) (3.8 ng) was incubated in 100 µl of 5 mM sodium acetate buffer, pH 5.0, containing 2.5 µM [1-^{3}H]cellopentaose. Samples were removed from the reaction mixture after various intervals and analyzed using TLC as described in Experimental Procedures. The slope of each line is the bond cleavage frequency of the substrate bond yielding the product (Gi). The curves represent the product ratios of [1-^{3}H]glucose (o), [1-^{3}H]cellobiose (●), [1-^{3}H]cellotriose (□) and [1-^{3}H]cellotetraose (■) and the substrate ratio of [1-^{3}H]cellopentaose (Δ).

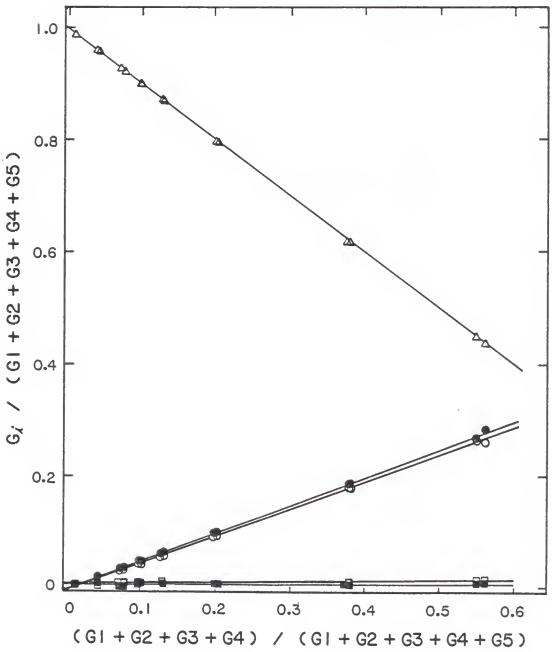
1.0
0.8
0.6
0.4
0.2
0
0
0.1
0.2
0.3
0.4
0.5
0.6
Gi / (G1 + G2 + G3 + G4 + G5)
(G1 + G2 + G3 + G4) / (G1 + G2 + G3 + G4 + G5)

Figure 6-10 Lineweaver-Burk and Eadie-Hofstee plots for hydrolysis of [1-^{3}H]cellopentaose by CBH I(D)

Initial rates for hydrolysis of [1-^{3}H]cellopentaose (0.25-5 μM) were used to construct Lineweaver-Burk (A) and Eadie-Hofstee (B) plots.

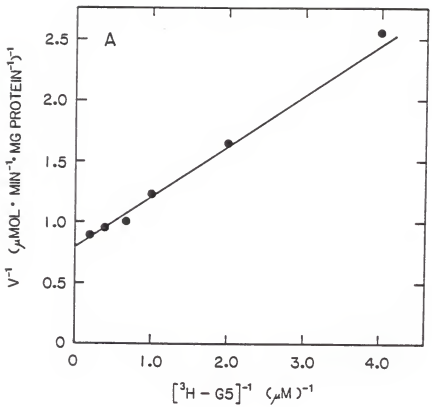
A
2.5
2.0
1.5
1.0
0.5
0
0
1.0
2.0
3.0
4.0
V⁻¹ (μMOL • MIN⁻¹• MG PROTEIN⁻¹)⁻¹
[³H – G5]⁻¹ (μM)⁻¹

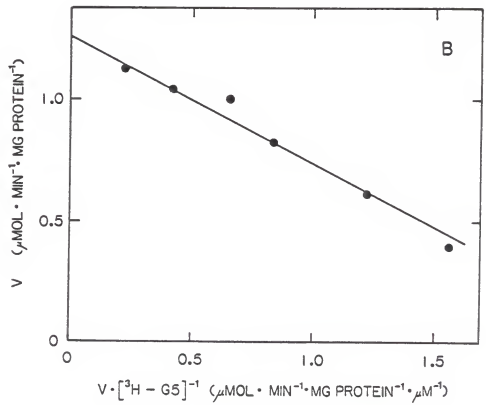
B
1.0
0.5
0
0
0.5
1.0
1.5
V (μMOL • MIN⁻¹• MG PROTEIN⁻¹)
V • [³H – G5]⁻¹ (μMOL • MIN⁻¹• MG PROTEIN⁻¹ • μM⁻¹)

Figure 6-11 Time course hydrolysis of [1-^{3}H]cellohexaose by CBH I(D)

Cellobiohydrolase I(D) (3.2 ng) was incubated in 100 µl of 5 mM sodium acetate buffer, pH 5.0, containing 2.5 µM [1-^{3}H]cellohexaose. Samples were removed from the reaction mixture after various intervals and analyzed using ILC as described in Experimental Procedures. The early, linear region of [1-^{3}H]cellohexaose degradation curve yielded the initial velocity. The curves represent the distribution of [1-^{3}H]glucose (o), [1-^{3}H]cellobiose (●), [1-^{3}H]cellotriose (□), [1-^{3}H]cellotetraose (■), [1-^{3}H]cellopentaose (△) and [1-^{3}H]cellohexaose (▲).

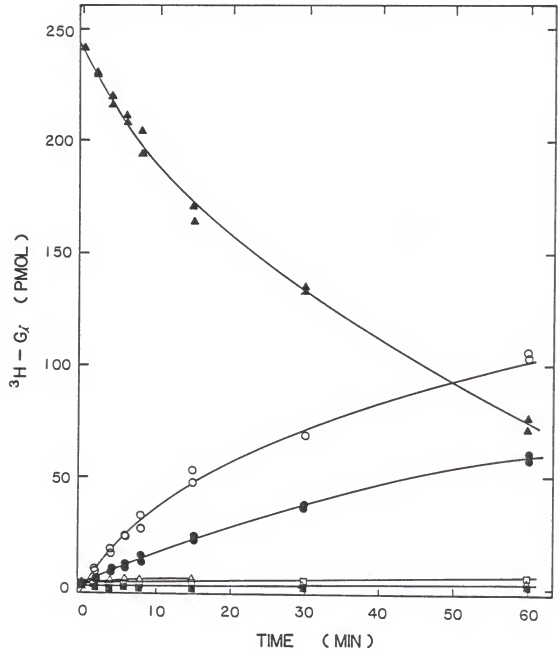
250
200
150
100
50
0
$^3H - G_\alpha$ (PMOL)
0
10
20
30
40
50
60
TIME (MIN)

Figure 6-12 Bond cleavage frequency plot for hydrolysis of [1-^{3}H]cellohexaose by CBH I(D)

Cellobiohydrolase I(D) (3.2 ng) was incubated in 100 µl of 5 mM sodium acetate buffer, pH 5.0, containing 2.5 µM [1-^{3}H]cellohexaose. Samples were removed from the reaction mixture after various intervals and analyzed using TLC as described in Experimental Procedures. The slope of each line is the bond cleavage frequency of the substrate bond yielding the product (Gi). The curves represent the product ratios of [1-^{3}H]glucose (o), [1-^{3}H]cellobiose (●), [1-^{3}H]cellotriose (□), [1-^{3}H]cellotetraose (■) and [1-^{3}H]cellopentaose (△) and the substrate ratio of [1-^{3}H]cellohexaose (▲).

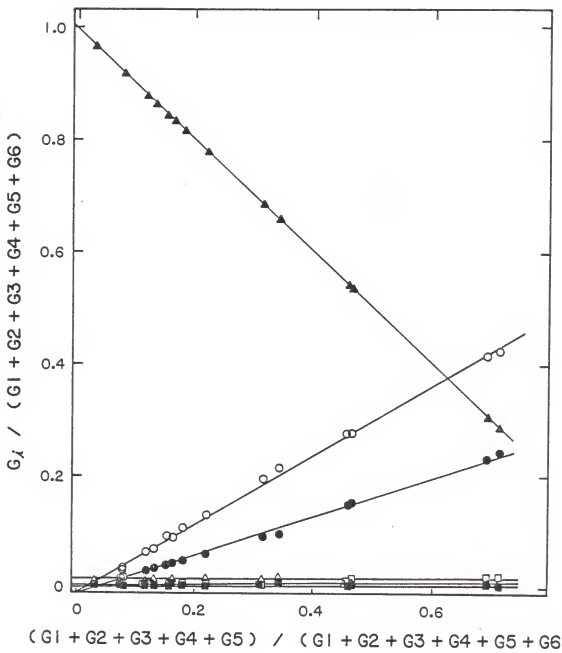
1.0
0.8
0.6
0.4
0.2
0
0
0.2
0.4
0.6
Gi / (G1 + G2 + G3 + G4 + G5 + G6)
(G1 + G2 + G3 + G4 + G5) / (G1 + G2 + G3 + G4 + G5 + G6)

construct linear Lineweaver-Burk and Eadie-Hofstee plots (Fig. 6-13). Values of K_m and V_{max} for hydrolysis of [1-^{3}H]cellohexaose are 1.1 ± 0.2 μM and 2.7 ± 0.2 μmol/min/mg, respectively.

Initial bond cleavage frequencies of CBH I(D) catalyzed hydrolysis of [1-^{3}H]cellotriose through [1-^{3}H]cellohexaose are summarized in Fig. 6-14. Although the major point of cleavage changes with each [1-^{3}H]cellooligosaccharide, CBH I(D) shows a strong preference for the reducing end. Cellobiohydrolases reportedly remove cellobiosyl residues from the nonreducing end (36); however, CBH I(D) may attack cellulosic substrates from the opposite direction. Since nonlabeled products were not monitored in these experiments, the assignment of processivity to one and only one direction cannot be demonstrated conclusively. Double label experiments with combined [1-^{3}H]cellooligosaccharides and [^{14}C-U]cellooligosaccharides described below provide more information regarding processivity.

The change seen in bond cleavage frequencies with concentration of [1-^{3}H]cellotriose may result from the binding of a second molecule of [1-^{3}H]cellotriose to subsites which bind glucosyl residues toward the nonreducing end of cellooligosaccharides. In order to favor cleavage at bond 1, [1-^{3}H]cellotriose must shift one subsite over toward the reducing end. At high concentrations, [1-^{3}H]cellotriose may compete for the mutual subsite and influence the bond cleavage frequencies. If each glucosyl residue of the

Figure 6-13 Lineweaver-Burk and Eadie-Hofstee plots for hydrolysis of [1-^{3}H]cellohexaose by CBH I(D)

Initial rates for hydrolysis of [1-^{3}H]cellohexaose (0.25-2.5 μM) by CBH I(D) were used to construct Lineweaver-Burk (A) and Eadie-Hofstee (B) plots.

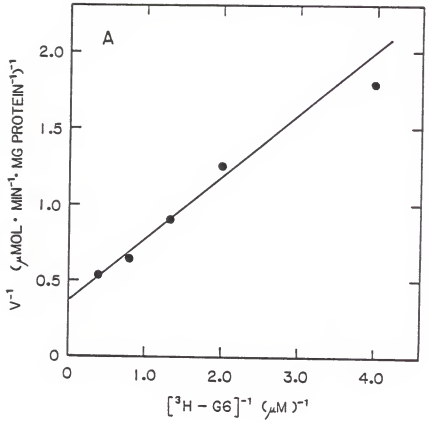
A
2.0
1.5
1.0
0.5
0
0
1.0
2.0
3.0
4.0
V^{-1} (μMOL • MIN^{-1}• MG $PROTEIN^{-1}$)$^{-1}$
$[^3H - G6]^{-1}$ (μM)$^{-1}$

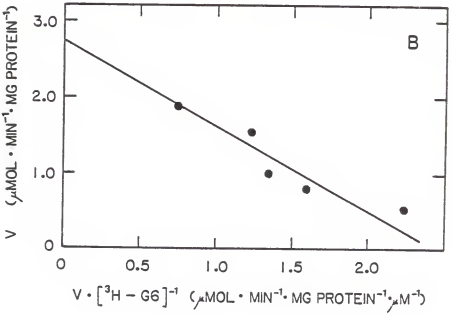
B
3.0
2.0
1.0
0
0.5
1.0
1.5
2.0
V (μMOL • MIN^{-1}• MG $PROTEIN^{-1}$)
V • $[^3H - G6]^{-1}$ (μMOL • MIN^{-1}• MG $PROTEIN^{-1}$•μM^{-1})

Figure 6-14 Bond cleavage frequencies of [1-^{3}H]cellooligosaccharide hydrolysis by CBH I(D)

Values shown are initial bond cleavage frequencies of [1-^{3}H]cellotriose (A and B), [1-^{3}H]cellotetraose (C), [1-^{3}H]cellopentaose (D) and [1-^{3}H]cellohexaose (E) hydrolysis by CBH I(D). Bond cleavage frequencies for [1-^{3}H]cellotriose were obtained at 0.015 (A) and 50 mM (B). The reducing end glucosyl residue is represented by (ø).

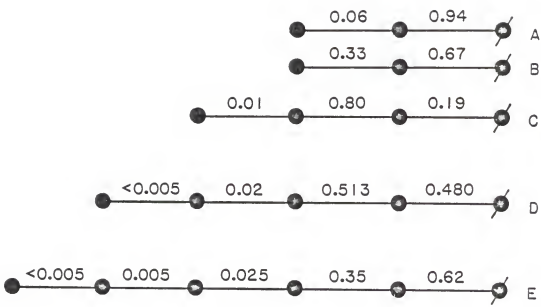
0.06
0.94
A
0.33
0.67
B
0.01
0.80
0.19
C
<0.005
0.02
0.513
0.480
D
<0.005
0.005
0.025
0.35
0.62
E

second molecule of [1-^{3}H]cellotriose binds to a specific subsite and the cleavage is catalyzed at bond 1 of the molecule bound at the above site, then a minimum of 4 subsites are located on the nonreducing side of the catalytic groups. Two molecules of substrate of chain length greater than 3 may not physically fit into the active site; therefore, initial bond cleavage frequencies of [1-^{3}H]cellotretraose through [1-^{3}H]cellohexaose are independent of concentration of substrate.

Kinetic constants determined from initial rates of hydrolysis of [1-^{3}H]cellooligosaccharides are summarized in Table 6-1. Values of K_m decrease with increasing chain length; however, the K_m of [1-^{3}H]cellohexaose is approximately 2-fold greater than that of [1-^{3}H]cellopentaose. Values of V_{max} increase with increasing chain length. A similar dependence is reflected in the V_{max}/K_m values, which apparently plateau at [1-^{3}H]cellopentaose. Reducing end-labeled cellotriose, whose value for V_{max}/K_m is 250-fold lower than that of [1-^{3}H]cellotetraose, is a poor substrate for CBH I(D). Thus, values of K_m, V_{max} and V_{max}/K_m indicate that cellobiohydrolase I(D) preferentially cleaves longer cellooligosaccharides. In contrast, the value of k_{cat}/K_m for [1-^{3}H]cellotriose hydrolysis by β-glucosidase is 170-fold higher than that for hydrolysis by CBH I(D) (Appendix F). Values of k_{cat}/K_m for [1-^{3}H]cellopentaose and [1-^{3}H]cellohexaose hydrolysis by CBH I(D) are approximately 3-fold higher than those for hydrolysis of β-glucosidase

Table 6-1

Kinetic Constants for [1-^{3}H]Cellooligosaccharide Hydrolysis by Cellobiohydrolase I(D)

Activity of cellobiohydrolase I(D) was measured at various concentrations of [1-^{3}H]cellooligosaccharides in the presence of 5 mM sodium acetate buffer, pH 5.0, containing 3 mM sodium azide. Kinetic constants were determined from initial rates of hydrolysis using Cleland's HYPER program (70).

[1-^{3}H]Cellooligosaccharide	K_m (μM)	V_{max} (μmole/min mg)	V_{max}/K_m
Cellotriose 1.	9.0 ± 4.5	0.016±0.002	$(1.8\pm0.9)\times10^{-3}$
2.	3400 ±600	0.26 ±0.02	$(7.4\pm1.4)\times10^{-5}$
Cellotetraose	3.1 ± 0.2	1.51 ±0.05	$(4.8\pm0.2)\times10^{-1}$
Cellopentaose	0.52± 0.04	1.26 ±0.03	2.4±0.2
Cellohexaose	1.1 ± 0.2	2.7 ±0.2	2.4±0.3

(Appendix F). Thus, comparing values of k_{cat}/K_m for [1-^{3}H]cellooligosaccharide hydrolysis by CBH I(D) and ß-glucosidase suggests that during the saccharification of cellulose the role of CBH I(D) is to hydrolyze longer cello-oligosaccharides, whereas the role of the ß-glucosidase is to hydrolyze cellobiose and cellotriose.

Hydrolysis of [1-^{3}H]Cellooligosaccharides and [^{14}C-U]Cellooligosaccharides

Since activity of CBH I(D) on [1-^{3}H]cellooligosaccharides does not provide information regarding the fate of unlabeled products, [^{14}C-U]cellooligosaccharides were used in conjunction with [1-^{3}H]cellooligosaccharides as substrates for CBH I(D). Products formed during the time course of hydrolysis of [1-^{3}H]cellopentaose and [^{14}C-U]cellopentaose are listed in Table 6-2. The ratio of [^{14}C-U]glucose/[1-^{3}H]glucose is approximately 1 indicating that glucose produced from cellopentaose by CBH I(D) arises exclusively from cleavage at bond 4. However, the amount of [^{14}C-U]cellotetraose produced does not equal that of [1-^{3}H]glucose or [^{14}C-U]glucose suggesting that CBH I(D) repetitively attacks cellopentaose. The efficiency of repetitive attack estimated from the concentrations of [^{14}C-U]cellotetraose and [^{14}C-U]glucose at 4 min is 97 percent for successive cleavage of bonds 4 and 2 of cellopentaose. Since essentially all glucose arises from cleavage at bond 4 and the resulting cellotetraose is immediately

Table 6-2

Hydrolysis of [1-^{3}H]Cellopentaose and [^{14}C-U]Cellopentaose by Cellobiohydrolase I(D)

Cellobiohydrolase I(D) (8.62×10^{-5} mg) was incubated at 40°C in 100 µl of 5 mM sodium acetate buffer, pH 5.0, containing 0.55 µCi of [1-^{3}H]cellopentaose and 0.22 µCi of [^{14}C-U]cellopentaose. Total concentration of cellopentaose was 83 µM.

Cellooligosaccharide	Pmol TIME (min) 0	4	8	15	60	Ratio [^{14}C-U]/[1-^{3}H]
[1-^{3}H]Glucose	0	230 ±10	420±10	670±50	1680±140	1.11 ±0.05
[^{14}C-U]Glucose	0	260 ±20	500±10	750±40	1850±120	
[1-^{3}H]Cellobiose	0	297 ± 9	539± 2	880±40	2340±180	2.39 ±0.06
[^{14}C-U]Cellobiose	0	710 ±40	1340±20	2140±80	5400±400	
[1-^{3}H]Cellotriose	0	36 ± 1	60± 2	98± 4	261± 6	8 ±1
[^{14}C-U]Cellotriose	0	293 ± 7	550±10	860±20	2170±120	
[1-^{3}H]Cellotetraose	0	<2	<2	<2	2± 11	ND[a]
[^{14}C-U]Cellotetraose	0	7 ±10	17±20	42±20	190± 20	
[1-^{3}H]Cellopentaose	8125±4	7560 ±30	7120±10	6480±90	3840±320	0.941±0.004
[^{14}C-U]Cellopentaose	7640±10	7120 ±50	6660±10	6090±50	3650±240	

[a] ND = Not determined.

cleaved at bond 2, the direction of attack must be from the reducing end (Fig. 6-15a). Repetitive attack from the nonreducing end beginning at bond 1 would have resulted in a higher ratio of [^{14}C-U]glucose/[1-^{3}H]glucose (Fig. 6-15b). Repetitive attack from the nonreducing end beginning at bond 2 would furnish [^{14}C-U]/[1-^{3}H] ratios identical to those for repetitive attack beginning at bond 4. However, repetitive attack beginning at bond 2 would produce [1-^{3}H]cellotricse, a poor substrate for CBH I(D). Cellobiose arises from initial cleavage at bonds 3 or 2 of cellopentaose and from cleavage of cellotetraose, which was produced from initial cleavage of cellopentaose. Thus, the ratio of [^{14}C-U]cellobiose/[1-^{3}H]cellobiose (2.4) results from the sum of the concentrations of [1-^{3}H]cellobiose, [1-^{3}H]cellotriose, and twice that of [1-^{3}H]glucose divided by the concentration of [1-^{3}H]cellobiose. Cellotriose is produced from cleavages at either bonds 2 or 3.

Initial rates of formation of [1-^{3}H] products and [^{14}C-U]products from CBH I(D)-catalyzed hydrolysis of [1-^{3}H]cellopentaose and [^{14}C-U]cellopentaose are listed in Table 6-3. The rates of [1-^{3}H]cellopentaose and [^{14}C-U]cellopentaose hydrolysis are within experimental error indicating the absence of a detectable kinetic isotope effect. The ratio of ^{14}C/^{3}H rates of formation of products are similar to [^{14}C-U]/[1-^{3}H] product distributions supporting the idea that these distributions of products result from the same bond cleavage frequencies.

Figure 6-15 Possible types of repetitive attack of CBH I(D) with [1-^{3}H]cellopentaose and [^{14}C-U]cellopentaose

Cellobiohydrolase I(D) may repetitively attack cellopentaose in several possible modes some of which are shown: (A) attack toward the nonreducing end initiated at bond 4 and followed by attack at bond 2, (B) attack toward the reducing end initiated at bond 1 and followed by attack at bond 3, (C) attack toward the reducing end initiated at bond 2 and followed by attack at bond 4. Bonds are numbered from the nonreducing end. The reducing end glucosyl residue is represented by (ø).

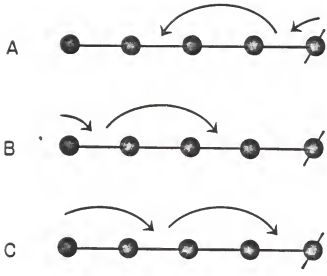
A
B
C

Table 6-3

Initial Rates of Cellobiohydrolase I(D) Activity on [1-^{3}H]Cellopentaose and [^{14}C-U]Cellopentaose

Cellobiohydrolase I(D) (8.62×10^{-5} mg) was incubated at 40°C in 100 µl of 5 mM sodium acetate buffer, pH 5.0, containing 0.55 µCi of [1-^{3}H]cellopentaose and 0.22 µCi of [^{14}C-U]cellopentaose. Total concentration of cellopentaose was 83 µM.

Cellooligosaccharide	Initial Velocity (pmol/min)	Ratio [^{14}C-U]/[1-^{3}H]
[1-^{3}H]Glucose	58 ± 3	1.12 ± 0.09
[^{14}C-U]Glucose	65 ± 4	
[1-^{3}H]Cellobiose	74 ± 2	2.40 ± 0.13
[^{14}C-U]Cellobiose	178 ± 8	
[1-^{3}H]Cellotriose	9.1 ± 0.3	8.0 ± 0.3
[^{14}C-U]Cellotriose	73 ± 2	
[1-^{3}H]Cellotetraose	-0.55 ± 0.05	ND[a]
[^{14}C-U]Cellotetraose	2 ± 3	
[1-^{3}H]Cellopentaose	-141 ± 6	0.91 ± 0.07
[^{14}C-U]Cellopentaose	-129 ± 8	

[a] ND = Not determined.

The distribution of products formed from hydrolysis of [^{14}C-U]cellohexaose and [1-^{3}H]cellohexaose is shown in Table 6-4. The ratio of [^{14}C-U]glucose/[1-^{3}H]glucose is approximately 1 indicating that glucose is produced exclusively from hydrolysis at bond 5 of cellohexaose. Formation of [^{14}C-U]cellopentaose was negligible and did not correspond with the formation of [1-^{3}H]glucose indicating that CBH I(D) repetitively attacks cellohexaose after initiating cleavage at bond 5. The distribution of [^{14}C-U]cellotriose is similar to that of [1-^{3}H]glucose and [^{14}C-U]glucose indicating that cellopentaose, which results from initial cleavage of cellohexaose at bond 5, is cleaved to cellobiose and cellotriose (Fig. 6-16a). Although cellobiose and cellotriose may be produced from cleavage at either bond 2 or 3 of the resulting cellopentaose, bond cleavage frequencies of cellopentaose (Fig. 6-14) suggest that bond 3 is more likely to be cleaved than bond 2. The accumulation of cellotriose supports the idea that it is a poor substrate even when formed in the active site of CBH I(D). Cellobiose is formed from cellohexaose by three routes: (1) cleavage of cellopentaose, which was initially formed from cleavage at bond 5 of cellohexaose (Fig. 6-16a), (2) cleavage at bond 4 of cellohexaose (Fig. 6-16b) and (3) cleavage of cellotetraose, which was initially formed from cleavage at bond 4 of cellohexaose (Fig. 6-16b). The ratio of 4.6 for [^{14}C-U]cellobiose/[1-^{3}H]cellobiose results from the sum of concentrations of [1-^{3}H]glucose and 3 times that of

Table 6-4

Hydrolysis of [1-^{3}H]Cellohexaose and [^{14}C-U]Cellohexaose by Cellobiohydrolase I(D)

Cellobiohydrolase I(D) (6.19×10^{-5} mg) was incubated at 40°C in 100 µl of 5 mM sodium acetate buffer, pH 5.0, containing 0.55 µCi of [1-^{3}H]cellohexaose and 0.19 µCi of [^{14}C-U]cellohexaose. Total concentration of cellohexaose was 59 µM.

Cellooligosaccharide	Pmol TIME (min) 0	4	8	15	60	Ratio [^{14}C-U]/[1-^{3}H]
[1-^{3}H]Glucose	0	280± 2	440 ±20	670±20	1690 ± 50	1.10±0.02
[^{14}C-U]Glucose	0	300±20	470 ± 4	750± 6	1880 ± 30	
[1-^{3}H]Cellobiose	0	140± 7	226 ± 4	350±10	930 ± 40	4.6 ±0.2
[^{14}C-U]Cellobiose	0	640±20	1030 ±40	1600±10	3990 ±150	
[1-^{3}H]Cellotriose	0	22± 1	34 ± 4	58± 1	170 ± 10	14.7 ±0.2
[^{14}C-U]Cellotriose	0	338± 4	540 ±20	810±10	2090 ± 40	
[1-^{3}H]Cellotetraose	0	10± 1	16.1± 0.1	23± 1	71.0± 0.4	3.8 ±0.9
[^{14}C-U]Cellotetraose	0	40±20	47 ± 6	84± 7	216 ± 5	
[1-^{3}H]Cellopentaose	0	70±60	39 ± 1	140±60	120 ± 20	0.5 ±0.2
[^{14}C-U]Cellopentaose	0	40±70	12.0± 0.2	110±70	50 ± 30	
[1-^{3}H]Cellohexaose	5840±0	5320±50	5090 ±20	4610±30	2870±120	0.86±0.03
[^{14}C-U]Cellohexaose	5194±0	4700±60	4460 ±20	3980±60	2320±100	

Figure 6-16 Possible types of repetitive attack of CBH I(D) with [1-^{3}H]cellohexaose and [^{14}C-U]cellohexaose

Cellobiohydrolase I(D) repetitively attacks cellohexaose in 2 possible modes: (A) attack toward the nonreducing end initiated at bond 5 and followed by attack at bond 3, (B) attack toward the nonreducing end initiated at bond 4 and followed by attack at bond 2. Bonds are numbered from the nonreducing end. The reducing end glucosyl residue is represented by (ø).

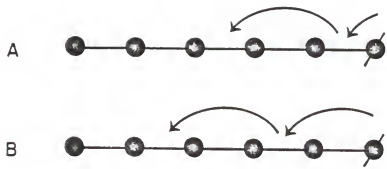
A
B

[1-^{3}H]cellobiose divided by the concentration of [1-^{3}H]cellobiose. The efficiency of repetitive attack initiated at bond 5 of cellohexaose and estimated from the concentration of [^{14}C-U]cellopentaose at 60 min is 97 percent. The efficiency of repetitive attack initiated at bond 4 of cellohexaose and estimated from the concentration of [^{14}C-U]cellotetraose excluding [1-^{3}H]cellotetraose is approximately 82 percent. The [^{14}C-U]cellotriose/[1-^{3}H]cellotriose ratio of 14.7 results from the sum of the concentrations of 2 times [1-^{3}H]cellotriose and [1-^{3}H]glucose divided by [1-^{3}H]cellotriose. Cellobiohydrolase I(D) exhibits little tendency to cleave bonds 1 and 2 of cellohexaose.

Initial rates of formation of products from CBH I(D)-catalyzed hydrolysis of [1-^{3}H]cellohexaose and [^{14}C-U]cellohexaose are within experimental error indicating the absence of a detectable kinetic isotope effect (Table 6-5). The ratios of formation of [^{14}C-U]/[1-^{3}H] products are similar to ratios of [^{14}C-U]/[1-^{3}H] product distributions supporting that the distribution of products results from the same initial cleavage frequencies.

The activity of CBH I(D) on [^{14}C-U] and [1-^{3}H]cellooligosaccharides indicates that CBH I(D) repetitively attacks long cellooligosaccharides from the reducing end. Cellobiohydrolase I(D) was shown by van Tilbeurgh et al. (30) to preferentially hydrolyze 4-methylumbelliferyl glycosides of cellooligosaccharides at the reducing end. Since

Table 6-5

Initial Rates of Hydrolysis of Cellobiohydrolase I(D) Activity on [1-^{3}H]Cellohexaose and [^{14}C-U]Cellohexaose

Cellobiohydrolase I(D) (8.62×10^{-5} mg) was incubated at 40°C in 100 µl of 5 mM sodium acetate buffer, pH 5.0, containing 0.55 µCi of [1-^{3}H]cellohexaose and 0.19 µCi of [^{14}C-U]cellohexaose. Total concentration of cellohexaose was 59 µM.

Cellooligosaccharide	Initial Velocity (pmol/min)	Ratio [^{14}C-U]/[1-^{3}H]
[1-^{3}H]Glucose	70.0 ± 0.6	1.08 ± 0.07
[^{14}C-U]Glucose	76 ± 5	
[1-^{3}H]Cellobiose	35 ± 2	4.6 ± 0.3
[^{14}C-U]Cellobiose	161 ± 4	
[1-^{3}H]Cellotriose	5.5 ± 0.3	15.4 ± 0.8
[^{14}C-U]Cellotriose	84.6 ± 0.8	
[1-^{3}H]Cellotetraose	2.5 ± 0.2	3.8 ± 1.6
[^{14}C-U]Cellotetraose	9.6 ± 4	
[1-^{3}H]Cellopentaose	18 ± 14	0.53 ± 0.99
[^{14}C-U]Cellopentaose	10 ± 17	
[1-^{3}H]Cellohexaose	-130 ± 10	0.94 ± 0.16
[^{14}C-U]Cellohexaose	-120 ± 20	

no evidence for repetitive attack or direction of attack was reported, products resulting from 4-methylumbelliferyl glycoside hydrolysis may not represent initial products. Examination of the frequency at which CBH I(D) of T. viride cleaves reduced cellooligosaccharides revealed little tendency to hydrolyze bonds linking the sorbityl residue at the former reducing end of the substrate (98). High performance liquid chromatographic analysis of cellooligosaccharide hydrolysis also showed that CBH I(D) repetitively attacks longer cellooligosaccharides (6).

Subsite Mapping of Cellobiohydrolase I(D)

Two methods are available in the literature to evaluate subsite affinities of polysaccharide depolymerases which bind substates in more than one productive mode. The method of Suganuma et al. (45) uses V_{max}/K_m values and bond cleavage frequencies for a series of cellooligosaccharides to estimate subsite affinities. The method of Allen and Thoma (49) uses bond cleavage frequencies to estimate subsite affinities; however, they also require values for K_m, V_{max} and K_{int}. (The dissociation constant for a substrate that completely spans the catalytic site is termed K_{int}.) Equations pertinent to the method of Suganuma et al. (45) and Allen and Thoma (49) are presented in Appendix A.

Subsite affinities calculated by the method of Suganuma et al. (45) using the major bond cleavage frequencies and values of V_{max}/K_m for a series of cellooligosaccharides are listed in Table 6-6. Only major bond cleavage frequencies

Table 6-6

Subsite Affinities of CBH I(D) Calculated Using Values of V_{max}/K_m and Bond Cleavage Frequencies From [1-^{3}H]Cellooligosaccharides

Numbers in brackets indicate mode of calculation using bond cleavage frequencies of cellooligosaccharides at glycosidic bonds denoted by superscripts in parentheses.

Subsite	Mode of Calculation	Subsite Affinity (cal/mol)
1	$[G_5^{(4)}/G_6^{(5)}]$	-160± 80
2	$[G_4^{(3)}/G_5^{(4)}]$	-1580± 30
	$[G_5^{(3)}/G_6^{(4)}]$	230± 90
3	$[G_3^{(2)}/G_4^{(3)}]$	-2500±300
	$[G_4^{(2)}/G_5^{(3)}]$	-730± 50
4	$[G_3^{(1)}/G_4^{(2)}]$	-5100±400
7	$[G_3^{(2)}/G_4^{(2)}]$	-3400±300
	$[G_4^{(3)}/G_5^{(3)}]$	-1620± 80
	$[G_5^{(4)}/G_6^{(4)}]$	190± 30

were used because they are less susceptible to error. The active site of CBH I(D) consists of 7 subsites with catalytic groups located between subsites 5 and 6 (Fig. 6-17). Affinities of subsites 2, 3 and 7 were calculated using more than one combination of V_{max}/K_m values and bond cleavage frequencies for cellooligosaccharides differing in length by one glucosyl residue. The various combinations used to calculate subsite affinities are listed in Table 6-6 and subsite affinities are shown in Fig. 6-17. Since subsites 5 and 6 are common to all productive complexes, their subsite affinities cannot be evaluated by this method. The significant affinity of subsites 1 through 4 for glucosyl residues is consistent with a repetitive attack mode of CBH I(D) toward the nonreducing end of cellooligosaccharides. For example, after hydrolysis of bond 5 of cellohexaose, subsites 1-4 would strongly bind cellopentaose. When product glucose dissociates from the active site, the bound cellopentaose would relocate into subsites 3-7 without leaving the active site. Cellopentaose would then be cleaved at bond 3 forming cellobiose and cellotriose.

The method of Suganuma et al. (45) permits calculation of a particular subsite affinity from various combinations of bond cleavage frequencies and V_{max}/K_m values for n-mer and n+1-mer oligosaccharides. However, differences of up to 1800 cal/mole were obtained when affinities for subsites 2, 3 and 7 were calculated for CBH I(D). Since the method of Suganuma et al. (45) provides no means to evaluate the

Figure 6-17 Subsite map for CBH I(D) constructed using values of V_{max}/K_m and bond cleavage frequencies for [1-^{3}H]cellooligosaccharides

Subsite affinities were estimated using the method of Suganuma et al. (45) from values of V_{max}/K_m and bond cleavage frequencies for [1-^{3}H]cellooligosaccharide hydrolysis by CBH I(D). The arrow shows the position of the catalytic groups. Since subsites adjacent to catalytic groups are common to all productive complexes, their affinities cannot be evaluated using this method. Shaded bars indicate that more than one combination of V_{max}/K_m values and bond cleavage frequencies for [1-^{3}H]cellooligosaccharides differing in chain length by one glucosyl residue were used to evaluate affinities at a particular subsite (Table 6-6).

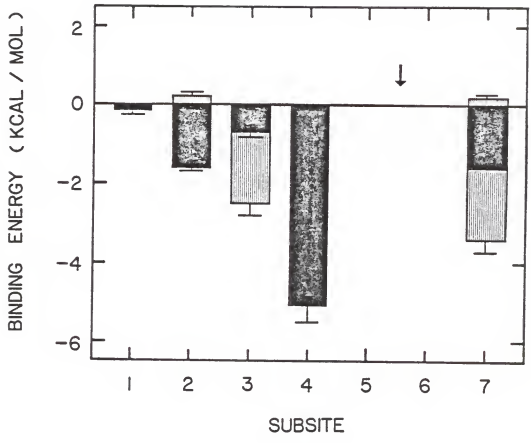
BINDING ENERGY (KCAL / MOL)
2
0
-2
-4
-6
1
2
3
4
5
6
7
SUBSITE

reliability of a particular affinity, the three estimates which range from -176 to 3431 cal/mol, for the affinity of subsite 7 suggest that the method of Suganuma et al. (45) is not adequate to evaluate subsite affinities of CBH I(D).

The subsite map constructed using the computer model for depolymerases developed by Allen and Thoma (49) was first optimized to account for bond cleavage frequencies and location of catalytic groups. Then, subsite affinities were optimized using experimental values of K_m and V_{max} for [1-^{3}H]cellotriose through [1-^{3}H]cellohexaose. Values of K_m and V_{max} for the high affinity site detected during [1-^{3}H]cellotriose hydrolysis were used in the calculations because they are more relevant to concentrations of cellotriose usually encountered during depolymerization of cellulose. Previously determined inhibition constants for glucose (0.476 M) and cellobiose (90.4 μM) (31) and apparent V_{max} for hydrolysis of cellobiose (8.84×10^{-4} μmol/min/mg, data not shown) were also used in the evaluation of subsite affinities. The value of K_m observed for cellohexaose hydrolysis was used as an estimate of K_{int}.

The subsite map for CBH I(D) that gave the lowest residual error for bond cleavage frequencies, K_m, V_{max} and K_{int} is shown in Fig. 6-18. A minimum of 7 subsites with the catalytic groups located between subsites 5 and 6 were required to account for the bond cleavage frequencies. Affinities decrease in order from subsites 5-3 with significant affinity at subsites 1 and 2. The potential of

Figure 6-18 Subsite map for CBH I(D) constructed using values of K_m, V_{max} and bond cleavage frequencies for [1-^{2}H]cellooligosaccharides

The number of subsites and the position of the catalytic groups were determined using the method of Allen and Thoma (48) from values of K_m, V_{max} and bond cleavage frequencies for [1-^{2}H]cellooligosaccharides. The arrow shows the position of the catalytic groups. The bars depict the estimated binding energies including the contribution of the acceleration factor (551 cal/mol).

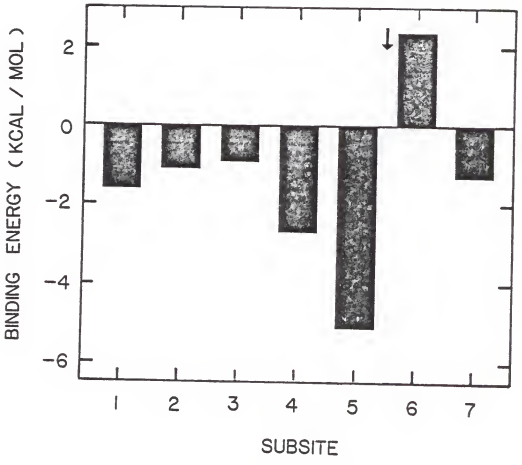
BINDING ENERGY (KCAL / MOL)
2
0
−2
−4
−6
1
2
3
4
5
6
7
SUBSITE

subsites 1-5 to bind glucosyl residues is consistent with the repetitive attack toward the nonreducing end catalyzed by CBH I(D). Unfavorable binding at subsite 6 may promote catalysis by distorting the glucosyl residue adjacent to the catalytic groups. The method of Allen and Thoma (49) permits the hydrolytic rate coefficient (k_{+2}) to vary with chain length in order to obtain good agreement between predicted and experimentally derived values of V_{max}, K_m and bond cleavage frequencies. The approximate decrease in the activation energy caused by the binding of a glycosyl residue and enhancing the rate of bond cleavage is termed the acceleration factor. Although the acceleration factor for subsites was determined to be 551 cal/mol, it only slightly improved the residuals.

The subsite maps constructed using the methods of Suganuma et al. (45) or Allen and Thoma (49) indicate that the active site of CBH I(D) is composed of 7 subsites (Figs. 6-17 and 6-18). Although each map shows favorable binding at subsites 1-4, the map constructed using the method of Suganuma et al. (45) results in different and sometimes conflicting affinities for subsites 2, 3 and 7. Discrepancies in subsite affinities calculated using the method of Suganuma et al. (45) may indicate that the hydrolytic rate coefficient (k_{+2}) for cellooligosaccharide hydrolysis is dependent on chain length of cellooligosaccharides. Suganuma et al. (45) assume that hydrolytic rate coefficients are equal.

Conclusions

Bond cleavage frequencies determined for CBH I(D)-catalyzed hydrolysis of [1-^{3}H]cellooligosaccharides indicate that CBH I(D) binds cellooligosaccharides in multiple productive modes. Furthermore, CBH I(D) preferentially hydrolyzes bonds at the reducing end of [1-^{3}H]cellotriose through [1-^{3}H]cellohexaose. Michaelis parameters for hydrolysis of [1-^{3}H]cellooligosaccharides decrease with increasing chain length demonstrating preferential binding of longer cellooligosaccharides. Activity of CBH I(D) on [^{14}C-U]cellooligosaccharides in conjunction with [1-^{3}H]cellooligosaccharides indicates that CBH I(D) repetitively attacks longer cellooligosaccharides towards the nonreducing end. Subsite maps constructed by two methods using kinetic parameters and bond cleavage frequencies show that the active site of CBH I(D) is composed of 7 subsites with catalytic groups located between subsites 5 and 6.

CHAPTER 7
MODE OF ACTION OF CELLOBIOHYDROLASE II

Introduction

The cellulase system of T. reesei comprises endoglucanases, cellobiohydrolases and ß-glucosidases which act sequentially and cooperatively to convert crystalline cellulose to glucose. Endoglucanases preferentially hydrolyze internal glycosidic bonds of cellulose producing chain ends from which cellobiohydrolases remove cellobiosyl residues. The role of the ß-glucosidase is to convert cellobiose, an inhibitor of depolymerizing enzymes, and oligosaccharides to glucose. Although the role of cellobiohydrolases in saccharification of cellulose has been demonstrated, the mode of action, the topography of the active site, the direction from which enzymes attack and the mechanism by which cellobiohydrolases synergistically degrade crystalline cellulose have not been described.

Two cellobiohydrolases [CBH I(D) and CBH II] have been purified and partially characterized from extracellular culture filtrates of T. reesei (6,7). The mode of action of CBH II has been investigated using HPLC analysis of products formed during enzymic hydrolysis of cellooligosaccharides (6). Cellobiohydrolase II exhibits a 2-fold increase in the rate of hydrolysis of cellohexaose compared to cellotetraose

and cellopentaose. Cellobiohydrolase II yields exclusively cellobiose from cellotetraose or a mixture of cellobiose and cellotriose from cellopentaose or cellohexaose. Cellobiose is produced from hydrolysis of cellohexaose without concomitant formation of cellotetraose, indicating a sequential cleavage of cellobiosyl residues. Strong synergism has been shown to exist between CBH II and CBH I(D) in depolymerizing crystalline cellulose; however, the mechanism by which synergism occurs has not been described (7). Fagerstam and Pettersson (7) have referred to this synergism as exo-exo synergism in order to distinguish it from the well-documented endo-exo synergism.

The identity of some glycosidic bonds cleaved by CBH II cannot be determined by examination of products formed during enzymic hydrolysis of cellooligosaccharides, because identical product ratios can be obtained from hydrolysis at different bonds. In this report, the action patterns resulting from CBH II hydrolysis of a series of [1-^{3}H]cello-oligosaccharides are described. In addition, the sensitivity afforded by the [1-^{3}H]cellooligosaccharides permits measurement of initial rates of hydrolysis at micromolar substrate concentrations and evaluation of Michaelis parameters. The action patterns of CBH II on [1-^{3}H]cellooligosaccharides indicate that CBH II preferentially hydrolyzes glycosidic bonds at the nonreducing end. Action patterns of CBH II on [1-^{3}H]cellohexaose suggest that cellobiosyl residues are sequentially removed from the nonreducing end.

Values of K_m, V_{max} and bond cleavage frequencies are used to construct a subsite map of CBH II.

Results and Discussion

Hydrolysis of [1-^{3}H]Cellooligosaccharides

Initial bond cleavage frequencies and initial rates of CBH II catalyzed hydrolysis of [1-^{3}H]cellooligosaccharides were determined by removing samples from enzymic digests and separating products using TLC followed by scintillation counting of zones removed from TLC plates.

Cellobiohydrolase II catalyzes the hydrolysis of [1-^{3}H]cellotriose at bond 2 (numbered from the nonreducing end) forming predominantly [1-^{3}H]glucose (Fig. 7-1). A negligible amount of [1-^{3}H]cellobiose is also produced. Bond cleavage frequency analysis indicates that bond 1 and 2 are cleaved with a frequency of 0.01 and 0.99, respectively (Fig. 7-2). Furthermore, the linear relationship between product ratios and extent of reaction indicates that the mode of action of CBH II is maintained during the time course of reaction. In contrast to the dependence of bond cleavage frequencies on initial concentration of [1-^{3}H]cellotriose observed during CBH I(D)-catalyzed hydrolysis, bond cleavage frequencies resulting from CBH II hydrolysis of [1-^{3}H]cellotriose remain essentially constant for substrate concentrations ranging from 2.5 μM to 1 mM.

Lineweaver-Burk and Eadie-Hofstee plots constructed from initial rates of hydrolysis of [1-^{3}H]cellotriose were linear from 2.5 to 50 μM (Fig. 7-3). In contrast, CBH I(D)

Figure 7-1 Time course hydrolysis of [1-^{3}H]cellotriose by CBH II

Cellobiohydrolase II (1.2 µg) was incubated in 100 µl of 5 mM sodium acetate buffer, pH 5.0, containing 25 µM [1-^{3}H]cellotriose. Samples were removed from the reaction mixture after various intervals and analyzed using TLC as described in Experimental Procedures. The early, linear region of [1-^{3}H]cellotriose degradation curve yielded the initial velocity. The curves represent the distribution of [1-^{3}H]glucose (●), [1-^{3}H]cellobiose (o) and [1-^{3}H]cellotriose (□).

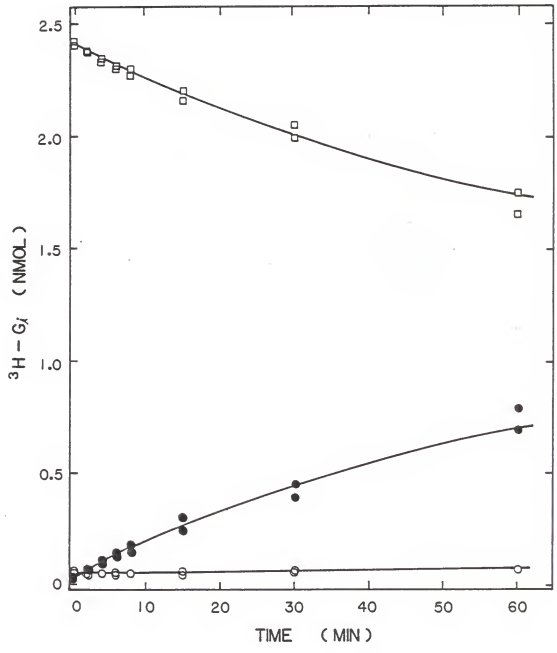
2.5
2.0
1.5
1.0
0.5
0
$^3H-G_i$ (NMOL)
0
10
20
30
40
50
60
TIME (MIN)

Figure 7-2 Bond cleavage frequency plot for hydrolysis of [1-^{3}H]cellotriose by CBH II

Cellobiohydrolase II (1.2 µg) was incubated in 100 µl of 5 mM sodium acetate buffer, pH 5.0, containing 25 µM [1-^{3}H]cellotriose. Samples were removed from the reaction mixture and analyzed using TLC as described in Experimental Procedures. The initial slope of each line is the bond cleavage frequency of the substrate bond yielding the product (Gi). The curves represent the product ratios of [1-^{3}H]glucose (●), [1-^{3}H]cellobiose (o) and [1-^{3}H]cellotriose (□).

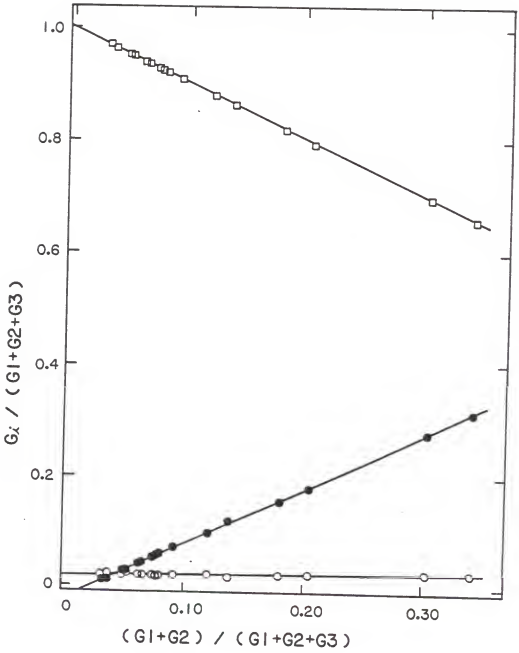
1.0
0.8
0.6
0.4
0.2
0
Gi / (G1+G2+G3)
0
0.10
0.20
0.30
(G1+G2) / (G1+G2+G3)

Figure 7-3 Lineweaver-Burk and Eadie-Hofstee plots for hydrolysis of [1-^{3}H]cellotriose by CBH II

Initial rates of hydrolysis of [1-^{3}H]cellotriose (2.5-50 μM) by CBH II were used to construct Lineweaver-Burk (A) and Eadie-Hofstee (B) plots.

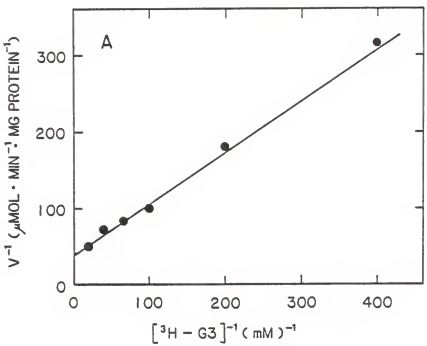
A
300
200
100
0
0
100
200
300
400
V^{-1} (μMOL · MIN^{-1}· MG PROTEIN^{-1})
$[^3H - G3]^{-1}$ (mM)$^{-1}$

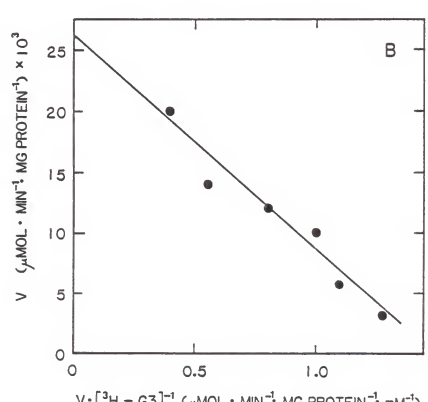
B
25
20
15
10
5
0
0
0.5
1.0
V (μMOL · MIN^{-1}· MG PROTEIN^{-1}) × 10^3
V·$[^3H - G3]^{-1}$ (μMOL · MIN^{-1}· MG PROTEIN^{-1}· mM^{-1})

activity on [1-^{3}H]cellotriose indicated the presence of high and low affinity binding sites. Values of K_m and V_{max} were determined to be 18 ± 3 μM and 0.026 ± 0.002 μmol/min/mg, respectively.

The time course of hydrolysis of [1-^{3}H]cellotetraose by CBH II is shown in Fig. 7-4. Reducing end-labeled cellobiose formed from hydrolysis at bond 2 is the predominant product. A negligible amount of [1-^{3}H]cellotriose accumulates by 60 min. Bond cleavage frequency analysis showed a linear relationship between product ratios and extent of reaction indicating no change in mode of action (Fig. 7-5). Bond cleavage frequencies estimated from the slopes for [1-^{3}H]glucose, [1-^{3}H]cellobiose and [1-^{3}H]cellotriose are <0.005, 0.99 and 0.01, respectively. In contrast, CBH I(D) produces [1-^{3}H]glucose from hydrolysis of [1-^{3}H]cellotetraose with a frequency of 0.19.

Initial velocities obtained from the early, linear region of the time course of hydrolysis of [1-^{3}H]cellotetraose were used to construct linear Lineweaver-Burk and Eadie-Hofstee plots (Fig. 7-6). Values of K_m and V_{max} were determined to be 2.6 ± 0.3 μM and 7.7 ± 0.3 μmol/min/mg, respectively.

Reducing end-labeled cellobiose and [1-^{3}H]cellotriose were produced from CBH II hydrolysis of [1-^{3}H]cellopentaose indicating that bonds 2 and 3 were cleaved (Fig. 7-7). Initial bond cleavage frequencies derived from the slope of product ratio versus extent of reaction for [1-^{3}H]glucose,

Figure 7-4 Time course hydrolysis of [1-^{3}H]cellotetraose by CBH II

Cellobiohydrolase II (2.0 ng) was incubated in 100 µl of 5 mM sodium acetate buffer, pH 5.0, containing 3.8 µM [1-^{3}H]cellotetraose. Samples were removed from the reaction mixture after various intervals and analyzed using TLC as described in Experimental Procedures. The early, linear region of [1-^{3}H]cellotetraose degradation curve yielded the initial velocity. The curves represent the distribution of [1-^{3}H]glucose (o), [1-^{3}H]cellobiose (●), [1-^{3}H]cellotriose (□) and [1-^{3}H]cellotetraose (■).

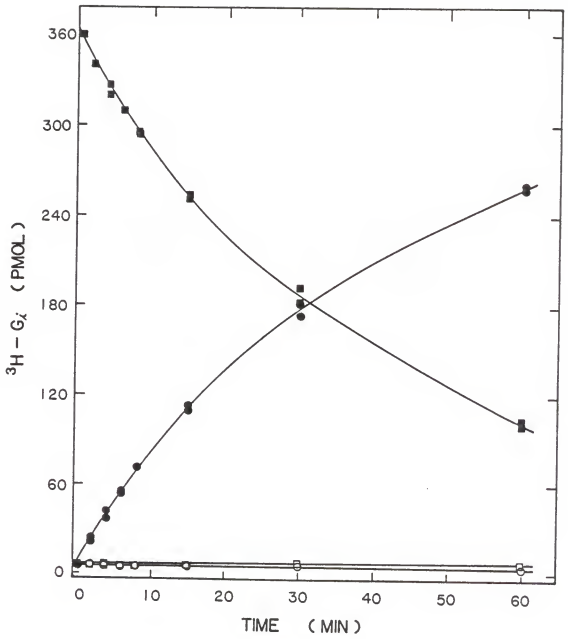
360
300
240
180
120
60
0
$^3H - G_i$ (PMOL)
0
10
20
30
40
50
60
TIME (MIN)

Figure 7-5 Bond cleavage frequency plot for hydrolysis of [1-^{3}H]cellotetraose by CBH II

Cellobiohydrolase II (2.0 ng) was incubated in 100 µl of 5 mM sodium acetate buffer, pH 5.0, containing 3.8 µM [1-^{3}H]cellotetraose. Samples were removed from the reaction mixture and analyzed using TLC as described in Experimental Procedures. The initial slope of each line is the bond cleavage frequency of the substrate bond yielding the product (Gi). The curves represent the product ratios of [1-^{3}H]glucose (○), [1-^{3}H]cellobiose (●), [1-^{3}H]cellotriose (□) and the substrate ratio of [1-^{3}H]cellotetraose (■).

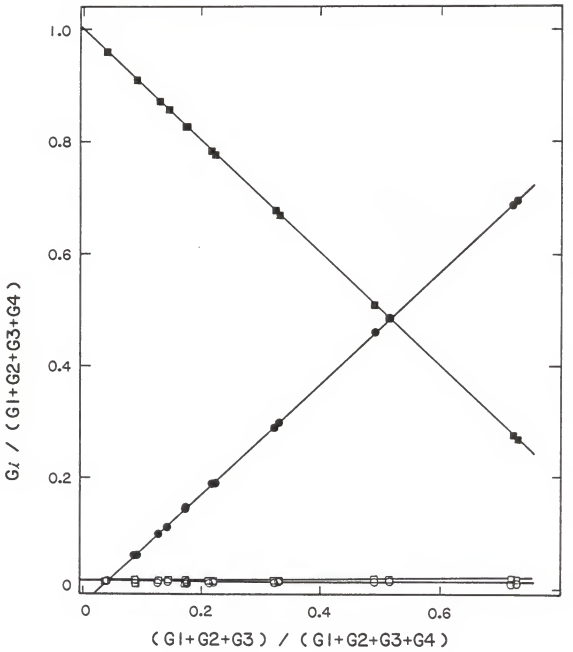
1.0
0.8
0.6
0.4
0.2
0
0
0.2
0.4
0.6
Gi / (G1+G2+G3+G4)
(G1+G2+G3) / (G1+G2+G3+G4)

Figure 7-6 Lineweaver-Burk and Eadie-Hofstee plots for hydrolysis of [1-^{2}H]cellotetraose by CBH II

Initial rates of hydrolysis of [1-^{3}H]cellotetraose (0.5-15 μM) by CBH II were used to construct Lineweaver-Burk (A) and Eadie-Hofstee (B) plots.

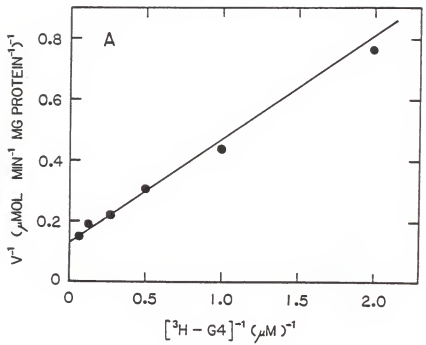
A
0.8
0.6
0.4
0.2
0
0
0.5
1.0
1.5
2.0
V^{-1} (μMOL MIN^{-1} MG PROTEIN^{-1})$^{-1}$
$[^3H - G4]^{-1}$ (μM)$^{-1}$

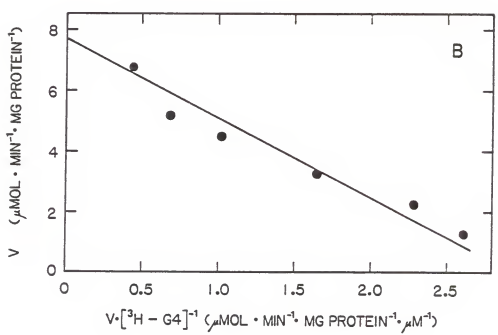
B
8
6
4
2
0
0
0.5
1.0
1.5
2.0
2.5
V (μMOL • MIN^{-1} • MG PROTEIN^{-1})
V•$[^3H - G4]^{-1}$ (μMOL • MIN^{-1}• MG PROTEIN^{-1}•μM^{-1})

Figure 7-7 Time course hydrolysis of [1-^{3}H]cellopentaose by CBH II

Cellobiohydrolase II (0.32 ng) was incubated in 100 µl of 5 mM sodium acetate buffer, pH 5.0, containing 0.25 µM [1-^{3}H]cellopentaose. Samples were removed from the reaction mixture after various intervals and analyzed using TLC as described in Experimental Procedures. The early, linear region of [1-^{3}H]cellopentaose degradation curve yielded the initial velocity. The curves represent the distribution of [1-^{3}H]glucose (o), [1-^{3}H]cellobiose (●), [1-^{3}H]cellotriose (□), [1-^{3}H]cellotetraose (■) and [1-^{3}H]cellopentaose (Δ).

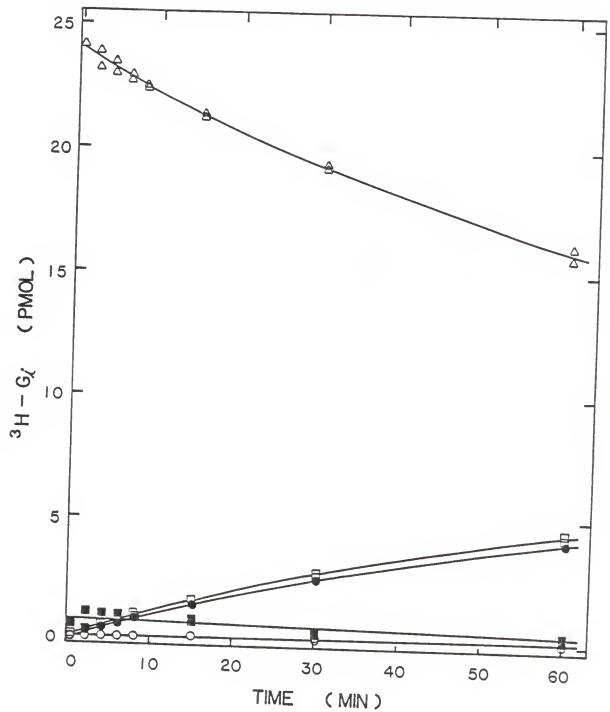
25
20
15
10
5
0
$^3H - G_i$ (PMOL)
0
10
20
30
40
50
60
TIME (MIN)

[1-^{3}H]cellobiose, [1-^{3}H]cellotriose and [1-^{3}H]cellotetraose are <0.005, 0.483, 0.524 and <0.005, respectively (Fig. 7-8). Bond cleavage frequencies were essentially constant during the time course of reaction and were also constant for substrate concentrations ranging from 0.25 to 2.5 μM. Cellobiohydrolase I(D), however, predominantly forms [1-^{3}H]glucose and [1-^{3}H]cellobiose from [1-^{3}H]cellopentaose.

Linear Lineweaver-Burk and Eadie-Hofstee plots were obtained using initial velocities derived from the early, linear region of time course of hydrolysis of [1-^{3}H]cellopentaose (Fig. 7-9). Values of K_m and V_{max} for hydrolysis of [1-^{3}H]cellopentaose are 0.98 ± 0.10 μM and 2.20 ± 0.09 μmol/min/mg, respectively.

The time course of hydrolysis of [1-^{3}H]cellohexaose by CBH II is shown in Fig. 7-10. Two predominant products, [1-^{3}H]cellobiose and [1-^{3}H]cellotriose, are formed by the action of CBH II. Bond cleavage frequency analysis indicates that the frequencies for production of [1-^{3}H]glucose, [1-^{3}H]cellobiose, [1-^{3}H]cellotriose, [1-^{3}H]cellotetraose and [1-^{3}H]cellopentaose are <0.005, 0.43, 0.54, 0.035 and <0.005, respectively (Fig. 7-11). Bond cleavage frequencies were essentially constant during the time course of hydrolysis and showed little tendency to vary from 0.125 to 2.5 μM [1-^{3}H]cellohexaose. In contrast, CBH I(D) predominantly

Figure 7-8 Bond cleavage frequency plot for hydrolysis of [1-^{3}H]cellopentaose by CBH II

Cellobiohydrolase II (0.32 ng) was incubated in 100 µl of 5 mM sodium acetate buffer, pH 5.0, containing 0.25 µM [1-^{3}H]cellopentaose. Samples were removed from the reaction mixture and analyzed using TLC as described in Experimental Procedures. The initial slope of each line is the bond cleavage frequency of the substrate bond yielding the product (Gi). The curves represent the product ratios of [1-^{3}H]glucose (o), [1-^{3}H]cellobiose (●), [1-^{3}H]cellotriose (□), [1-^{3}H]cellotetraose (■) and the substrate ratio of [1-^{3}H]cellopentaose (Δ).

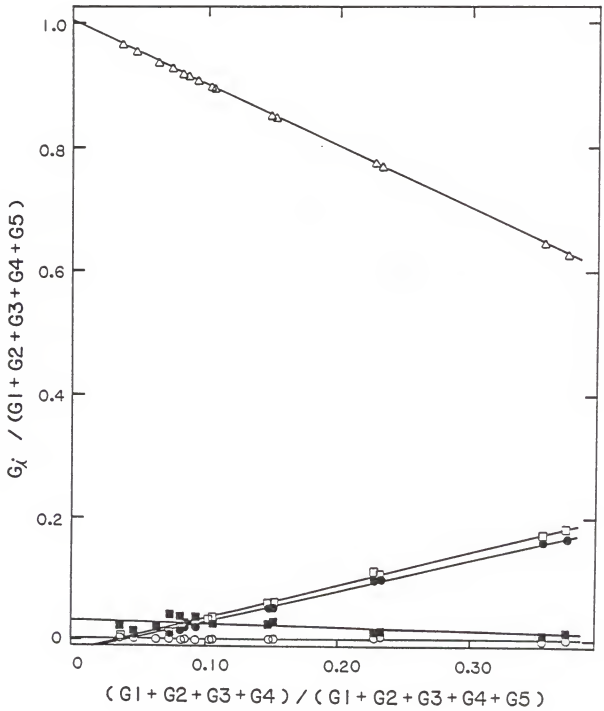
1.0
0.8
0.6
0.4
0.2
0
0
0.10
0.20
0.30
Gi / (G1 + G2 + G3 + G4 + G5)
(G1 + G2 + G3 + G4) / (G1 + G2 + G3 + G4 + G5)

Figure 7-9 Lineweaver-Burk and Eadie-Hofstee plots for hydrolysis of [1-^{3}H]cellopentaose by CBH II

Initial rates for hydrolysis of [1-^{3}H]cellopentaose (0.25-5 μM) by CBH II were used to construct Lineweaver-Burk (A) and Eadie-Hofstee (B) plots.

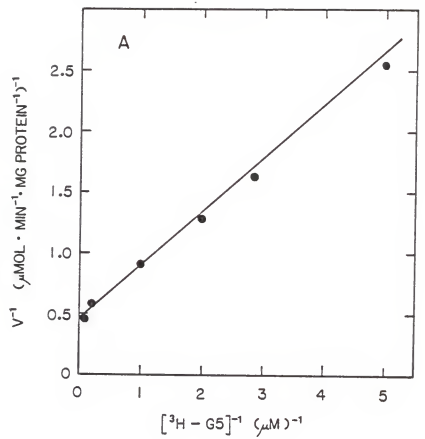
A
2.5
2.0
1.5
1.0
0.5
0
0
1
2
3
4
5
V^{-1} (μMOL · MIN^{-1} · MG PROTEIN^{-1})$^{-1}$
$[^3H - G5]^{-1}$ (μM)$^{-1}$

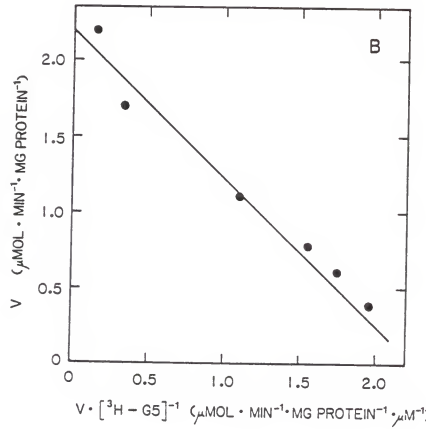
B
2.0
1.5
1.0
0.5
0
0.5
1.0
1.5
2.0
V (μMOL · MIN^{-1} · MG PROTEIN^{-1})
V · $[^3H - G5]^{-1}$ (μMOL · MIN^{-1} · MG PROTEIN^{-1} · μM^{-1})

Figure 7-10 Time course hydrolysis of [1-^{3}H]cellohexaose by CBH II

Cellobiohydrolase II (0.29 ng) was incubated in 100 µl of 5 mM sodium acetate buffer, pH 5.0, containing 0.25 µM [1-^{3}H]cellohexaose. Samples were removed from the reaction mixture after various intervals and analyzed using TLC as described in Experimental Procedures. The early, linear region of [1-^{3}H]cellohexaose degradation curve yielded the initial velocity. The curves represent the distribution of [1-^{3}H]glucose (o), [1-^{3}H]cellobiose (●), [1-^{3}H]cellotriose (□), [1-^{3}H]cellotetraose (■), [1-^{3}H]cellopentaose (Δ) and [1-^{3}H]cellohexaose (▲).

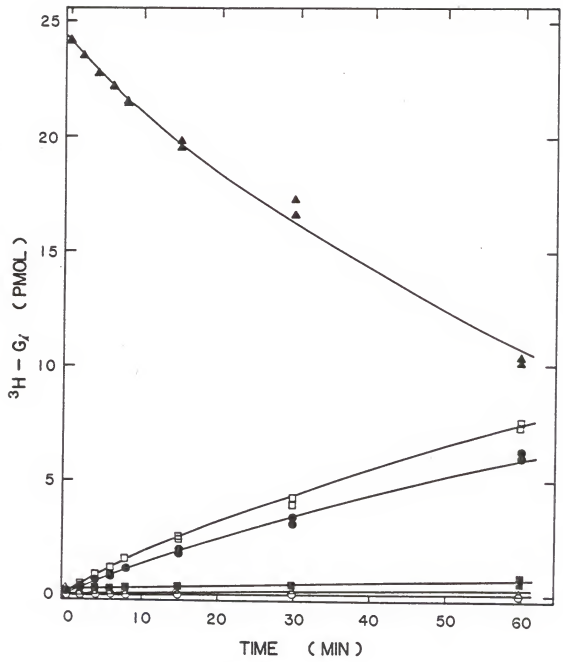
25
20
15
10
5
0
$^3H - G_i$ (PMOL)
0
10
20
30
40
50
60
TIME (MIN)

Figure 7-11 Bond cleavage frequency plot for hydrolysis of [1-^{3}H]cellohexaose by CBH II

Cellobiohydrolase II (0.29 ng) was incubated in 100 µl of 5 mM sodium acetate buffer, pH 5.0, containing 0.25 µM [1-^{3}H]cellohexaose. Samples were removed from the reaction mixture and analyzed using TLC as described in Experimental Procedures. The initial slope of each line is the bond cleavage frequency of the substrate bond yielding the product (Gi). The curves represent the product ratios of [1-^{3}H]glucose (○), [1-^{3}H]cellobiose (●), [1-^{3}H]cellotriose (□), [1-^{3}H]cellotetraose (■) and [1-^{3}H]cellopentaose (△) and the substrate ratio of [1-^{3}H]cellohexaose (▲).

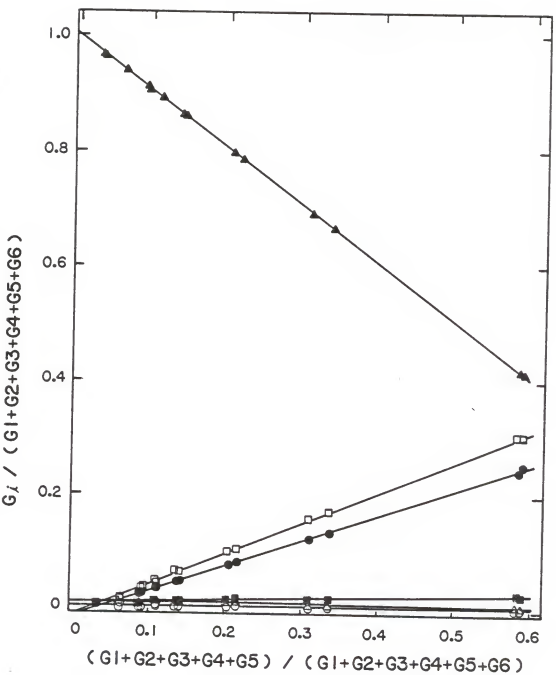
1.0
0.8
0.6
0.4
0.2
0
0
0.1
0.2
0.3
0.4
0.5
0.6
Gi / (G1+G2+G3+G4+G5+G6)
(G1+G2+G3+G4+G5) / (G1+G2+G3+G4+G5+G6)

hydrolyzes bonds 4 and 5 of [1-^{3}H]cellohexaose producing [1-^{3}H]cellobiose and [1-^{3}H]glucose, respectively.

The early, linear region of time course hydrolysis of [1-^{3}H]cellohexaose yielded initial rates used to construct linear Lineweaver-Burk and Eadie-Hofstee plots (Fig. 7-12). Values of K_m and V_{max} for hydrolysis of [1-^{3}H]cellohexaose were determined to be 0.67 ± 0.06 μM and 4.4 ± 0.2 μmol/min/mg, respectively.

A summary of bond cleavage frequencies for hydrolysis of [1-^{3}H]cellooligosaccharides by CBH II is presented in Fig. 7-13. Cellobiohydrolase II produces [1-^{3}H]glucose with a frequency of <0.005 from [1-^{3}H]cellotetraose through [1-^{3}H]cellohexaose, whereas the bond cleavage frequency of [1-^{3}H]glucose generated by CBH I(D) increases from 0.19 to 0.62 from [1-^{3}H]cellotetraose through [1-^{3}H]cellohexaose. During CBH II-catalyzed hydrolysis of [1-^{3}H]cellotriose or [1-^{3}H]cellotetraose bond 2 is cleaved predominantly; however, the bond at the nonreducing end of [1-^{3}H]cellotriose and [1-^{3}H]cellotetraose was cleaved with a frequency of 0.01. Cellobiohydrolase II binds [1-^{3}H]cellopentaose and [1-^{3}H]cellohexaose in predominantly two modes. Cleavage at bond 2 is slightly favored over cleavage at bond 3 of [1-^{3}H]cellopentaose. However, cleavage at bond 2 of [1-^{3}H]cellohexaose is 0.035 compared to bonds 3 and 4, which have frequencies of 0.54 and 0.43, respectively. Since CBH II repetitively hydrolyzes cellohexaose, the direction of attack significantly influences bond cleavage frequencies.

Figure 7-12 Lineweaver-Burk and Eadie-Hofstee plots for hydrolysis of [1-^{3}H]cellohexaose by CBH II

Initial rates of hydrolysis of [1-^{3}H]cellohexaose (0.125-2.5 μM) by CBH II were used to construct Lineweaver-Burk (A) and Eadie-Hofstee (B) plots.

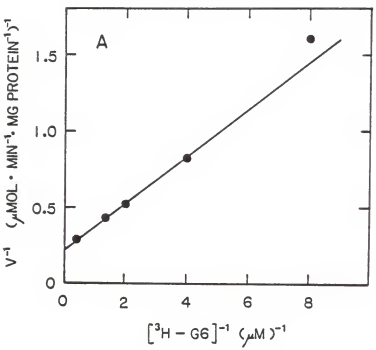
A
1.5
1.0
0.5
0
0
2
4
6
8
V^{-1} (μMOL • MIN^{-1}• MG PROTEIN^{-1})$^{-1}$
[^{3}H – G6]$^{-1}$ (μM)$^{-1}$

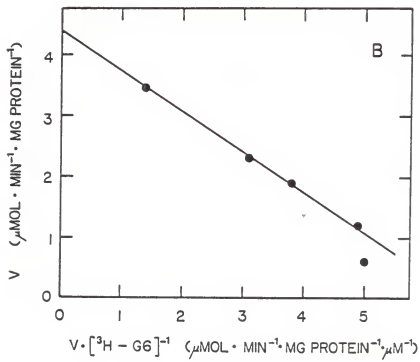
B
4
3
2
1
0
0
1
2
3
4
5
V (μMOL • MIN^{-1}• MG PROTEIN^{-1})
V • [^{3}H – G6]$^{-1}$ (μMOL • MIN^{-1}• MG PROTEIN^{-1}• μM^{-1})

Figure 7-13 Bond cleavage frequencies of [1-^{3}H]cellooligosaccharide hydrolysis by CBH II

Values shown are initial bond cleavage frequencies of [1-^{3}H]cellotriose (A), [1-^{3}H]cellotetraose (B), [1-^{3}H]cellopentaose (C), [1-^{3}H]cellohexaose (D) and [1-^{3}H]cellohexaose (assuming repetitive attack toward the reducing end) (E). The reducing end glucosyl residue is represented by (ø).

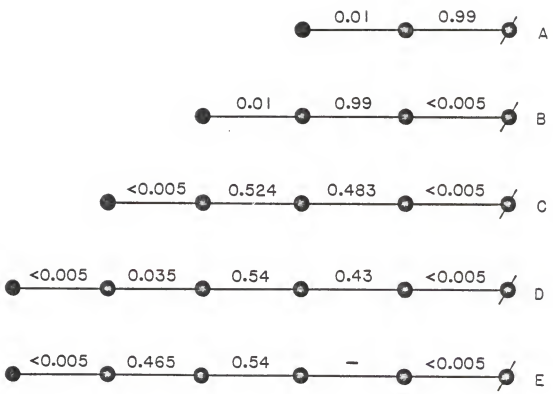
0.01
0.99
A
0.01
0.99
<0.005
B
<0.005
0.524
0.483
<0.005
C
<0.005
0.035
0.54
0.43
<0.005
D
<0.005
0.465
0.54
–
<0.005
E

If CBH II repetitively attacks [1-^{3}H]cellohexaose from the reducing end, the bond cleavage frequency analysis would accurately reflect initial points of cleavage. However, if attack is from the nonreducing end, then products of initial cleavages would not be detected, because they would not be radioactive. Evidence provided below using [^{14}C-U]cellohexaose in conjunction with [1-^{3}H]cellohexaose suggests that CBH II repetitively attacks cellohexaose removing cellobiosyl residues from the nonreducing end. Therefore, the true initial bond cleavage frequencies for CBH II activity on [1-^{3}H]cellohexaose are shown in Fig. 7-13e. Bond cleavage frequency analysis of CBH II-catalyzed hydrolysis of [1-^{3}H]cellooligosaccharides indicates a preference for the nonreducing end, whereas that for CBH I(D) indicates a preference for the reducing end.

Kinetic constants for hydrolysis of [1-^{3}H]cellooligosaccharides by CBH II are summarized in Table 7-1. Values of K_m decrease approximately 26-fold from [1-^{3}H]cellotriose to [1-^{3}H]cellohexaose indicating that CBH II preferentially binds longer cellooligosaccharides. However, a similar trend is not observed for values of V_{max}. Since CBH II repetitively attacks [1-^{3}H]cellohexaose, the V_{max} for [1-^{3}H]cellohexaose hydrolysis does not reflect the maximum number of glycosidic bonds cleaved per substrate encounter with enzyme. Approximately 3 moles of cellobiose are produced per mole of cellohexaose suggesting that the V_{max} for total glycosidic bond cleavage is 8.8 μmol/min/mg. The

Table 7-1

Kinetic Constants for [1-^{3}H]Cellooligosaccharide Hydrolysis by Cellobiohydrolase II

Activity of cellobiohydrolase II was measured at various concentrations of [1-^{3}H]cellooligosaccharides in the presence of 5 mM sodium acetate buffer, pH 5.0, containing 0.3 mM sodium azide. Kinetic constants were determined from initial rates of hydrolysis using Cleland's HYPER program (70).

[1-^{3}H]Cellooligo-saccharide	K_m (μM)	V_{max} (μmole/min mg)	V_{max}/K_m
Cellotriose	18 ±3	0.026±0.002	0.0015±0.0001
Cellotetraose	2.6 ±0.3	7.7 ±0.3	2.9 ±0.2
Cellopentaose	0.98±0.10	2.20 ±0.09	2.3 ±0.2
Cellohexaose	0.67±0.06	4.4 ±0.2	6.6 ±0.4

comparatively low V_{max} for [1-^{3}H]cellopentaose hydrolysis may result from cellotriose (value of K_m is 18 μM) "sticking" to the active site after hydrolysis of [1-^{3}H]cellopentaose. The general increase in values of V_{max}/K_m as chain length increases confirms the preferential cleavage of longer cellooligosaccharides by CBH II.

Cellobiohydrolase II is more catalytically effective with longer cellooligosaccharides than is CBH I(D) as indicated by their respective values for k_{cat}/K_m of the cellooligosaccharide series (Appendix F). However, repetitive attack by CBH I(D) and CBH II makes comparison difficult. Values of k_{cat}/K_m for ß-glucosidase action on [1-^{3}H]cellooligosaccharides of chain length >3 are greater than 3-fold lower than those reported for CBH I(D) and CBH II indicating that the role of the ß-glucosidase in saccharification of cellulose is to convert cellobiose and cellooligosaccharides (especially cellotriose) to glucose; cellooligosaccharides of longer chain length are rapidly hydrolyzed by CBH I(D) and CBH II (Appendix F).

Hydrolysis of [1-^{3}H]Cellooligosaccharides and [^{14}C-U]Cellooligosaccharides

The activity of CBH II on [1-^{3}H]cellooligosaccharides provides little information regarding the fate of unlabeled products. Therefore, [^{14}C-U]cellooligosaccharides were used in conjunction with [1-^{3}H]cellooligosaccharides as substrates for CBH II.

The distribution of products formed from hydrolysis of [^{14}C-U]cellopentaose and [1-^{3}H]cellopentaose by CBH II is shown in Table 7-2. The formation of [^{14}C-U]glucose and the corresponding absence of [1-^{3}H]glucose suggests that CBH II hyrolyzes bond 1. The absence of a corresponding amount of [1-^{3}H]cellotetraose suggests that CBH II repetitively attacks cellopentaose initiating attack at bond 1 followed by attack at bond 3. The efficiency of repetitive attack estimated from the concentrations of [^{14}C-U]glucose and [1-^{3}H]cellotetraose is 80 percent. Since cellobiose and cellotriose are produced from cleavages at bonds 2 and 3, the [^{14}C-U]cellobiose/[^{14}C-U]cellotriose ratio is 1. The [^{14}C-U]cellobiose/[1-^{3}H]cellobiose ratio of 2 corresponds with the sum of concentrations of [1-^{3}H]cellobiose and [1-^{3}H]cellotriose divided by [1-^{3}H]cellobiose. Similarly, the [^{14}C-U]cellotriose/[1-^{3}H]cellotriose ratio of 1.6 corresponds with the sum of the concentrations of [1-^{3}H]cellobiose and [1-^{3}H]cellotriose divided by [1-^{3}H]cellotriose. Thus, the distribution of [^{14}C-U] products and [1-^{3}H] products resulting from hydrolysis of bond 2 and 3 indicate that one bond is hydrolyzed per encounter with CBH II.

Initial rates of formation of products from CBH II catalyzed hydrolysis of [^{14}C-U]cellopentaose and [1-^{3}H]cellopentaose are listed in Table 7-3. Initial rates of hydrolysis of [^{14}C-U]cellopentaose and [1-^{3}H]cellopentaose are within experimental error indicating no detectable kinetic isotope effect. Ratios of formation of [^{14}C-U]/

Table 7-2

Hydrolysis of [1-^{3}H]Cellopentaose and [^{14}C-U]Cellopentaose by Cellobiohydrolase II

Cellobiohydrolase II (6.28×10^{-5} mg) was incubated at 40°C in 100 µl of 5 mM sodium acetate buffer, pH 5.0, containing 0.55 µCi of [1-^{3}H]cellopentaose and 0.22 µCi of [^{14}C-U]cellopentaose. Total concentration of cellopentaose was 83 µM.

Cellooligosaccharide	Pmol Time (min) 0	4	8	15	60	Ratio [^{14}C-U]/[1-^{3}H]
[1-^{3}H]Glucose	0	3± 2	5± 3	10± 5	15± 3	9 ±3
[^{14}C-U]Glucose	0	21±17	53± 3	76± 6	190± 70	
[1-^{3}H]Cellobiose	0	380±13	522±10	840±120	2110± 560	2.0±0.2
[^{14}C-U]Cellobiose	0	600±80	1080±40	1700±260	4300±1200	
[1-^{3}H]Cellotriose	0	380±40	660±40	1000±160	2520± 740	1.6±0.2
[^{14}C-U]Cellotriose	0	580±70	1020±50	1640±220	4200±1200	
[1-^{3}H]Cellotetraose	0	6± 6	11± 5	16± 17	37± 16	ND[a]
[^{14}C-U]Cellotetraose	0	<3	10±10	<3	<3	
[1-^{3}H]Cellopentaose	8111± 6	7420±70	6910±40	6220±280	3400±1300	0.96±0.1
[^{14}C-U]Cellopentaose	7638±13	7060±50	6590±40	5960±230	3400±1200	

[a] ND = not determined.

Table 7-3

Initial Rates of Cellobiohydrolase II Activity on [1-^{3}H]Cellopentaose and [^{14}C-U]Cellopentaose

Cellobiohydrolase II (6.28×10^{-5}mg) was incubated at 40°C in 100 µl of 5 mM sodium acetate buffer, pH 5.0, containing 0.55 µCi of [1-^{3}H]cellopentaose and 0.22 µCi of [^{14}C-U]cellopentaose. Total concentration of cellopentaose was 83 µM.

Cellooligosaccharide	Initial Velocity (pmol/min)	Ratio [^{14}C-U]/[1-^{3}H]
[1-^{3}H]Glucose	0.8± 0.4	6.25±5.9
[^{14}C-U]Glucose	5 ± 4	
[1-^{3}H]Cellobiose	76 ± 6	2.0 ±0.3
[^{14}C-U]Cellobiose	149 ± 20	
[1-^{3}H]Cellotriose	94 ± 10	1.5 ±0.2
[^{14}C-U]Cellotriose	144 ± 17	
[1-^{3}H]Celltetraose	2 ± 2	ND[a]
[^{14}C-U]Celltetraose	-4 ± 2	
[1-^{3}H]Cellopentaose	-172 ± 18	0.84±0.13
[^{14}C-U]Cellopentaose	-144 ± 17	

[a] ND = Not determined

[1-^{3}H] products agree well with ratios of [^{14}C-U]/[1-^{3}H] product distributions supporting the contention that products result from hydrolysis at the same bonds.

The distribution of products formed from hydrolysis of [^{14}C-U]cellohexaose and [1-^{3}H]cellohexaose are listed in Table 7-4. Although bond cleavage frequency at bond 1 resulting in the formation of [1-^{3}H]cellopentaose (<0.005) could not be precisely determined because of high background, the formation of [^{14}C-U]glucose may indicate that cleavage occurs at bond 1. However, [^{14}C-U]glucose may arise from cleavage at other bonds.

The formation of [1-^{3}H]cellobiose indicates that CBH II catalyzes hydrolysis at bond 4; however, the [^{14}C-U]cellobiose/[1-^{3}H]cellobiose concentration ratio of 2.9 indicates that cellobiose also arises from cleavage at bonds other than bond 4. The 2.9-fold greater concentration of [^{14}C-U]cellobiose compared to cellohexaose during the reaction indicates that CBH II repetitively attacks cellohexaose. Cellobiose may arise from cleavage at bond 2 and then at bond 4 (Fig. 7-14a) or from cleavage at bond 4 and then at bond 2 (Fig. 7-14b). Since repetitive attack from either direction results in the same ratio of [^{14}C-U]cellobiose to [1-^{3}H]cellobiose, the direction of repetitive attack must be ascertained from the [^{14}C-U]/[1-^{3}H] ratios of other products, especially cellotetraose. Initial cleavage at a bond resulting in the formation of cellobiose will also result in the formation of an equal amount of

Table 7-4

Hydrolysis of [1-^{3}H]Cellohexaose and [^{14}C-U]Cellohexaose by Cellobiohydrolase II

Cellobiohydrolase II (4.52×10^{-5} mg) was incubated at 40°C in 100 µl of 5 mM sodium acetate buffer, pH 5.0, containing 0.55 µCi of [1-^{3}H]cellohexaose and 0.19 µCi of [^{14}C-U]cellohexaose. Total concentration of cellopentaose was 59 µM.

Cellooligosaccharide	Pmol TIME (min) 0	2	6	15	60	Ratio [^{14}C-U]/[1-^{3}H]
[1-^{3}H]Glucose	0	5 ± 2	5.9± 0.7	11± 1	24± 4	10 ±2
[^{14}C-U]Glucose	0	26 ± 6	52 ±28	123± 14	270± 50	
[1-^{3}H]Cellobiose	0	187.8± 0.1	443 ±20	830± 50	1570± 80	2.90 ±0.03
[^{14}C-U]Cellobiose	0	552.0± 0	1300 ±50	2400±180	4600±270	
[1-^{3}H]Cellotriose	0	243 ± 2	580 ±20	1060± 60	2090±220	1.84 ±0.31
[^{14}C-U]Cellotriose	0	447 ± 1	1070 ±40	1950±100	3850±400	
[1-^{3}H]Cellotetraose	0	28.3± 0.7	68 ± 4	135± 1	280± 10	1.0 ±0.1
[^{14}C-U]Cellotetraose	0	27 ±10	80 ±10	140± 10	270± 10	
[1-^{3}H]Cellopentaose	0	<1	1 ±15	38± 38	<1	ND[a]
[^{14}C-U]Cellopentaose	0	<1	<1	<1	<1	
[1-^{3}H]Cellohexaose	5763±0	4320 ±10	4670 ±30	3690±150	1840±300	0.886±0.007
[^{14}C-U]Cellohexaose	5147±0	4741 ± 4	4140 ±30	3280±160	1600±280	

[a] ND = Not determined.

Figure 7-14 Possible types of repetitive attack of CBH II with [1-^{3}H]cellohexaose and [^{14}C-U]cellohexaose

Cellobiohydrolase II may repetitively attack cellohexaose in either of two possible directions: (A) attack toward the reducing end initiated at bond 2 and followed by attack at bond 4, (B) attack toward the nonreducing end initiated at bond 4 and followed by attack at bond 2. Bonds are numbered from the nonreducing end. The reducing end glucosyl residue is represented by (ø).

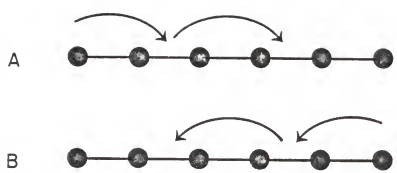
A
B

cellotetraose. If all resulting cellotetraose remains associated with CBH II and is immediately converted to cellobiose, then repetitive attack is 100 percent efficient. The efficiency of repetitive attack in either direction estimated from the concentration of [^{14}C-U]cellotetraose and [1-^{3}H]cellobiose at 60 min is 83 percent. If repetitive attack occurs toward the nonreducing end and is initiated at bond 4, then no [1-^{3}H]cellotetraose should be formed. However, if repetitive attack occurs toward the reducing end and is initiated at bond 2, then [1-^{3}H]cellotetraose should be formed and the [^{14}C-U]cellotetraose/[1-^{3}H]cellotetraose ratio should be equal to 1. The ratio of [^{14}C-U]cellotetraose/[1-^{3}H]cellotetraose concentration is found to be equal to 1 supporting the model (Fig. 7-14a) that the direction of repetitive attack is toward the reducing end of cellohexaose. Distribution of [^{14}C-U] products and [1-^{3}H] products resulting from CBH II-catalyzed hydrolysis of [^{14}C-U]cellopentaose and [1-^{3}H]cellopentaose is also consistent with repetitive attack toward the reducing end. The preference of CBH II for the nonreducing end is supported by the accumulation of [^{14}C-U]glucose arising from cleavage at bond 1. The negligible accumulation of [1-^{3}H]glucose indicates that CBH II has little tendency to cleave the terminal reducing end bond (bond 5).

Initial rates of formation of products from CBH II catalyzed hydrolysis of [^{14}C-U]cellohexaose and

[1-^{3}H]cellohexaose are listed in Table 7-5. Initial rates of hydrolysis of [^{14}C-U]cellohexaose and [1-^{3}H]cellohexaose are within experimental error indicating no detectable kinetic isotope effect. Ratios of initial rates of formation of [^{14}C-U]/[1-^{3}H] products agree well with ratios of [^{14}C-U]/[1-^{3}H] product distribution supporting the contention that products result from hydrolysis at the same bonds.

In contrast to CBH I(D), evidence from hydrolysis of [1-^{3}H]cellohexaose in conjunction with [^{14}C-U]cellohexaose supports that CBH II repetitively attacks cellohexaose from the nonreducing end. The β-glucosidase also prefers the nonreducing end of cellooligosaccharides; however, no evidence for repetitive attack by the β-glucosidase has been obtained. The difference between CBH I(D) and CBH II with respect to their directions of repetitive attack suggests a synergistic mechanism by which CBH I(D) and CBH II may degrade crystalline cellulose. Possible mechanisms to explain exo-exo synergism are presented in the following chapter.

Subsite Mapping of Cellobiohydrolase II

The methods of Suganuma et al. (45) and Allen and Thoma (49) were used to construct subsite maps of CBH II. The method of Suganuma et al. (45) requires bond cleavage frequencies and values of V_{max}/K_m for a series of oligosaccharides to estimate subsite affinities. The method of Allen and Thoma (49) requires bond cleavage frequencies;

Table 7-5

Initial Rates of Cellobiohydrolase II Activity on [1-^{3}H]Cellohexaose and [^{14}C-U]Cellohexaose

Cellobiohydrolase II (4.52×10^{-5}mg) was incubated at 40°C in 100 µl of 5 mM sodium acetate buffer, pH 5.0, containing 0.55 µCi of [1-^{3}H]cellohexaose and 0.19 µCi of [^{14}C-U]cellohexaose. Total concentration of cellohexaose was 59 µM.

Cellooligosaccharide	Initial Velocity (pmol/min)	Ratio [^{14}C-U]/[1-^{3}H]
[1-^{3}H]Glucose	1.4± 0.1	11.4±0.8
[^{14}C-U]Glucose	15.8± 0.2	
[1-^{3}H]Cellobiose	85 ± 2	2.9 ±0.1
[^{14}C-U]Cellobiose	240 ± 10	
[1-^{3}H]Cellotriose	107 ± 2	1.83±0.06
[^{14}C-U]Cellotriose	196 ± 6	
[1-^{3}H]Celltetraose	13 ± 1	1.3 ±0.2
[^{14}C-U]Celltetraose	17 ± 3	
[1-^{3}H]Cellopentaose	18 ± 4	0.9 ±0.3
[^{14}C-U]Cellopentaose	16 ± 5	
[1-^{3}H]Cellohexaose	-224 ± 8	0.92±0.07
[^{14}C-U]Cellohexaose	-207 ± 13	

however, values for K_m, V_{max} and K_{int} are also required. Equations essential to the formulation of both methods are presented in Appendix A.

Subsite affinities calculated by the method of Suganuma et al. (45) using major bond cleavage frequencies and values of V_{max}/K_m for [1-^{3}H]cellotriose through [1-^{3}H]cellohexaose are listed in Table 7-6. The active site of CBH II consists of 7 subsites with catalytic groups located between subsites 3 and 4 (Fig. 7-15). Subsite 2 contributes the greatest proportion of binding energy, whereas subsites 1, 6 and 7 provide maximum binding energies of approximately -800 cal/mol/subsite. Subsites 3 and 4 are common to all productive modes, therefore individual affinities cannot be evaluated. More than one combination of bond cleavage frequencies and V_{max}/K_m values are used to calculate affinities for subsites 1 and 6. However, affinities for subsite 6 were determined to be 560 cal/mol and -740 cal/mol. Unfavorable and favorable binding affinities for subsite 1 were also obtained: 600 and -680 cal/mol. Since the importance of subsites 1 and 6 cannot be ascertained using bond cleavage frequencies and values of V_{max}/K_m, the method of Suganuma et al. (45) is not adequate for mapping subsites in the active site of CBH II.

The subsite map constructed using the computer model for depolymerases developed by Allen and Thoma (49) was first optimized for experimental bond cleavage frequencies and location of catalytic groups. Bond cleavage frequencies

Table 7-6

Subsite Affinities of CBH II Calculated Using Values of V/K and Bond Cleavage Frequencies From [1-^{3}H]Cellooligosaccharides

Numbers in brackets indicate mode of calculation using bond-cleavage frequencies of cellooligosaccharides at glycosidic bonds denoted by superscripts in parentheses.

Subsite	Mode of Calculation	Subsite Affinity (cal/mol)
1	$[G_4^{(2)}/G_5^{(3)}]$	600± 70
	$[G_5^{(2)}/G_6^{(3)}]$	-680± 70
2	$[G_3^{(1)}/G_4^{(2)}]$	-7600±1200
5	$[G_3^{(2)}/G_4^{(2)}]$	-4720± 70
6	$[G_4^{(2)}/G_5^{(2)}]$	560± 70
	$[G_5^{(3)}/G_6^{(3)}]$	-740± 70
7	$[G_5^{(2)}/G_6^{(2)}]$	-590± 70

Figure 7-15 Subsite map for CBH II constructed using values of V_{max}/K_m and bond cleavage frequencies for [1-^{2}H]cellooligosaccharides

Subsite affinities were estimated using the method of Suganuma et al. (45) from values of V_{max}/K_m and bond cleavage frrequencies for [1-^{2}H]cellooligosaccharides. The arrow shows the position of catalytic groups. Since subsites adjacent to catalytic groups are common to all productive complexes, their affinities cannot be evaluated using this method. Shaded bars indicate that more than one combination of V_{max}/K_m values and bond cleavage frequencies for [1-^{2}H]cellooligosaccharides differing in chain length by one glucosyl residue were used to evaluate affinities at a particular subsite (Table 7-6).

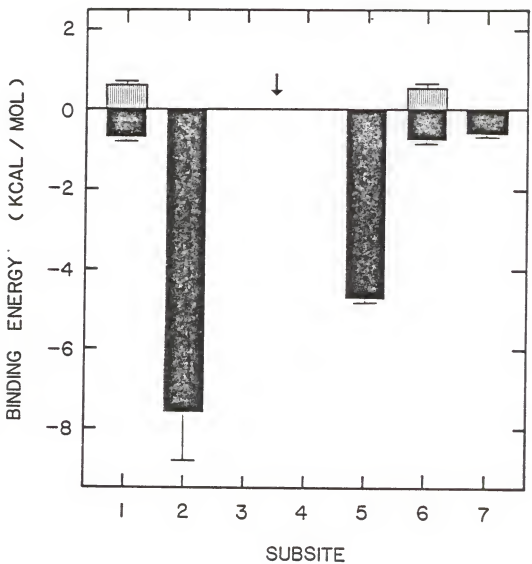
2
0
-2
-4
-6
-8
BINDING ENERGY (KCAL / MOL)
1
2
3
4
5
6
7
SUBSITE

calculated from the optimized subsite map agreed within 5 percent of experimentally derived bond cleavage frequencies. The resulting subsite map was then optimized for values of K_m and V_{max} for [1-^{3}H]cellotriose through [1-^{3}H]cellohexoase. Values of K_m and V_{max} calculated from the optimized subsite map for 7 of 11 constants agreed within 20 percent of experimentally derived values of K_m and V_{max}. Inhibition constants for glucose (24 mM) and cellobiose (204 μM) and apparent V_{max} for hydrolysis of cellobiose (1.13×10^{-3} μmol/min/mg, data not shown) were also used in the evaluation of subsite affinities. Inhibition constants for glucose and cellobiose were determined during inhibition of CBH II hydrolysis of [1-^{3}H]cellotetraose.

A minimum of 7 subsites with the catalytic groups located between subsites 3 and 4 was required to account for the bond cleavage frequencies. The value of K_{int} was estimated from the K_m of cellohexaose. The subsite map for CBH II yielding the lowest residual error for bond cleavage frequencies, K_m, V_{max} and K_{int} is shown in Fig. 7-16. Subsite 2 contributes the greatest proportion of binding energy, whereas the affinity at subsite 4 is unfavorable. Subsites 5-7 favorably bind glucosyl residues and may retain products of cellooligosaccharide hydrolysis in the active site for another cleavage. Unfavorable binding at subsite 4 may promote catalysis by straining the glycosidic bond positioned near catalytic groups. When the approximation was made that the binding of a glucosyl residue

Figure 7-16 Subsite map for CBH II constructed using values of K_m, V_{max} and bond cleavage frequencies for [1-^{3}H]cellooligosaccharides

The number of subsites and the position of the catalytic groups were determined using the method of Allen and Thoma (48) from values of K_m,$^3V_{max}$ and bond cleavage frequencies for [1-^{3}H]cellooligosaccharides. The arrow shows the position of the catalytic groups. The bars depict the estimated binding energies including the contribution of the acceleration factor (500 cal/mol).

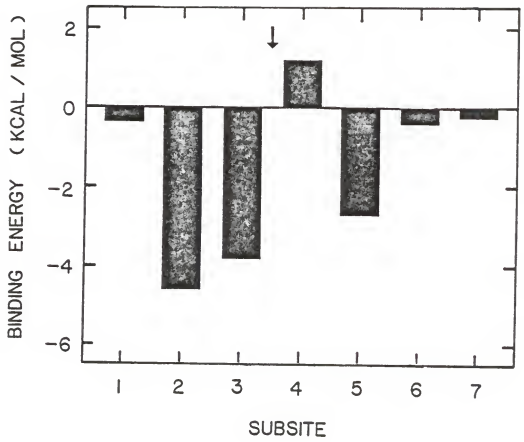
BINDING ENERGY (KCAL / MOL)
2
0
-2
-4
-6
1
2
3
4
5
6
7
SUBSITE

decreases the activation energy for hydrolysis by CBH II by a constant amount enhancing the rate of bond cleavage, agreement between predicted and experimentally derived values significantly improved. The approximation, which is termed the acceleration factor, was estimated to be 500 cal/mol.

The subsite maps constructed for CBH II using the method of Suganuma et al. (45) and Allen and Thoma (49) indicate that the active site of CBH II consists of 7 subsites with subsite 2 contributing the greatest proportion of binding energy. Although subsites 5-7 on each map indicate favorable binding, subsite 6 on the map constructed using the method of Suganuma et al. (45) also shows unfavorable binding.

Subsite maps reveal that the active sites of CBH I(D) and CBH II consists of 7 subsites; however, the location of catalytic groups is different. The catalytic groups are located between subsites 5 and 6 of CBH I(D), whereas they are located between subsites 3 and 4 of CBH II. Favorable binding affinities at subsites 1-5 may enable CBH I(D) to repetitively attack cellohexaose toward the nonreducing end. Similarly, subsites 5-7 of CBH II may promote repetitive attack of cellohexaose toward the reducing end.

Conclusions

Action patterns of [1-^{3}H]cellooligosaccharides indicate that CBH II preferentially hydrolyzes cellooligosaccharides in two productive modes. Michaelis parameters for

[1-^{3}H]cellooligosaccharide hydrolysis decrease with increasing chain length indicating that CBH II preferentially hydrolyzes longer cellooligosaccharides. Examination of action patterns of [1-^{3}H]cellohexaose and [^{14}C-U]cellohexaose revealed that CBH II repetitively attacks cellohexaose from the nonreducing end. Subsite maps constructed by two methods using kinetic parameters of bond cleavage frequencies showed that the active site of CBH II consists of 7 subsites with the catalytic groups located between subsites 3 and 4.

CHAPTER 8
GENERAL DISCUSSION

Hydrolysis of [1-^{3}H]Cellooligosaccharides

The synthesis of [1-^{3}H]cellooligosaccharides and their subsequent use with β-glucosidase, CBH I(D) and CBH II permitted identification of precise glycosidic bonds cleaved by these enzymes and estimation of K_m and V_{max} for substrate hydrolysis. Asymmetrically modified cellooligosaccharides, such as 4-methylumbelliferyl glycosides of cellooligosaccharides (30) and reduced cellooligosaccharides (98), have been used to investigate the action patterns of cellulolytic enzymes. However, the influence of the derivatization on the activity of cellulolytic enzymes has not been determined.

van Tilbeurgh et al. (30) reported that the K_m for cellotriose hydrolysis by CBH I(D) is 12 mM, which is approximately 1000-fold and 4-fold higher than the high and low affinity sites, respectively, reported here. The discrepancies may be due to the difference in the assay used in this report and that used by van Tilbeurgh et al. (30). The formation of glucose was measured by van Tilbeurgh et al. (30) using the glucose oxidase-peroxidase reagent, the sensitivity of which does not permit measurement of initial rates of glucose formation at micromolar substrate

concentrations. Hydrolysis of the aglycone bond of MeUmb(Glc$\underline{p}$)$_2$ was shown to have a K_m of 35 μM, approximately 4-fold higher than K_m for the high affinity site of cellotriose reported here. This may indicate that subsite 5 of CBH I(D) has less affinity for hydrophobic aglycones than for glucosyl residues. A comparison of the action patterns resulting from CBH I(D) hydrolysis of MeUmb(Glc$\underline{p}$)$_2$ through MeUmb(Glc$\underline{p}$)$_6$ with those of [1-^{3}H]cellotriose through [1-^{3}H]cellohexaose indicates that the 4-methylumbelliferyl aglycone alters the action patterns of CBH I(D). Hydrolysis of MeUmb(Glc$\underline{p}$)$_4$ produces bond cleavage frequencies of bonds 2, 3 and 4 of 0.30, 0.53 and 0.13 estimated by this author using peak heights reported in (30), respectively, whereas the corresponding bond cleavage frequencies for [1-^{3}H]cellopentaose are 0.02, 0.513, 0.480, respectively. The lower bond cleavage frequency at bond 4 of MeUmb(Glc$\underline{p}$)$_4$ is consistent with the idea that subsite 5 is more specific for glucosyl residues than for hydrophobic methylumbelliferyl groups. However, hydrolysis of MeUmb(Glc$\underline{p}$)$_5$ results in a bond cleavage frequency at bond 5 of approximately 0.75. Bond cleavage frequency at bond 5 of [1-^{3}H]cellohexaose is 0.62 suggesting that subsite 1 is crucial to the positioning of cellooligosaccharides as well as MeUmb(Glc$\underline{p}$) glycosides in the active site of CBH I(D). The change in bond cleavage frequencies with derivatization confirms the utility of using [1-^{3}H]cellooligosaccharides to investigate the action patterns of cellulolytic enzymes.

Gum (98) investigated the action patterns of CBH I(D) of T. viride using reduced cellooligosaccharides. When reduced cellohexaose was used as substrate, CBH I(D) exhibited little tendency to cleave bond 5, which links the sorbityl residue to previous reducing end of the cellooligosaccharide. The decrease in the formation of glucose may be explained in two ways: (1) if bond 5 is normally hydrolyzed by CBH I(D), then the subsite, which is adjacent to the catalytic groups and may position the glucosyl residue properly, rejects the sorbityl residue or (2) if bond 1 is normally hydrolyzed, then the subsite, which is 5 subsites away from the catalytic groups and may be essential to positioning cellohexaose properly, rejects the sorbityl residue and bond 1 is no longer hydrolyzed. Cellobiohydrolase I(D) produces [1-^{3}H]glucose by hydrolysis at bond 5, therefore explanation (1) above is correct. The loss in specificity of cleavage at bond 5 resulting from the reduction of cellohexaose emphasizes the importance of using [1-^{3}H]cellooligosaccharides to investigate the action patterns of cellulolytic enzymes.

Gritzali (6) investigated the action patterns of CBH I(D) and CBH II on cellotriose through cellohexaose. Since the observed molar ratios of products could have arisen from more than one combination of cleavages, the precise identity of glycosidic bonds cleaved could not be determined.

Synergism of Cellulolytic Enzymes

Mixtures of purified endoglucanases, cellobiohydrolases and ß-glucosidases of T. koningii, F. solani and P. funiculosum synergistically degrade various types of cellulose (100). Cotton is degraded with a high degree of synergism, whereas phosphoric acid-swollen cellulose shows less synergism and CM-cellulose is not synergistically degraded. Mixtures of component cellulolytic enzymes of T. reesei have also been shown to synergistically degrade cellulose (6,7). Furthermore, Fagerstam and Pettersson (7) have shown that CBH I(D) and CBH II synergistically degrade cellulose and have referred to this synergism as exo-exo synergism.

Endo-exo synergism is believed to result from the concerted action of endoglucanases and cellobiohydrolases. Endoglucanases hydrolyze internal glycosidic bonds of cellulose producing chain ends from which cellobiohydrolases remove cellobiosyl residues. Wood and McCrae (18) have suggested that a "loose complex" between cellobiohydrolases and endoglucanases may form at the surface of cellulose. After endoglucanase cleaves a glycosidic bond, cellobiohydrolase immediately binds to a chain end and begins removing cellobiosyl residues before the glycosidic bond reforms. The difference in the specificity of endoglucanases and cellobiohydrolases provides a basis for synergism.

The exo-exo synergism described by Fagerstam and Pettersson (7) for CBH I(D) and CBH II is not readily

explained by a difference in specificity, because each enzyme removes cellobiosyl residues from chain ends. However, evidence provided in this report suggests that CBH I(D) removes cellobiosyl and glucosyl residues from the reducing end of [1-^{3}H]cellooligosaccharides, whereas CBH II removes cellobiosyl residues from the nonreducing end. Since no evidence for the formation of a complex between CBH I(D) and CBH II has been provided, alternative explanations must be offered for synergism. To explain how CBH I(D) and CBH II by removing cellobiosyl residues from chain ends in opposite directions results in synergism, the structure of cellulose needs to be considered. Two major forms of cellulose, cellulose I and cellulose II, have been described (9). Cellulose I, native crystalline cellulose, is considered from X-ray diffraction studies to be arranged in parallel chains, whereas the arrangement of chains in cellulose II are antiparallel. However, Atalla and VanderHart (11) has recently reported that native celluloses isolated from various sources contain different degrees of cellulose I and cellulose II. The amount of cellulose I decreases in order of Acetobacter xylinium, Valonia ventricosa, cotton, ramie and cellulose II (regenerated cellulose I). Avicel, which was the substrate used during the assay showing exo-exo synergism, is isolated from α-cellulose and is presumably cellulose II (18).

Microfibrils of cellulose I and cellulose II may be diagrammatically represented as in Fig. 8-1. Cellulose I

Figure 8-1 Structure of cellulose I and cellulose II

The structure of cellulose I (A) and cellulose II (B) have parallel and antiparallel chains, respectively. Reducing end glucosyl residues are represented by ø.

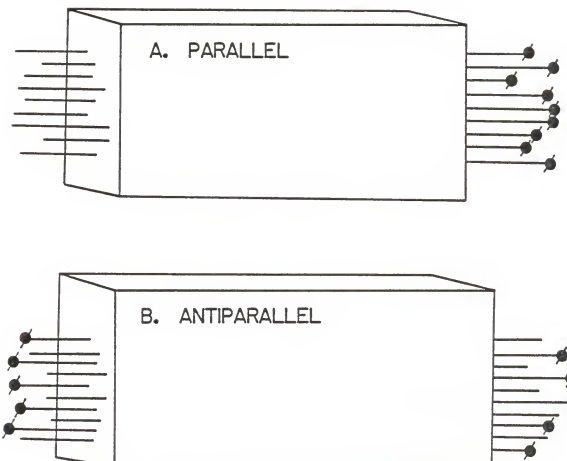
A. PARALLEL
B. ANTIPARALLEL

may be considered as a block with nonreducing chain ends protruding into solution on one side and on the other side reducing chain ends protruding into solution. If CBH I(D) and CBH II acted on cellulose I, the product would be a truncated version of that shown in Fig. 8-1a; however, the activity of either enzyme would not produce appropriate chain ends for the other. Therefore, synergism would not be expected. If CBH I(D) acted on cellulose II (Fig. 8-1b), then CBH I(D) would expose reducing chain ends from which cellobiosyl residues may be removed by CBH II. Cellobiohydrolase II, on the other hand, would expose reducing chain ends from which CBH I(D) would remove cellobiosyl residues. The production of more accessible chain ends by either enzyme would result in synergism.

Another important feature of cellulose is the cellobiose repeating unit. Wood (100) has noted that the glycosidic bonds of contiguous glucosyl residues, which are held in position by hydrogen bonds, are in different planes. An enzyme proceeding down a cellulose chain encounters an array of hydroxyl groups and hydrogen bonding which is different from those of the adjacent residue (Fig. 8-2). The ability of CBH I(D) and CBH II to bind [1-^{3}H]cellooligosaccharides in two productive modes allows them to hydrolyze the appropriate chain ends regardless of the orientation of the first glycosidic bond they encounter. The alternating position of the glycosidic bonds may also explain the action pattern of CBH I(D) on [1-^{3}H]cellohexaose. The bond cleavage

Figure 8-2 Orientation of glycosidic bonds in cellulose

Glycosidic bonds of contiguous glucosyl residues in cellulose are in different planes.

frequencies for bonds 1, 2, 3, 4 and 5 of [1-^{3}H]cellohexaose are <0.005, 0.005, 0.025, 0.35 and 0.62, respectively. The action patterns of CBH I(D) on [1-^{3}H]cellohexaose and [^{14}C-U]cellohexaose indicate that attack at bond 5 is immediately followed by attack at bond 3. Since the bond cleavage frequency at bond 4 of [1-^{3}H]cellopentaose yielding [1-^{3}H]glucose is 0.48, bond 4 of the original cellohexaose might be more likely cleaved than bond 3 after hydrolysis at bond 5. However, cleavage of the resulting cellopentaose at bond 4 would produce a significantly higher [^{14}C-U]glucose/[1-^{3}H]glucose ratio than observed. When the stereochemistry of the cellulosic substrate is considered, bonds 1, 3 and 5 have the same orientation, whereas bonds 2 and 4 have the opposite orientation. Therefore, repetitive attack initiated at bond 5 must immediately proceed to bond 3.

Individual Roles of Cellulolytic Enzymes

The cellulase system of T. reesei comprises endoglucanases, CBH I(D), CBH II and ß-glucosidases which together act sequentially and cooperatively to degrade crystalline cellulose to glucose. Through the use of [1-^{3}H]cellooligosaccharides and [^{14}C-U]cellooligosaccharides the roles of CBH I(D), CBH II and ß-glucosidase are more clearly understood. The increase in the affinity of ß-glucosidases for cellooligosaccharides as chain length increases suggested to Shewale (90) that the primary role of the ß-glucosidase is to convert cellooligosaccharides to glucose during the saccharification of cellulose. Comparison of k_{cat}/K_m values

for hydrolysis of [1-^{3}H]cellotriose by ß-glucosidase, CBH I(D) and CBH II indicates that [1-^{3}H]cellotriose is hydrolyzed 170- and 200-fold more efficiently by ß-glucosidase than by CBH I(D) and CBH II, respectively (Appendix F). Although the k_{cat}/K_m value of [1-^{3}H]cellotetraose hydrolysis by ß-glucosidase is approximately 2-fold higher than that of CBH I(D), the k_{cat}/K_m value for [1-^{3}H]cellotetraose hydrolysis by CBH II is approximately 3.6-fold higher than that of ß-glucosidase. The k_{cat}/K_m values for hydrolysis of [1-^{3}H]cellopentaose and [1-^{3}H]cellohexaose by CBH I(D) and CBH II are greater than 3-fold higher than the corresponding values for the ß-glucosidase. Furthermore, CBH I(D) and CBH II show little tendency to hydrolyze cellobiose. Thus, the role of the ß-glucosidase is primarily to hydrolyze cellobiose and cellotriose.

The role of the ß-glucosidase is reflected in the topography of its active site, which consists essentially of three subsites. The first subsite may serve to anchor substrate and position the scissile bond across the catalytic groups. Binding affinity for glucosyl residues at subsite 2 is negligible; however, subsite 2 has strong affinity for hydrophobic aglycones of glucosides; such as p-nitrophenyl-ß-D-glucoside and methylumbelliferyl-ß-D-glucoside. Values of V_{max}/K_m for p-nitrophenyl-ß-D-glucoside and methylumbelliferyl-ß-D-glucoside have been reported to be 30- and 125-fold higher than that for cellobiose (8). Low affinity for glucosyl residues at subsite 2 may promote

diffusion of product after hydrolysis. Significant affinity for glucosyl residues at subsite 3 permits the ß-glucosidase to scavenge cellotriose, which is a poor substrate for CBH I(D) and CBH II, produced during saccharification of cellulose. Affinities at subsites 4, 5 and 6 may represent nonspecific interactions between ß-glucosidase and longer cellooligosaccharides. Cellooligosaccharides of chain length greater than three will be rapidly hydrolyzed by CBH I(D) or CBH II. The ß-glucosidase exhibits little tendency to repetitively attack cellooligosaccharides supporting the idea that its role in the cellulase system of T. reesei is primarily to convert cellobiose and cellotriose to glucose rather than to depolymerize cellooligosaccharides.

The roles of CBH I(D) and CBH II are to remove cellobiosyl residues from reducing and nonreducing chain ends of cellulose, respectively. Furthermore, CBH I(D) and CBH II repetitively attack [1-^{3}H]cellooligosaccharides. Repetitive attack of cellooligosaccharides by CBH I(D) and CBH II has been shown previously by Gritzali (6). Berghem and Pettersson (101) have shown that a cellobiohydrolase from T. viride successively removes cellobiosyl residues from phosphoric acid-swollen cellulose. The lower activity of CBH I(D) on [1-^{3}H]cellooligosaccharides compared to CBH II may explain why T. reesei secretes more CBH I(D) than CBH II; the amount of CBH I(D) and CBH II in extracellular filtrates has been estimated at 60 and 25 percent (weight of protein), respectively (5).

The subsite maps of CBH I(D) constructed using the methods of Suganuma et al. (45) and Allen and Thoma (48) show significant binding affinity for glucosyl residues at subsites 1-4 and 7. The catalytic groups are located between subsites 5 and 6. Subsites distant from the catalytic groups and toward the nonreducing end may permit CBH I(D) to hold a portion of the substrate in the active site after hydrolysis. The absence of significant binding beyond subsite 7 may indicate the end of the active site. A physical block at the nonreducing end of the active site of glucoamylase has been proposed to explain the formation of only one productive complex in glucoamylase-catalyzed hydrolysis of maltooligosaccharides (44). Unfavorable affinity at subsite 6 may promote catalysis by introducing strain into the scissile glycosidic bond or by promoting diffusion of product away from the active site after hydrolysis. Unfavorable binding at one of the binding sites adjacent to catalytic groups has been reported for glucoamylases (44,47), B. amyloliquefaciens α-amylase (49) and lysozyme (40). Aspergillus oryzae α-amylase is a repetitive attack enzyme for which a subsite map has been constructed using the method of Allen and Thoma (49). The substrate binding region is composed of 7 subsites of which subsite 2 contributes the greatest proportion of binding energy. The catalytic groups are located between subsites 3 and 4. Subsite 7 has unfavorable binding and acts as a "barrier subsite" reducing hydrolysis of certain binding modes.

The unusual dependence of bond cleavage frequencies on concentration of [1-^{3}H]cellotriose may be explained by the topography of the active site of CBH I(D). Since the major product of [1-^{3}H]cellotriose hydrolysis at low concentrations is [1-^{3}H]glucose, [1-^{3}H]cellotriose must reside in subsites 4, 5 and 6 with the reducing end glucosyl residue bound in subsite 6. At high concentrations of [1-^{3}H]cellotriose, a second molecule of [1-^{3}H]cellotriose may bind to subsites 2, 3 and 4, which have significant affinity for glucosyl residues, and shift [1-^{3}H]cellotriose in subsites 4, 5 and 6 to subsites 5, 6 and 7. Thus a larger proportion of [1-^{3}H]cellobiose would be produced.

Subsite maps, constructed using the methods of Suganuma et al. (48) and Allen and Thoma (45), for CBH II show that catalytic groups are located between subsites 3 and 4. Subsites 5, 6 and 7 at the reducing end of the active site have significant affinity for glucosyl residues. Significant binding affinity for glucosyl residues at subsites 5, 6 and 7 located toward the reducing end of substrates may serve to retain cellooligosaccharides in the active site for subsequent hydrolysis. Unfavorable binding at subsite 4 may promote catalysis by straining the scissile bond or facilitating diffusion of products from the active site.

Methods of Subsite Mapping

There are several methods available in the literature to evaluate subsite affinities of polysaccharide depolymerizing enzymes (45,45,48,71). The application of a method

depends on the number of productive binding modes that an enzyme forms with oligosaccharide substrates. Since the method of Hiromi et al. (44) can be applied to enzymes that bind substrates in only one productive complex, this method was used to evaluate subsite affinities of the ß-glucosidase. The method of Roeser and Legler (71) was originally used to assess the contribution of individual parts of substrate to binding in glycoside hydrolysis by ß-glucosidase from A. wentii. However, the method of Roeser and Legler (71) may also be applied to evaluating the contributions of individual glucosyl residues of cellooligosaccharides. When the formation of more than one productive complex is detected, the methods of Suganuma et al. (45) and Allen and Thoma (48) are more appropriate, because they partition affinities of different subsites according to bond cleavage frequencies. Since CBH I(D) and CBH II bind cellooligosaccharides in more than one productive complex, the methods of Suganuma et al. (45) and Allen and Thoma (48) were used to evaluate their subsite affinities. The equations essential to the formulation of each subsite mapping procedure are presented in Appendix A.

The method of Roeser and Legler (71) was used to evaluate the contribution of glucosyl residues of cellooligosaccharides to binding by measuring cellobiose through cellohexaose inhibition of methylumbelliferyl-ß-D-glucoside hydrolysis catalyzed by the ß-glucosidase. Subsite affinities will be accurate if inhibition constants

represent true dissociation constants. Since cellooligosaccharides are substrates for the β-glucosidase, their inhibition constants may not be true dissociation constants. However, Lineweaver-Burk and Dixon plots of inhibition by cellobiose through cellohexaose of MUG hydrolysis are linear indicating that the inhibitors are not significantly degraded during the time course of the assay. The stability of cellooligosaccharides in the assay mixture is expected, because the value of V_{max}/K_m for MUG hydrolysis (8) by β-glucosidase is approximately 4-fold higher than that for cellooligosaccharide hydrolysis. Each cellooligosaccharide competitively inhibits the β-glucosidase suggesting that cellooligosaccharides bind to the same subsites. Thus, the ratio of inhibition constants for an n-mer and n+1-mer provides an estimate of the subsite affinity for the n+1-mer glucosyl residue. Since previously reported substrate specificity studies (8) suggest that glucose primarily binds toward the nonreducing side of the catalytic groups and that the region of the β-glucosidase which binds the aglycone is hydrophobic, the binding affinity of subsite 1 was evaluated from the K_i for glucose. Affinity at subsite 2 was evaluated from the ratio of inhibition constants for glucose and cellobiose.

Hiromi et al. (44) evaluated subsite affinities of glucoamylase from R. delemar using first order rate constants (V_{max}/K_m) for hydrolysis of a series of maltooligosaccharides. Three important assumptions made by the

authors are (1) 1/Km for each oligosaccharide approximates its association constant, (2) the value of the hydrolytic rate coefficient (k+2) is independent of chain length and (3) subsite affinities are additive. The values of K_m for cellooligosaccharide hydrolysis by the ß-glucosidase are similar to inhibition constants supporting the validity of assumption (1) for ß-glucosidase. The values of V_{max} for cellobiose through cellohexaose are similar supporting the assumption (2) that k+2 is independent of chain length. Assumption (3) is made by all subsite mapping procedures and is necessary to calculate individuals subsite affinities. Values of V_{max}/K_m for [1-^{3}H]cellobiose through [1-^{3}H]cellohexaose provided estimates for affinities of subsites 3-6 using the method of Hiromi et al. (44). Affinity of subsite 1 and the value of k_{+2} were evaluated from the intercepts of a linear plot of $\exp(-\Delta G_{n+1}/RT)$ versus $[E_o/V_n]$. However, this plot was not linear when corresponding values for the ß-glucosidase were used. Since the affinity at subsite 1 cannot be estimated for the ß-glucosidase by Hiromi's method; the affinity at subsite 2 can not be evaluated. Examination of the plot reported for glucoamylase reveals that the linearity of the plot is completely dependent on the value of V_{max} for maltose (44). The value of V_{max} for maltose is 5-fold higher than any of the other maltooligosaccharide substrates. Thus, the method of Hiromi et al. (44) does not provide an estimate for ΔG_1 when V_{max} is constant. Affinities of subsite 1 and 2 must be evaluated

using other experimental approaches. The methods of Roeser and Legler (71) and Hiromi et al. (44) provide similar affinities for subsites 3-6, supporting the validity of using either ratios of V_{max}/K_m or K_i to determine these subsite affinities.

The method of Suganuma et al. (45) was used to construct subsite maps for CBH I(D) and CBH II using bond cleavage frequencies and V_{max}/K_m values for [1-^{3}H]cellotriose through [1-^{3}H]cellohexaose. The three assumptions made by Hiromi et al. (44) are also made by Suganuma et al. (45). Values of V_{max}/K_m, which provide a direct estimate of subsite affinities, are partitioned using bond cleavage frequencies. Comparisons of hydrolytic rates for pairs of substrates differing in chain length by one glucosyl residue provide estimates for affinities of all subsites except the two subsites adjacent to catalytic groups. Since V_{max}/K_m values provide information about productive complexes only and subsites adjacent to catalytic groups are common to all productive complexes, affinities of subsites adjacent to catalytic groups can not be evaluated. The method of Suganuma et al. (45) does not require values of K_m and V_{max}, which provide information about nonproductive complexes and are essential to evaluating affinities of subsites adjacent to catalytic groups.

The method of Suganuma et al. (45) provides estimates of affinities of a particular subsite from more than one combination of substrate and bond cleavage frequencies. The

authors suggest that the most reliable value is that obtained for the major products. However, equally reliable favorable and unfavorable affinities for subsites 2, 3 and 7 of CBH I(D) and 1 and 6 of CBH II were calculated using the method of Suganuma et al. (45). The discrepancies in subsite affinities may indicate that hydrolytic rate coefficients (k+2) for cellooligosaccharide hydrolysis by CBH I(D) and CBH II are dependent on chain length. Another disadvantage of the method of Suganuma et al. (45) is that it does not provide estimates of affinities of subsites adjacent to catalytic groups.

The subsite mapping method of Allen and Thoma (48) requires quantitative determination of bond cleavage frequencies and Michaelis parameters (K_m and V_{max}) for a series of oligosaccharides to evaluate a complete subsite map. Substrates of chain length equal to or greater than the entire binding region are used to measure the sum of the subsite binding energies. Since the method of Allen and Thoma (48) does not assume that hydrolytic rate coefficients (k_{+2}) are independent of chain length, ratio of bond cleavage frequencies for a pair of oligosaccharides provide a measure of the difference between 2 subsite energies and the ratio of hydrolytic rate coefficients. The sum of binding energies for subsites adjacent to the catalytic groups can be partitioned between the two subsites using K_{int}, (microscopic dissociation constant for a binding mode in which the entire binding region is occupied) and

Michaelis parameters for all other sites. Allen and Thoma (48) also use an acceleration factor, which is the average contribution a glucosyl residue makes to the binding energy, in order to obtain good fits between experimental and predicted bond cleavage frequencies, K_{int}, K_m and V_{max}.

Subsite maps for CBH I(D) and CBH II were constructed using the method of Allen and Thoma (48) and experimental values of bond cleavage frequencies, K_m and V_{max} for [1-^{3}H]cellotriose through [1-^{3}H]cellohexaose. The minimum number of subsites required to account for the bond cleavage frequencies of each enzyme is 7. The value of K_m for [1-^{3}H]cellohexaose was used as an approximation of K_{int}. However, this is not an adequate approximation, because [1-^{3}H]cellohexaose is not equal to or greater than the substrate binding region. Cellooligosaccharides of chain length greater than 6 show limited solubility in water. Therefore, the subsite maps for CBH I(D) and CBH II must be considered approximations of true subsite maps. Subsite mapping is also limited, because CBH I(D) and CBH II repetitively attack cellooligosaccharides. For example, the apparent V_{max} for hydrolysis of [1-^{3}H]cellohexaose underestimates the catalytic abilities of CBH I(D) and CBH II, because more than one bond is hydrolyzed per enzyme-substrate encounter. Although values of K_m and V_{max} derived from initial rates of [1-^{3}H]cellooligosaccharide hydrolysis by CBH I(D) and CBH II and those predicted from subsite binding energies agree within 20 percent, several differ by

5-fold. The lack of agreement probably reflects the need for values of bond cleavage frequencies, K_m and V_{max} for [1-^{3}H]cellooligosaccharides of chain length greater than the substrate binding region. Thus, refinement of subsite maps for CBH I(D) and CBH II requires (1) experimental conditions where repetitive attack is minimized and (2) the use of [1-^{3}H]cellooligosaccharides of chain length greater than 6. The synthesis and use of longer [1-^{3}H]cellooligosaccharides may require solvents other than water.

Future Experiments

The topography of the active sites of β-glucosidase, CBH I(D) and CBH II may be further investigated using the sensitive assay afforded by [1-^{3}H]cellooligosaccharides. The specificity of particular subsites may be examined using different glycosyl inhibitors. Lactones of cellooligosaccharide aldonic acids may also be used as inhibitors to provide information about subsites which bind nonreducing ends of substrates.

Although evidence provided in this report suggests that CBH I(D) and CBH II attack cellooligosaccharides from reducing and nonreducing ends, respectively, evidence confirming the direction of processivity may be obtained by measuring their ability to hydrolyze derivatized reducing and nonreducing ends of cellulose. The mechanism of exo-exo synergism may be further investigated by measuring the activities of CBH I(D) and CBH II on celluloses of different forms and crystallinities.

Subsite maps of CBH I(D) and CBH II may be refined by synthesizing [1-^{3}H]celloheptaose and [1-^{3}H]cellooctaose and then measuring bond cleavage frequencies, K_m and V_{max} for their hydrolysis.

CHAPTER 9
SUMMARY

To understand the process by which component enzymes of the cellulase system of T. reesei convert native crystalline cellulose to glucose, cellooligosaccharides that are asymmetrically and radioactively labeled are required. In this report, a method was developed for synthesizing cellooligosaccharides labeled at carbon one of the reducing end glucosyl residue with tritium. Asymmetry in [1-^{3}H]cellooligosaccharides permits identification of precise glycosidic bonds cleaved by cellulolytic enzymes. Sensitivity afforded by radioactively labeled cellooligosaccharides allows determination of initial velocities of cellooligosaccharide hydrolysis at micromolar substrate concentrations. A TLC method for separating [1-^{3}H]glucose through [1-^{3}H]cellohexaose with high resolution and extracting [1-^{3}H]cellooligosaccharides quantitatively is described. This method is superior to previously reported TLC methods for separating cellooligosaccharides and will facilitate analysis of cellulolytic enzymes.

Activity on [1-^{3}H]cellooligosaccharides indicated that the ß-glucosidase binds [1-^{3}H]cellooligosaccharides in one productive mode and removes glucosyl residues from the nonreducing end. The ß-glucosidase exhibits little tendency to

repetitively attack [1-^{3}H]cellooligosaccharides. Values of V_{max} for [1-^{3}H]cellooligosaccharide hydrolysis remain essentially constant as chain length increases, whereas values of K_m decrease. Cellooligosaccharides were used to inhibit methylumbelliferyl-ß-D-glucoside hydrolysis by ß-glucosidase. Inhibition constants for cellooligosaccharides are similar to corresponding values of K_m indicating that $1/K_m$ approximates association constant. Subsite maps constructed using the methods of Hiromi et al. (44) and Roeser and Legler (71) show that the active site consists primarily of 3 subsites. Subsite 1 contributes the greatest proportion of binding energy and the catalytic groups are located between subsites 1 and 2. Thus, the role of the ß-glucosidase during saccharification of cellulose is to convert primarily cellobiose and cellotriose to glucose.

Cellobiohydrolase I(D) was shown to bind [1-^{3}H]cellooligosaccharides in more than one productive mode. Values of V_{max}/K_m increase with increasing chain length. Activity on [1-^{3}H]cellooligosaccharides and [^{14}C-U]cellooligosaccharides indicate that CBH I(D) repetitively attacks cellooligosaccharides from the reducing end. Subsite maps constructed for CBH I(D) using the methods of Suganuma et al. (45) and Allen and Thoma (48) show that the active site consists of at least 7 subsites and the catalytic groups are located between subsites 5 and 6.

Cellobiohydrolase II also binds [1-^{3}H]cellooligosaccharides in more than one productive mode. Values of V_{max}/K_m

increase with increasing chain length. Action patterns resulting from cleavage of [1-^{3}H]cellooligosaccharides and [^{14}C-U]cellooligosaccharides suggest that CBH II repetitively attacks cellooligosaccharides from the nonreducing end. Subsite maps constructed for CBH II using methods of Suganuma et al. (45) and Allen and Thoma (48) show that the active site consists of at least 7 subsites and that the catalytic groups are located between subsites 3 and 4.

The difference in the direction from which cellobiosyl residues are repetitively removed from cellooligosaccharides by CBH I(D) and CBH II suggests that exo-exo synergism may result from the ability of CBH I(D) to expose nonreducing chain ends for CBH II by hydrolyzing surrounding reducing ends. Similarly, CBH II may expose reducing chain ends for CBH I(D) by hydrolyzing surrounding nonreducing chain ends.

APPENDIX A
SUBSITE MAPPING OF ENZYMES

A synopsis of equations used to evaluate subsite affinities of polysaccharide depolymerases is presented below. Detailed theoretical treatments of subsite mapping have been reported previously (37,41,43-46,48). Although the subsite mapping procedures of Hiromi et al. (44), Suganuma et al. (45) and Allen and Thoma (48) originate from a common theoretical base, some assumptions, which are described below, distinguish the methods. To facilitate comparisons among the methods, the nomenclature of Allen (37) will be used below. A list of symbols and notations is presented at the end of this section.

The object of subsite mapping is to partition enzymic processes into measurable macroscopic constants, which describe the net association of substrate with enzyme, and microscopic constants, which describe processes associated with one particular binding mode. For example, the positional binding modes of a trisaccharide with a four-subsite enzyme are shown in Fig. A-1. Each binding mode (1,3-6,3) is characterized by a microscopic association constant and each productive E-S complex (3,3 and 4,3) has, in addition, a microscopic hydrolytic rate coefficient. A combination of microscopic association constants will define

Figure A-1 Binding modes of cellotriose on a hypothetical four-subsite enzyme

Cellotriose may bind to a four-subsite enzyme in several binding modes. The arrow shows the position of catalytic groups. Reducing end glucosyl residues are represented by ø. The broken line shows the position of bond cleavage. The nomenclature of Allen (37) is used to describe the binding modes.

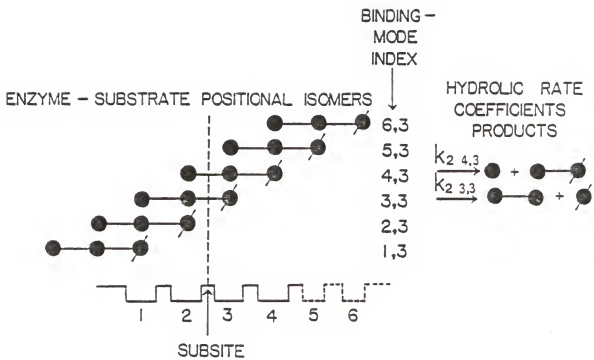
BINDING – MODE INDEX
ENZYME – SUBSTRATE POSITIONAL ISOMERS
6,3
5,3
4,3
3,3
2,3
1,3
HYDROLIC RATE COEFFICIENTS PRODUCTS
$K_{2\ 4,3}$
$K_{2\ 3,3}$
1 2 3 4 5 6
SUBSITE

each measurable macroscopic association constant, whereas a specific combination of microscopic rate coefficients and microscopic association constants may define a measurable macroscopic velocity.

The Michaelis scheme for binding and hydrolysis of a polymeric substrate may be desribed as (37,41,43-46,48):

$$E + A_n \underset{k_{-1,r,n}}{\overset{k_{+1,r,n}}{\rightleftharpoons}} E\,A_{r,n} \xrightarrow{k_{+2,r,n}} E + P_{r,n-m} + P_{r,m} \qquad (1)$$

where E is enzyme, A_n is substrate of n monomeric units in length, $P_{r,n-m}$ is product of chain length n-m arising from the nonreducing end and $P_{r,m}$ is product of chain length m arising from the reducing end of substrate. The microscopic rate coefficients $k_{+1,r,n}$ and $k_{-1,r,n}$ describe the binding and dissociation of substrate and enzyme in binding mode r. The term r specifies a binding mode in which the real or virtual subsite occupied by the reducing end glycosyl residue. The microscopic hydrolytic rate coefficient is $k_{+2,r,n}$. A feature which distinguishes the method of Hiromi et al. (44) from that of Allen and Thoma (48) is the assumption by Hirmoi et al. (44) that the hydrolytic rate coefficient is independent of chain length n.

When rapid equilibrium between E and A_n is assumed ($k_{-1,r,n} \gg k_{+2,r,n}$), a rate equation of the same form as the Michaelis-Menton type is obtained where the inverse of the macroscopic Michaelis constant ($\tilde{K}_{m,n}$) is the sum of the

inverse of microscopic Michaelis constants. The inverse of the microscopic Michaelis constant ($\tilde{K}_{h,n}$) approaches an association constant ($K'_{h,n}$):

$$\frac{1}{\tilde{K}_{m,n}} = \sum_{h=1}^{l+n-1} \frac{1}{\tilde{K}_{h,n}} = \sum_{h=1}^{l+n-1} K'_{h,n} \qquad (2)$$

where h is the general binding-mode index, specifying the real or virtual subsite occupied by the reducing end glycosyl residue and l is the number of real subsites comprising the binding region of the enzyme. The macroscopic maximum velocity ($\tilde{V}_n/E_o$) is expressed as:

$$\frac{\tilde{V}_n}{E_o} = \frac{\sum_{h=c}^{c+n-2} \frac{k_{+2,h,n}}{\tilde{K}_{h,n}}}{\sum_{h=1}^{l+n-1} \frac{1}{\tilde{K}_{h,n}}} = \frac{\sum_{h=c}^{c+n-2} k_{+2,h,n} K'_{h,n}}{\sum_{h=1}^{l+n-1} K'_{h,n}} \qquad (3)$$

where c is the index position of the catalytic site, specifiying the subsite to the right of the position of bond cleavage. The first order rate constant for enzymic hydrolysis at low concentration of substrate ($A_n << \tilde{K}_{m,n}$) is $\tilde{k}'_n$:

$$\tilde{k}'_n = \frac{\tilde{V}_n}{\tilde{K}_{m,n}[E_o]} = \sum_{h=2}^{c+n-2} \frac{k_{+2,h,n}}{\tilde{K}_{h,n}} . \qquad (4)$$

The first order rate constant contains terms for productive binding only, whereas $\tilde{K}_{m,n}$ and $\tilde{V}_n$ contain terms for

productive and nonproductive binding. The macroscopic constants $\tilde{K}_{m,n}$, $\tilde{V}_n$ and $\tilde{k}'_n$ are measurable and are related to microscopic constants by equations (2)-(4).

The free energy of binding of a glycosyl residue to a particular subsite is assumed to be constant and not affected by binding at another subsite. Therefore, the macroscopic association constant for each binding mode of an n-mer ($K'_{r,n}$) is related to the sum of the binding energies of occupied subsites by:

$$\sum_{i=r-n+1}^{r} \Delta G_i + 2500 = -RT \ln K'_{r,n} \qquad (5)$$

where ΔG_i is the unitary free energy of binding for subsite i. The 2500 cal/mol arises from the entropy of mixing in water at 40°C and is referred to as the cratic free energy contribution to binding (102,103).

Application of Subsite Mapping by Hiromi et al. (44)

Since a true exoenzyme binds substrate in only one productive mode, equation (4) may be expressed as:

$$k'_n = \frac{k_{+2,h,n}}{K_{h,n}} = k_{+2,h,n} K'_{r,n} \qquad (6)$$

insofar as the inverse of the Michaelis constant approximates the association constant. The ratio of first order rate constants for an n-mer and n+1-mer are expressed in terms of subsite binding energies by using equations (5) and (6):

$$\frac{\tilde{k}'_n}{\tilde{k}'_{n+1}} = \frac{k_{+2,r,n}}{k_{+2,r+1,n+1}} \exp(\Delta G_{n+1}/RT) \quad . \qquad (7)$$

Ratios of first order rate constants provide an estimate of affinities of subsites c+1 and larger, if hydrolytic rate coefficients are independent of n. Affinities of subsites 3-7 of glucoamylase from R. delemar (44) and A. saito (47) have been evaluated using equation (7).

Hiromi et al. (44) showed that the binding energy for maltose calculated using equations (2) and (5) is higher than could be accounted for by subsites 3-7. Therefore, Hiromi et al. (44) assumed that only subsites 1 and 2 contribute significantly to the binding of oligosaccharides and calculated the binding energy for subsite 1 by expressing equation (3) in terms of subsite binding affinities to yield:

$$\exp(-\Delta G_{n+1}/RT) = \left[\frac{k_{+2,r,n}}{\tilde{V}_n/E_o} - 1 \right] \exp(-\Delta G_1/RT) \quad . \qquad (8)$$

If only subsites 1 and 2 contribute significantly to binding of oligosaccharides and hydrolytic rate coefficients are independent of n, then a plot of $\exp(\Delta G_{n+1}/RT)$ versus $[E_o]/\tilde{V}_n$ should be linear. Vertical and horizontal intercepts give ΔG_1 and $k_{+2,r,n}$, respectively.

The affinity at subsite 2 can be evaluated using two methods. The Michaelis constant for each n-mer can be used

to estimate the sum of affinities of occupied subsites. Since the binding energy for all subsites except subsite 2 have been evaluated, they can be used to evaluate the binding energy at subsite 2. Alternatively, k_{+2} and first order rate constants can be used with equations (5) and (6) to calculate the affinity at subsite 2.

Affinities for subsites 3-6 of the β-glucosidase were calculated using first order rate constants by the method of Hiromi et al. (44). For example, the free energy of binding to subsite 3 was calculated using the first order rate constants of [1-^{3}H]cellobiose and [1-^{3}H]cellotriose hydrolysis and equation (7):

$$\frac{\tilde{k}'_n}{\tilde{k}'_{n+1}} = \exp\left(\Delta G_{n+1}/RT\right)$$

$$RT \ln\left(\frac{0.0200}{0.217}\right) = \Delta G_{n+1}$$

$$-1480 \text{ cal/mol} = \Delta G_{n+1}$$

However, k_{+2} and ΔG_1 could not be evaluated using the method of Hiromi et al. (44), because a plot of $\exp(\Delta G_{n+1}/RT)$ versus $[E_o]/\tilde{V}_n$ was not linear [equation (8)]. Since ΔG_1 and k_{+2} could not be estimated, ΔG_2 could not be evaluated.

Application of Subsite Mapping by Allen and Thoma (48)

The method of Allen and Thoma (48) uses four approximately accessible paramters: $\tilde{K}_m$, $\tilde{V}$, bond cleavage

frequencies and $\tilde{K}_{int}$ to evaluate subsite affinities. Substrates that cover the entire binding region of the active site can be used to measure the sum of subsite binding affinities. All binding modes in which subsites are completely occupied are assumed to have the same dissociation constant, K_{int}. Equation (2) can be written in terms of K_{int} by partitioning it into:

$$\frac{1}{\tilde{K}_{m,n}} = \sum_{h=1}^{l-1} \frac{1}{K_{h,m}} + (n-l+1)\frac{1}{K_{int}} + \sum_{h=n+1}^{n+l-1} \frac{1}{K_{h,n}} \quad . \qquad (9)$$

The term $^1/K_{h,n}$ accounts for binding modes in which subsites on the right side of the binding region are vacant; the middle term accounts for binding in which all subsites are occupied and the last term accounts for binding modes when subsites on the left side of the binding region are vacant. Equation (9) is in a linear form and $^1/K_{int}$ is obtained from a plot of (n-l+1) versus $^1/K_{m,n}$ for $n \geq l$.

Information about subsites can also be obtained from the relative rates of formation of each product, i.e., bond cleavage frequencies. Specific productive bonding modes of a subsite are characterized by formation of specific products. The relative rate of formation of a product resulting from binding in a particular mode is proportional to the population of that enzyme-substrate complex multiplied by the corresponding hydrolytic rate coefficient. The relative rate of formation of product from

two adjacent binding modes is

$$\frac{[\dot{P}_{r,m}]}{[\dot{P}_{r+1,m+1}]} = \frac{k_{+2,r,n}/K_{r,n}}{k_{+2,r+1,n}/K_{r+1,n}} \qquad (10)$$

where $[\dot{P}_{r,m}]=d[P_{r,m}]/dt$. Since the k_{+2} term goes to zero in the numerator of equation (1) for nonproductive complexes, bond cleavage frequencies provide information about only productive complexes. Bond cleavage frequencies also provide information about subsite-binding affinities and hydrolytic rate coefficients. Equation (5) may be solved for $K'_{r,n}$ and then substituted into equation (10):

$$RT\ln\frac{[\dot{P}_{r,m}]}{[\dot{P}_{r+1,m+1}]} = \Delta G_{r+1} - \Delta G_{r-n+1} + RT\ln\left(\frac{k_{+2,r,n}}{k_{+2,r+1,n}}\right) . \qquad (11)$$

Thus, a bond cleavage frequency provides information about the difference between two subsite affinities and the ratio of hydrolytic rate coefficients. Affinities of all subsites with the exception of the two adjacent to the catalytic groups can be evaluated using bond cleavage frequencies for a series of oligosaccharides. Since subsites adjacent to catalytic groups are common to all productive complexes, their affinities cannot be evaluated.

If hydrolytic rate coefficients (k_{+2}) are assumed equal, then bond cleavage frequencies provide a direct estimate of subsite affinities [equation (11)]. The method

of Suganuma et al. (45) assumes that hydrolytic rate coefficients are equal. However, Thoma et al. (43) found that binding energies estimated from equation (11) and used in equations (2), (3) and (5) yielded values of $\tilde{K}_{m,n}$ and $\tilde{V}_n/E_o$ that did not agree well with values of $\tilde{K}_{m,n}$ and $\tilde{V}_n/E_o$ calculated from experimental initial velocities. Agreement between predicted and experimentally derived values significantly improved when the approximation was made that the binding of a glycosyl residue decreases the activation energy by a constant amount enhancing the rate of bond cleavage. Thus, the hydrolytic rate coefficient (k_{+2}) may be expressed as a function of the number of occupied subsites:

$$k_{+2,r,n} \propto \exp\left(\sum_{i=r}^{r-n+1} \Delta G_{a,i}/RT\right) \qquad (12)$$

where $\Delta G_{a,i}$ is the contribution of the i-th real subsite to acceleration of bond cleavage. Equation (11) can be partitioned as:

$$RT\ln\frac{[\dot{P}_{r,m}]}{[\dot{P}_{r+1,m+1}]} = (\Delta G_{r+1} - \Delta G_{a,r+1}) - (\Delta G_{r-n+1} - \Delta G_{a,r-n+1})$$

$$= \Delta\tilde{G}_{r+1} - \Delta\tilde{G}_{r-n+1} \qquad (13)$$

revealing that apparent subsite affinities must be increased by an average acceleration factor to provide true binding

affinities. When an acceleration factor was used by Thoma et al. (43) values of $\tilde{K}_{m,n}$ and $\tilde{V}_n/E_o$ predicted from subsite energies agreed well with corresponding values estimated using experimental initial velocities.

Allen and Thoma (48) have incorporated the basic equations of subsite mapping into a depolymerase computer model which generates a subsite map that gives an optimum fit to experimentally derived paramters: $\tilde{K}_{m,n}$, $\tilde{V}_n$, bond cleavage frequencies and $\tilde{K}_{int}$. Bond cleavage frequencies are first used to estimate apparent subsite binding energies and the location of the catalytic groups [equations (5) and (10)]. The next step is to optimize binding energies for the two subsites adjacent to the catalytic groups while binding energy of the other subsites are constrained at values estimated from bond cleavage frequencies. All four parameters are then optimized by varying binding energies for all subsites, while the acceleration factor is not allowed to vary. Finally, the acceleration factor is varied and an optimum subsite map is obtained providing the minimum error between predicted values of $\tilde{K}_{m,n}$, $\tilde{V}_n$, bond cleavage frequencies and $\tilde{K}_{int}$ and those derived from experimental initial velocities. Optimized subsite maps for CBH I(D) and CBH II were generated using the depolymerase computer model, of which a tape and a test data set were kindly provided by J. D. Allen, Biotrack, Inc., Sunnyvale, CA.

Application of Subsite Mapping by Suganuma et al. (45)

The subsite mapping procedure for exoenzymes described by Hiromi et al. (44) was adapted for use with endoenzymes by Suganuma et al. (45). Since endoenzymes can bind substrate in more than one productive mode, the values of first order rate constants (k'_n) alone do not provide estimates of subsite affinities [equation (6)]. However, comparison of rate constants for the reactions yielding labeled m-mer and m+1-mer products from reducing end-labeled n-mer and n+1-mer substrates provides a basis for estimation of the affinity of the subsite to which the n+1 glycosyl residue binds. Since Suganuma et al. (45) assume that the hydrolytic rate coefficent is independent of n, equation (10) reduces to:

$$\frac{[\dot{P}_{r,m}]}{[\dot{P}_{r+1,m+1}]} = \frac{K'_{r,n}}{K'_{r+1,n+1}} \quad . \tag{14}$$

Equation (14) used in conjunction with equation (5) yields:

$$RT \ln \left(\frac{[\dot{P}_{r,m}]}{[\dot{P}_{r+1,m+1}]}\right) = \Delta G_{n+1} \tag{15}$$

where ΔG_{n+1} is the free energy of binding for subsite n+1. Comparison of first order rate constants ($\tilde{k}'_n$) and bond cleavage frequencies for pairs of substrates differing in

length by one glycosyl residue yields affinities of each subsite except those adjacent to the catalytic groups.

Subsite affinities of CBH I(D) and CBH II were evaluated using the method of Suganuma et al. (45). For example, subsites 4 and 7 of CBH I(D) were evaluated using first order rate constants and bond cleavage frequencies of [1-^{3}H]cellotriose and [1-^{3}H]cellotetraose in equation (16) derived from equations (4) and (5) (Figure A-2):

$$\Delta G_{n+1} = RT \ln \left(\frac{\tilde{k}'_n \, [\dot{P}_{r,m}]}{k'_{n+1} \, [P_{r+1,m+1}]} \right) \qquad (16)$$

$$\Delta G_7 = RT \ln \left(\frac{0.00177 \times 0.94}{0.479 \times 0.78} \right) = -3400 \text{ cal/mol}$$

$$\Delta G_4 = RT \ln \left(\frac{0.00177 \times 0.06}{0.479 \times 0.78} \right) = -5100 \text{ cal/mol}$$

Calculated bond cleavage frequencies of bonds 1 and 2 of [1-^{3}H]cellotriose are 0.06 and 0.94, respectively (Fig. 6-14). Bond cleavage frequency of bond 2 of [1-^{3}H]cellotetraose is found to be 0.79 (Fig. 6-14). Values of V_{max}/K_m for [1-^{3}H]cellotriose and [1-^{3}H]cellotetraose hydrolysis of CBH I(D) are 0.00177 and 0.479 μmol/min.mg.μM, respectively (Table 6-1).

Application of Subsite Mapping by Roser and Legler (71)

Roeser and Legler (71) calculated the contribution of individual parts of substrates to the free energy of binding of sugar analogs by ß-glucosidase A_3 from A. wentii using

Figure A-2 Combination of V_{max}/K_m values and bond cleavage frequencies for [1-^{3}H]cellotetraose and [1-^{3}H]cellotriose used to calculate subsite affinities

Schematic model for the productive ES complexes used to evaluate the affinities of subsites 4 (A) and 7 (B) of CBH I(D). The arrow shows the position of catalytic groups.

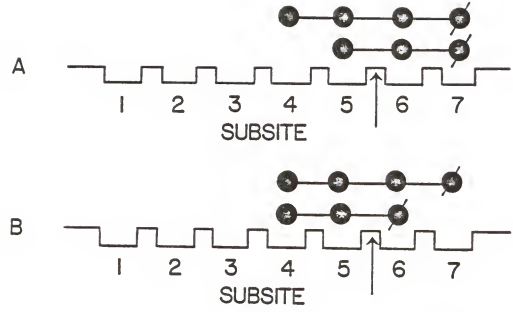
A
1 2 3 4 5 6 7
SUBSITE
B
1 2 3 4 5 6 7
SUBSITE

equation (17):

$$\Delta\Delta G^{o} = -RT \ln \left(\frac{K_i}{K_{i(ref)}}\right) \quad . \qquad (17)$$

Equation (16) was applied to determine affinities of subsites in the binding region of the β-glucosidase from T. reesei. For example, subsite 3 was calculated as follows:

$$\Delta\Delta G^{o}_{3} = -RT \ln \left(\frac{K_{i,2}}{K_{i,3}}\right)$$

$$= -RT \ln \left(\frac{1045}{58}\right) = -1800 \text{ cal/mol}$$

Affinity at subsite 1 was calculated using the inhibition constant of glucose (700 μM) (8) and equation (5):

$$\Delta G = -RT \ln (1/K_i) - 2500$$

$$= -RT \ln (1/7\times10^{-4}\text{M}) - 2500$$

$$= -7000 \text{ cal/mol}$$

Symbols and Notations Used in Subsite Mapping

A	Substrate
c	Index of the position of the catalytic site, specifying the subsite to the right of the position of bond cleavage
E	Enzyme
ΔG	Unitary free energy of binding
ΔG_a	Acceleration factor
h	General binding-mode index, specifying the real or virtual subsite occupied by the reducing-end glycosyl residue
i	Subsite index

j	Maximum chain length substrate for which experimental data are available
K	Microscopic dissociation constant
K'	Microscopic association constant
K_i	Inhibition constant
K_m	Michaelis constant
K_{int}	Microscopic dissociation constant for a binding mode in which the entire binding region is occupied
k	The first-order rate constant for enzymic hydrolysis
k_{+1}	Microscopic association rate constant
k_{-1}	Microscopic dissociation rate constant
k_{+2}	Hydrolytic rate coefficient
l	Number of real subsites comprising the binding region of an enzyme
m	Chain-length index for product
n	Chain-length index for substrate
P	Product
R	Gas constant
r	Specific binding-mode index, specifying the real or virtual subsite occupied by the reducing-end glycosyl unit
T	Absolute temperature
t	Sugar chain length
V	Maximum velocity
v_o	Measured velocity
$[^o]$	Concentration
$\tilde{}$	Measured or apparent value
$\cdot$	Time derivative

APPENDIX B
SAMPLE CALCULATIONS FOR BOND CLEAVAGE FREQUENCIES AND INITIAL RATES OF HYDROLYSIS OF [1-^{3}H]CELLOOLIGOSACCHARIDES

Bond cleavage frequencies and initial rates for hydrolysis of [1-^{3}H]cellooligosaccharides by exoglucanases were determined as described below for hydrolysis of [1-^{3}H]cellotetraose (15 μM) by CBH I(D):

1. The radioactivity of products ([1-^{3}H]glucose, [1-^{3}H]cellobiose and [1-^{3}H]cellotriose) and substrate ([1-^{3}H]cellotetraose) in TLC scrapings was measured at various time intervals. The sum of the radioactivity of products and substrate at each time interval was then calculated (Table B-1).
2. Product ratio for each product was determined at each time interval by dividing the radioactivity of each product by the sum of radioactivity of all products and substrate. Extent of reaction was calculated by dividing the sum of the radioactivity of the products by the sum of the radioactivity of products and substrate (Table B-2).
3. The amount of each product and substrate at each time interval was determined by multiplying the product and substrate ratios by the initial amount

Table B-1

Distribution of [1-^{3}H]Cellooligosaccharides from Hydrolysis of [1-^{3}H]Cellotetraose by CBH I(D)

Cellobiohydrolase I(D) (2.32×10^{-5} mg) was incubated at 40°C in 100 µl of 5 mM sodium acetate buffer, pH 5.0, containing 15 µM [1-^{3}H]cellotetraose.

Time (min)	DPM				
	[1-^{3}H]G1	[1-^{3}H]G2	[1-^{3}H]G3	[1-^{3}H]G4	Sum
0	531	798	672	45505	47506
2	958	2055	658	45307	48978
4	1281	3375	896	44551	50103
6	1599	4565	770	42823	49757
8	1904	5696	712	40556	48868
15	2727	9054	876	36902	49559
30	3810	14057	906	29202	47975
60	5825	21485	1103	21598	50011

Table B-2

Product Ratios for [1-^{3}H]Cellotetraose Hydrolysis by CBH I(D)

Time (min)	Product Ratio				Extent of Reaction
	[1-^{3}H]G1	[1-^{3}H]G2	[1-^{3}H]G3	[1-^{3}H]G4	
0	0.0112	0.0168	0.0141	0.958	0.0421
2	0.0196	0.0420	0.0134	0.925	0.0750
4	0.0256	0.0674	0.0179	0.889	0.111
6	0.0321	0.0917	0.0155	0.861	0.139
8	0.0390	0.117	0.0146	0.830	0.170
15	0.0550	0.183	0.0177	0.745	0.255
30	0.0794	0.293	0.0189	0.609	0.391
60	0.116	0.430	0.0220	0.432	0.568

of substrate; in this example, 1500 pmol (Table B-3).

4. Bond cleavage frequencies for each product were determined by plotting each product ratio versus extent of reaction (69). The slope of the line is the bond cleavage frequency. Linear regression analysis yielded bond cleavage frequencies for [1-^{3}H]G1, [1-^{3}H]G2, [1-^{3}H]G3 and [1-^{3}H]G4 of 0.197±0.002, 0.789±0.003, 0.0145±0.003 and -1.0±0.0, respectively. The corresponding R-squared values were found to be 99.9, 100.0, 80.8 and 100.0 percent, respectively.

5. Initial velocities for product formation and substrate degradation were determined by plotting the amount of product and substrate (pmol) versus time (min). Linear regression analysis of early, linear region yielded velocities determined from the slope for [1-^{3}H]G1, [1-^{3}H]G2, [1-^{3}H]G3 and [1-^{3}H]G4 of 5.40±0.51, 19.0±0.05, 1.40±1.12 and -25.8±0.6 pmol/min, respectively. The corresponding R-squared values were found to be 99.1, 100.0, 61.2 and 99.9 percent, respectively.

Table B-3

Concentration of [1-^{3}H]Cellooligosaccharides from Hydrolysis of [1-^{3}H]Cellotetraose by CBH I(D)

Time (min)	Pmol			
	[1-^{3}H]G1	[1-^{3}H]G2	[1-^{3}H]G3	[1-^{3}H]G4
0	16.8	25.2	21.2	1437
2	29.3	62.9	20.2	1387
4	38.4	101	26.8	1333
6	48.2	138	23.2	1291
8	58.4	175	21.8	1245
15	82.5	274	26.5	1117
30	119	440	28.3	913
60	175	644	33.1	648

APPENDIX C
KINETIC EQUATIONS

1. Cleland's HYPER program (70) was used to fit initial rates of [1-^{3}H]cellooligosaccharide hydrolysis to the hyperbola described by:

$$v = \frac{V_{max} \cdot A}{K_m + A} .$$

2. Cleland's TWO/ONE program was used to fit initial velocities determined for CBH I(D) hydrolysis of [1-^{3}H]cellotriose to:

$$v = \frac{V_{max1} \cdot A}{K_{m1} + A} + \frac{V_{max2} \cdot A}{K_{m2} + A} .$$

APPENDIX D
SUBSITE AFFINITIES FOR β-GLUCOSIDASE

Subsite	Binding Energy (cal/mol)	
	Determined from V_{max}/K_m values of [1-^{3}H]cellooligosaccharides	Determined from K_i values of cellooligosaccharides
1	-6880± 30	-7020±50
2		250±50
3	-1480± 70	-1800±30
4	-630± 90	-140±40
5	90± 70	-170±60
6	20±120	-70±70

APPENDIX E
KINETIC CONSTANTS FOR HYDROLYSIS OF β-LINKED DISACCHARIDES OF GLUCOSE BY β-GLUCOSIDASE

Activity of β-glucosidase was assayed at various concentrations of disaccharide in 50 mM sodium acetate buffer, pH 5.0, containing 3 mM sodium azide as described in Experimental Procedures. Kinetic constants were determined from initial rates of hydrolysis using Cleland's HYPER program (70).

Disaccharide	Linkage	K_m (μM)	V_{max} (μmole/min·mg)	V_{max}/K_m
Sophorose	β-1,2	1070±90	27 ± 1	0.025±0.001
Laminaribiose	β-1,3	460±20	22.6±0.4	0.048±0.002
Gentiobiose	β-1,6	960±60	8.3±0.2	0.0087±0.0004

APPENDIX F
KINETIC CONSTANTS FOR HYDROLYSIS OF
[1-^{3}H]CELLOOLIGOSACCHARIDES BY ß-GLUCOSIDASE,
CBH I(D), AND CBH II

To facilitate comparison of kinetic constants for hydrolysis of [1-^{3}H]cellooligosaccharides by the exoglucanases, kinetic constants found in Tables 5-1, 6-1, and 7-1 are expressed below as per mole of enzyme instead of per mg of protein. The molecular weights of ß-glucosidase, CBH I(D), and CBH II determined using sedimentation equilibrium analysis are reported to be 74600 (8), 53200 (6), and 54700 (6), respectively.

[1-^{3}H]Cellooligo-saccharide	K_m (M)x10^6	k_{cat} (s^{-1})	k_{cat}/K_m ($M^{-1}s^{-1}$)x10^{-6}
ß-Glucosidase			
G2	880 ± 40	22.0 ±0.2	0.0250±0.001
G3	74 ± 11	20.1 ±1.1	0.272 ±0.04
G4	35 ± 5	26.1 ±1.2	0.746 ±0.11
G5	35 ± 4	22.6 ±1.0	0.646 ±0.079
G6	37 ± 10	22.4 ±2.5	0.605 ±0.18
CBH I(D)			
G3	9 ± 4.5	0.014±0.002	(1.56 ±0.8)x10^{-3}
	3400 ±600	0.23 ±0.02	(6.76 ±1.3)x10^{-5}
G4	3.1 ± 0.2	1.34 ±0.04	0.432 ±0.03
G5	0.52± 0.04	1.12 ±0.03	2.15 ±0.18
G6	1.1 ± 0.2	2.4 ±0.2	2.18 ±0.44
CBH II			
G3	18 ± 3	0.024±0.002	0.0013±0.0002
G4	2.6 ± 0.3	7.0 ±0.3	2.69 ±0.3
G5	0.98± 0.10	2.01 ±0.08	2.05 ±0.2
G6	0.67± 0.06	4.0 ±0.2	5.97 ±0.6

REFERENCES

1. Ghose, T. K. (1977) Cellulase biosynthesis and hydrolysis of cellulosic substances. Adv. Biochem. Eng. 6, 39-76.

2. Humphrey, A. E. (1979) The hydrolysis of cellulosic materials to useful products. In: Hydrolysis of Cellulose: Mechanisms of Enzymatic and Acid Catalysis (Brown, R. D., Jr., and Jurasek, L., Eds.) pp. 25-53, American Chemical Society, Washington.

3. Ryu, D. D. Y., and Mandels, M. (1980) Cellulases: Biosynthesis and applications. Enzyme Microb. Technol. 2, 91-102.

4. Mandels, M. (1975) Microbial sources of cellulase. Biotechnol. Bioeng. Symp. 6, 81-105.

5. Gritzali, M., and Brown, R. D., Jr. (1979) The cellulase system of Trichoderma. Relationships between purified extracellular enzymes from induced or cellulose-grown cells. In: Hydrolysis of Cellulose: Mechanisms of Enzymatic and Acid Catalysis (Brown, R. D., Jr., and Jurasek, L., Eds.) pp. 237-260, American Chemical Society, Washington.

6. Gritzali, M. (1979) Purification and characterization of an endo-1,4-ß-D-glucanase and two exo-1,4-ß-D-glucanases from the cellulase system of Trichoderma reesei QM 9414. Ph.D. Dissertation, VPI and SU, Blacksburg, Virginia.

7. Fagerstam, L. G., and Pettersson, L. G. (1980) The 1,4-ß-glucan cellobiohydrolases of Trichoderma reesei QM 9414. FEBS Lett. 119, 97-100.

8. Chirico, W. J. (1980) Purification and characterization of an extracellular ß-glucosidase from Trichoderma reesei QM 9414. Master's Thesis, VPI and SU, Blacksburg, Virginia.

9. Blackwell, J. (1982) The marcomolecular organization of cellulose and chitin. In: Cellulose and Other Natural Polymer Systems (Brown, R. M., Jr., Ed.) pp. 403-428, Plenum Press, New York.

10. Ward, K., Jr., and Seib, P. A. (1970) Cellulose, lichenan, and chitin. In: The Carbohydrates (Pigman, W., and Horton, D., Eds.) Vol. IIA, pp. 413-298, Academic Press, New York.

11. Atalla, R. H., and VanderHart, D. L. (1984) Native cellulose: A composite of two distinct crystalline forms. Science 223, 283-285.

12. Gum, E. K., Jr., and Brown, R. D., Jr. (1976) Structural characterization of a glycoprotein cellulase, 1,4-ß-D-glucan cellobiohydrolase C from Trichoderma viride. Biochim. Biophys. Acta 446, 371-386.

13. Gum, E. K., Jr., and Brown, R. D., Jr. (1977) Comparison of four purified extracellular 1,4-ß-D-glucan cellobiohydrolase enzymes from Trichoderma viride. Biochim. Biophys. Acta 492, 225-231.

14. Shoemaker, S. P., and Brown, R. D., Jr. (1978) Enzymic activities of endo-1,4-ß-D-glucanases purified from Trichoderma viride. Biochim. Biophys. Acta 523, 133-146.

15. Shoemaker, S. P., and Brown, R. D., Jr. (1978) Characterization of endo-1,4-ß-D-glucanases purified from Trichoderma viride. Biochim. Biophys. Acta 523, 147-161.

16. Berghem, L. E. R., and Pettersson, L. G. (1974) The mechanism of enzymatic cellulose degradation. Isolation and some properties of a ß-glucosidase from Trichoderma viride. Eur. J. Biochem. 46, 295-305.

17. Häkansson, U., Fägerstam, L. E., Pettersson, L. G., and Anderson, L. (1979). A 1,4-ß-glucan glucanohydrolase from the cellulolytic fungus Trichoderma viride QM 9414. Biochem. J. 179, 141-149.

18. Wood, T. M., and McCrae, S. I. (1979) Synergism between enzymes involved in the solubilization of native cellulose. In: Hydrolysis of Cellulose: Mechanisms of Enzymic and Acid Catalysis (Brown, R. D., Jr., and Jurasek, L., Eds.) pp. 181-209, American Chemical Society, Washington.

19. Wood, T. M., and McCrae, S. I. (1982) Purification and some properties of the extracellular ß-D-glucosidase of the cellulolytic fungus Trichoderma koningii. J. Gen. Micro. 128, 2973-2982.

20. Kanda, T., Nakakubo, S., Wakabayashi, K., and Nisizawa, K. (1979) The mode of enzymic degradation of cellulose based on properties of cellulase components. In: Hydrolysis of Cellulose: Mechanisms of Enzymic and Acid Catalysis (Brown, R. D., Jr., and Jurasek, L., Eds.) pp. 211-236, American Chemical Society, Washington.

21. Emert, G. H., Gum, E. K., Jr., Lang, J. A., Liu, T. H., and Brown, R. D., Jr. (1974) Cellulases. In: Food Related Enzymes (Whitaker, J. R., Ed.) pp. 79-100, American Chemical Society, Washington.

22. Reese, E. T., Maguire, A. H., and Parrish, F. W. (1968) Glucosidases and exo-glucanases. Can. J. Biochem. 46, 25-34.

23. Ladisch, M. R., Gong, C. S., and Tsao, G. T. (1980) Cellobiose hydrolysis of endoglucanase (glucan glucanohydrolase) from Trichoderma reesei: Kinetics and mechanism. Biotechnol. Bioeng. 22, 1107-1126.

24. duMée, C. (1984) Structural characterization of carbohydrate attached to the glycoprotein cellulase enzymes of Trichoderma reesei QM 9414. Ph.D. Dissertation, Univ. of Florida, Gainesville, Florida.

25. Bhikhabhai, R., and Pettersson, L. G. (1984) The cellulolytic enzymes of Trichoderma reesei as a system of homologous proteins. FEBS Lett. 167, 301-308.

26. Mandels, M., Parrish, F. W., and Reese, E. T. (1962) Sophorose as an inducer of cellulase in Trichoderma viride. J. Bacteriol. 83, 406-408.

27. Fagerstam, L. G., Pettersson, L. G., and Engstrom, J. A. (1984) The primary structure of a 1,4-ß-glucan cellobiohydrolase from the fungus Trichoderma reesei QM 9414. FEBS Lett. 167, 309-315.

28. Shoemaker, S., Schweickart, V., Ladner, M., Gelfand, D., Kwok, S., Myambo, K., and Innish, M. (1983) Molecular cloning of exo-cellobiohydrolase I derived from Trichoderma reesei strain L27. Bio/Technology 1, 691-696.

29. Hsu, T., Gong, C., and Tsao, G. T. (1980) Kinetic studies of cellodextrins hydrolyses by exocellulase from Trichoderma reesei. Biotechnol. Bioeng. 22, 2305-2320.

30. van Tilbeurgh, H., Claeyssens, M., and de Bruyne, C.K. (1982) The use of 4-methylumbelliferyl and other chromophoric glycosides in the study of cellulolytic enzymes. FEBS Lett. 149, 152-156.

31. Brown, R. D., Jr., and Greenberg, B. (1980) Unpublished observations.

32. Nisizawa, K., and Hashimoto, Y. (1970) Glycoside hydrolases and glycosyl transferases. In: The Carbohydrates (Pigman, W., and Horton, D., Eds.) Vol. IIA, pp. 241-300, Academic Press, New York.

33. Sternberg, D. (1976) ß-Glucosidase of Trichoderma: Its biosynthesis and role in saccharification of cellulose. Appl. Environ. Microbiol. 31, 648-654.

34. Gong, C. S., Ladisch, R., and Tsao, G. T. (1977) Cellobiase from Trichoderma viride: Purification, properties, kinetics and mechanism. Biotechnol. Bioeng. 19, 959-981.

35. Emert, G. H. (1974) Purification and characterization of cellobiase from Trichoderma viride. Ph.D. Dissertation, VPI and SU, Blacksburg, Virginia.

36. Mandels, M. (1982) Cellulases. In: Annual Reports on Fermentation Processes (Tsao, G. T., Ed.) Vol. 5, pp. 35-78, Academic Press, New York.

37. Allen, J. D. (1980) Subsite mapping of enzymes: Application to polysaccharide depolymerases. In: Methods in Enzymology (Purich, D. L., Ed.) Vol. 64, pp. 248-277, Academic Press, New York.

38. Schechter, I., and Berger, A. (1967) On the size of the active site in proteases. I. Papain. Biochem. Biophys. Res. Commun. 27, 157-162.

39. Walz, F. G., Jr., and Terenna, B. (1976) Subsite interactions of Ribonuclease T_1: Binding studies of dimeric substrate analogues. Biochemistry 15, 2837-2842.

40. Chipman, D. M., Grisaro, V., and Sharon, N. (1967) The binding of oligosaccharides containing N-acetylglucosamine and N-acetylmuramic acid to lysozyme. J. Biol. Chem. 242, 4388-4394.

41. Hiromi, K., Ohnishi, M., and Tanaka, A. (1983) Subsite structure and ligand binding mechanism of glucoamylase. Molecular and Cellular Biochemistry 51, 79-95.

42. Biely, P., Krátký, Z., and Vrsanská, M. (1981) Substrate-binding site of endo-1,4-β-xylanase of the yeast Cryptococcus albidus. Eur. J. Biochem. 119, 559-564.

43. Thoma, J. A., Rao, G. V. K., Brothers, C., and Spradlin, J. (1971) Subsite mapping of enzymes. J. Biol. Chem. 246, 5621-5635.

44. Hiromi, K., Nitta, Y., Numata, C., and Ono, S. (1973) Subsite affinities of glucoamylase: Examination of the validity of the subsite theory. Biochem. Biophys. Acta 302, 362-375.

45. Suganuma, T., Matsuno, R., Ohnishi, M., and Hiromi, K. (1978) A study of the mechanism of action of Taka-amylase A on linear oligosaccharides by product analysis and computer simulation. J. Biochem. 84, 293-316.

46. Hiromi, K. (1970) Interpretation of dependency of rate parameters on the degree of polymerization of substrate in enzyme-catalyzed reactions. Evaluation of subsite affinities of exo-enzyme. Biochem. Biophys. Res. Commun. 40, 1-6.

47. Koyama, T., Inokuchi, N., Kikuchi, Y., Shimada, H., Iwama, M., Takahashi, T., and Irie, M. (1984) Subsite affinity of a glucoamylase from Aspergillus saitoi. Chem. Pharm. Bull. 32, 757-761.

48. Allen, J. D., and Thoma, J. A. (1976) Subsite mapping of enzymes: Depolymerase computer modelling. Biochem. J. 159, 105-120.

49. Allen, J. D., and Thoma, J. A. (1976) Subsite mapping of enzymes. Application of the depolymerase computer model to two α-amylases. Biochem. J. 159, 121-132.

50. Dubois, M., Gilles, K. A., Hamilton, S. K., Rebers, P. A. and Smith F. (1956) Colorimetric method for determination of sugars and related substances. Anal. Chem. 28, 350-356.

51. Nelson, N. J. (1944) A photometric adaptation of the Somogyi method for determination of glucose. J. Biol. Chem. 153, 375-380.

52. Somogyi, M. J. (1952) Notes on sugar determination. J. Biol. Chem. 195, 19-23.

53. Lowry, O. H., Rosebrough, N. J., Furr, A. L., and Randall, R. J. (1951) Protein measurement with the Folin-phenol reagent. J. Biol. Chem. 193, 265-273.

54. Bailey, J. L. (1967) Techniques in Protein Chemistry, 2nd Ed., pp. 345-346, Elsevier, Amsterdam.

55. Gum, E. K., Jr., and Brown, R. D., Jr. (1977) Two alternative HPLC separation methods for reduced and normal cellooligosaccharides. Anal. Biochem. 82, 372-375.

56. Miller, G. L., Dean, J., and Blum, R. (1960) A study of methods for preparing oligosaccharides from cellulose. Arch. Biochem. Biophys. 91, 21-26.

57. Diehl, H. W., Polorny, M., Zissis, E., Ness, R. K., and Fletcher, H. G., Jr. (1974) Crystalline cellobiono-1,5-lactone: Its preparation and growth-inhibitory activity in the Avena coleoptile section test. Carbohyd. Res. 38, 364-368.

58. Hudson, C. S., and Isbell, H. S. (1929) Relations between rotary power and structure in the sugar group. XIX. Improvements in the preparation of aldonic acids. J. Amer. Chem. Soc. 51, 2225-2229.

59. Conchie, J., Hay, A. J., Strachan, I., and Levvy, G. A. (1967) Inhibition of glycosidases by aldonolactones of corresponding configuration. Biochem. J. 102, 929-941.

60. Isbell, H. S., and Frush, H. L. (1963) Lactonization of aldonic acids. In: Methods in Carbohydrate Chemistry (Whistler, R. L. and Wolfrom, M. L., Eds.) Vol. II, pp. 16-18, Academic Press, New York.

61. Frush, H. L., and Isbell, H. S. (1956) Sodium bicarbonate reduction of aldonic lactones to glycitols. J. Amer. Chem. Soc. 78, 2844-2846.

62. Wolfrom, M. L., and Wood, H. B. (1951) Sodium borohydride as a reducing agent for sugar lactones. J. Amer. Chem. Soc. 73, 2933-2934.

63. Saif-ur-Rahman, S., Krishnamurti, C. R., and Kitts, W. D. (1968) Separation of cello-oligosaccharides by thin-layer chromatography. J. Chromatog. 38, 400-402.

64. Krebs, K. G., Heusser, D., and Wimmer, H. (1969) Spray reagents. In: Thin-Layer Chromatography (Stahl, E., Ed.) pp. 854-909, Springer-Verlag, New York.

65. Ghebregzabher, M., Rufini, S., Monaldo, B., and Lato, M. (1976) Thin-layer chromatography of carbohydrates. J. Chromatog. 127, 133-162.

66. Jermyn, M. A. (1955) Fungal cellulases. Australian J. Biol. Sci. 8, 541-602.

67. STATZYME. Worthington Diagnostics (1976) Worthington Statzyme Glucose, Freedhold, New Jersey.

68. Rosenthal, A. L., and Saifer, A. (1973) Continuous uv monitoring of fluorogenic substrates I. Kinetic analysis of N-acetyl-β-D-hexosaminidases. Anal. Biochem. 55, 85-92.

69. Allen, J. D. (1975) Bond-cleavage frequency analysis. Carbohyd. Res. 39, 303-315.

70. Cleland, W. W. (1979) Statistical analysis of enzyme kinetic data. In: Methods in Enzymology (Purich, D. L., Ed.) Vol. 63, pp. 103-138, Academic Press, New York.

71. Roeser, K-R., and Legler, G. (1981) Role of sugar hydroxyl groups in glycoside hydrolysis. Biochem. Biophys. Acta 657, 321-333.

72. Robyt, J. F., and French, D. (1970) The action pattern of porcine pancreatic α-amylase in relationship to the substrate binding site of the enzyme. J. Biol. Chem. 245, 3917-3927.

73. Whitaker, D. R., and Merler, E. (1956) Cleavage of cellotriose by Myrothecium cellulase. Can. J. Biochem. Physiol. 34, 83-89.

74. Vaheri, M., Leisola, M., and Kauppinen, V. (1979) Translycosylation products of cellulase system of Trichoderma reesei. Biotechnol. Lett. 1, 41-46.

75. Evans, E. A., Sheppard, H. C., Turner, J. C., and Warrell, D. C. (1974) A new approach to specific labelling of organic compounds with tritium: Catalyzed exchange in solution with tritium gas. J. Labelled Compounds 10, 569-587.

76. Friedberg, F., and Kaplan, L. (1957) The absence of an Amadori rearrangement in glucosazone formation. J. Am. Chem. Soc. 79, 2600-2601.

77. Isbell, H. S., Frush, H. L., Holt, N. B., and Moyer, J. D. (1960) Tritium-labeled compounds III. Aldoses-1-t. J. Research NSB 64A, 177-180.

78. Green, J. W. (1980) Reduction of carbohydrates. In: The Carbohydrates (Pigman, W. and Horton, D., Eds.) Vol. IB, pp. 989-1011, Academic Press, New York.

79. Takeo, K., Okushio, K., Fukuyama, K., and Kuge, T. (1983) Synthesis of cellobiose, cellotriose, cellotetraose, and lactose. Carbohydr. Res. 121, 163-173.

80. John, M., Trenel, G., and Dellweg, H. (1969) Quantitative chromatography of homologous glucose oligomers and other saccharides using polyacrylamide gel. J. Chromatog. 42, 476-484.

81. Tipson, R. S., and Parker, F. S. (1980) Infrared spectroscopy. In: The Carbohydrates (Pigman, W. and Horton, D., Eds.) Vol. IB, pp. 1394-1436, Academic Press, New York.

82. Biely, P., Vrsanska, M., and Kratky, Z. (1981) Mechanisms of substrate digestion by endo-1,4-β-xylanase of Cryptococcus albidus. Eur. J. Biochem. 119, 565-571.

83. Ladisch, M. R., and Tsao, G. T. (1978) Theory and practice of rapid liquid chromatography at moderate pressures using water as eluent. J. Chromatogr. 166, 85-100.

84. Vratny, P., Coupek, J., and Vozka, S. (1983) Accelerated reversed-phase chromatography of carbohydrate oligomers. J. Chromatogr. 254, 143-155.

85. Chen, C., and McGinnis, G. (1983) High-performance liquid chromatography of sugar oximes. Carbohydr. Res. 122, 322-326.

86. Brown, W., and Andersson, O. (1971) Preparation and xylodextrins and their separation by gel chromatography. J. Chromatogr. 57, 255-263.

87. Honda, S. (1984) High-performance liquid chromatography of mono- and oligosaccharides. Anal. Biochem. 140, 1-47.

88. Scott, R. W. (1970) Quantitative recovery of sugars from silica gel thin layers. J. Chromatogr. 49, 473-481.

89. Umezurike, G. M. (1972) The purification and properties of extracellular β-glucosidase from Botryodiplodia theobromae Pat. Biochem. Biophys. Acta 227, 419-428.

90. Shewale, J. G. (1982) β-Glucosidase: Its role in cellulase synthesis and hydrolysis of cellulose. Int. J. Biochem. 14, 435-443.

91. Cole, F. E., and King, K. W. (1964) Site of hydrolysis of cellulodextrins and reduced cellulodextrins by purified cellulase components. Biochim. Biophys. Acta 81, 122-129.

92. Hirayama, T., Horie, S., Nagayama, H., and Matsuda, K. (1978) Studies on cellulases of phytopathogenic fungus, Pyricularia oryzae Cavara. J. Biochem. 84, 27-37.

93. Tsujisaka, Y., Fukumota, J., and Yamamoto, T. (1958) Specificity of crystalline saccharogenic amylase of moulds. Nature 181, 770-771.

94. King, K. W., and Smibert, R. M. (1963) Distinctive properties of β-glucosidases and related enzymes derived from a commercial Aspergillus niger cellulase. Appl. Microbiol. 11, 315-319.

95. Shewale, J. G., and Sadana, J. (1981) Purification, characterization and properties of β-glucosidase enzymes from Sclerotium rolfsii. Arch. Biochem. Biophys. 207, 185-196.

96. Jencks, W. P. (1969) Catalysis in Chemistry and Enzymology, McGraw-Hill, New York, pp. 323-350.

97. Hiromi, K., Tanaka, A., and Ohnishi, M. (1982) Fluorometric studies on the binding of gluconolactone, glucose, and glucosides to the subsites of glucoamylase. Biochemistry 21, 102-107.

98. Gum, E. (1978) Unpublished observations.

99. Allen, J. D., and Thoma, J. A. (1978) Model for carbohydrase action. Aspergillus oryzae α-amylase degradation of maltotriose. Biochemistry 17, 2345-2350.

100. Wood, T. M. (1981) Enzyme interactions involved in fungal degradation of cellulosic materials. Ekman-Days Symp. 3, 31-38.

101. Berghem, L. E. R., Pettersson, L. G., and Axio-Frederiksson, U. (1975) The mechanism of enzymatic cellulose degradation. Eur. J. Biochem. 53, 55-62.

102. Gurney, R. W. (1953) Ionic Processes in Solution. McGraw-Hill, New York, pp 80-92.

103. Kauzman, W. (1959) Some factors in the interpretation of protein denaturation. In: Advances in Protein Chemistry, (Antinsen, C. B., Jr., Bailey, K., Anson, M. L. and Edsall, J. T., Eds.) Vol. XIV, pp. 1-64, Academic Press, New York.

BIOGRAPHICAL SKETCH

William J. Chirico was born on April 2, 1956, in Brooklyn, New York. After completing his education at Xaverian High School in Brooklyn, he attended Bucknell University in Lewisburg, PA, where he received a B.S. degree in biology. In September of 1978, he began his graduate studies at Virginia Tech, in the Department of Biochemistry and Nutrition, working with Dr. Ross D. Brown, Jr. He continued his graduate studies with Dr. Ross D. Brown, Jr., at the University of Florida, in the Department of Biochemistry and Molecular Biology. He has accepted a postdoctoral position in Dr. Günter Blobel's laboratory at The Rockefeller University.

I certify that I have read this study and that in my opinion it conforms to acceptable standards of scholarly presentation and is fully adequate, in scope and quality, as a dissertation for the degree of Doctor of Philosophy.

Ross D. Brown, Jr., Chairman
Associate Professor of
Biochemistry and Molecular
Biology

I certify that I have read this study and that in my opinion it conforms to acceptable standards of scholarly presentation and is fully adequate, in scope and quality, as a dissertation for the degree of Doctor of Philosophy.

Charles M. Allen, Jr.
Professor of Biochemistry and
Molecular Biology

I certify that I have read this study and that in my opinion it conforms to acceptable standards of scholarly presentation and is fully adequate, in scope and quality, as a dissertation for the degree of Doctor of Philosophy.

Kimon J. Angelides
Assistant Professor of
Biochemistry and Molecular
Biology

I certify that I have read this study and that in my opinion it conforms to acceptable standards of scholarly presentation and is fully adequate, in scope and quality, as a dissertation for the degree of Doctor of Philosophy.

Vincent Chau
Assistant Professor of
Biochemistry and Molecular
Biology

I certify that I have read this study and that in my opinion it conforms to acceptable standards of scholarly presentation and is fully adequate, in scope and quality, as a dissertation for the degree of Doctor of Philosophy.

R. Michael Roberts
Professor of Biochemistry and Molecular Biology

I certify that I have read this study and that in my opinion it conforms to acceptable standards of scholarly presentation and is fully adequate, in scope and quality, as a dissertation for the degree of Doctor of Philosophy.

Jesse F. Gregory
Associate Professor of Food Science and Human Nutrition

This dissertation was submitted to the Graduate Faculty of the College of Medicine and to the Graduate School, and was accepted as partial fulfillment of the requirements for the degree of Doctor of Philosophy.

December 1984

Dean, College of Medicine, 2/10/84

Dean for Graduate Studies and Research